AD-A168 949 ROCK MASS PERSISTENCE EXECUTIVE SUMMARY(U) 1/2
MASSACHUSETTS INST OF TECH CAMBRIDGE DEPT OF CIVIL
ENGINEERING H H EINSTEIN ET AL. FEB 86 R86-12-786
UNCLASSIFIED ARO-19291.4-GS DAAG29-83-K-0016 F/G 8/7 NL

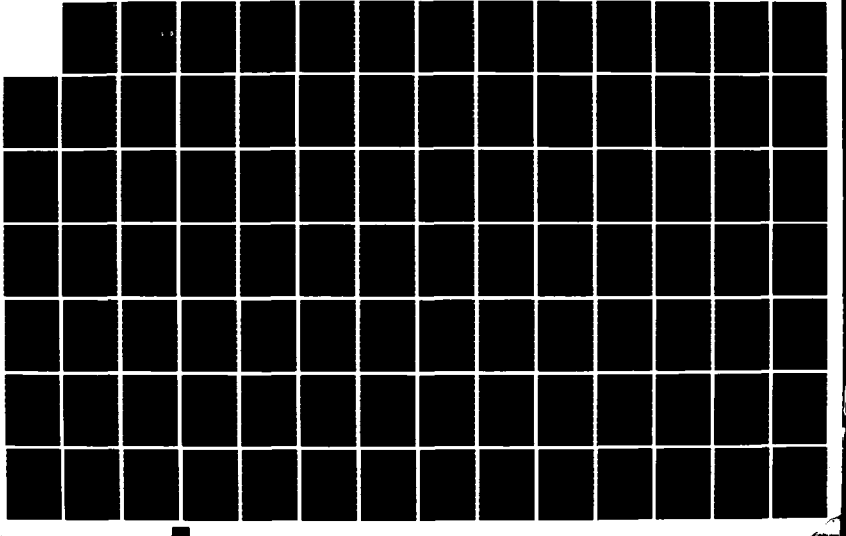

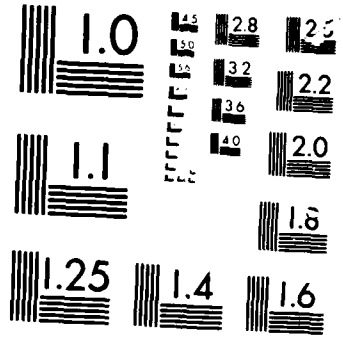

ROCK MASS PERSISTENCE

FINAL TECHNICAL REPORT
AND
EXECUTIVE SUMMARY

H.H. Einstein, G.B. Baecher, V. Li, D. Veneziano,
H. Herda, M. Gencer, W.S. Dershowitz,
J.C. Kafritsas, H.C. Chan

February 1986

U.S. Army Research Office
Grant No DAAG-29-83-K-0016

Department of Civil Engineering
Massachusetts Institute of Technology

SECURITY CLASSIFICATION OF THIS PAGE (When Data Entered)

REPORT DOCUMENTATION PAGE

READ INSTRUCTIONS BEFORE COMPLETING FORM

1. REPORT NUMBER	2. GOVT ACCESSION NO.	3. RECIPIENT'S CATALOG NUMBER
ARO 19291.4-GS	N/A	N/A

4. TITLE (and Subtitle)	5. TYPE OF REPORT & PERIOD COVERED
ROCK MASS PERSISTENCE	Final Technical Report Dec. 1, 1982 - Nov. 30, 1985
	6. PERFORMING ORG. REPORT NUMBER R86-11-786

7. AUTHOR(s)	8. CONTRACT OR GRANT NUMBER(s)
H.H. Einstein, G.B. Baecher, V. Li, D. Veneziano, H. Herda, M. Gencer, W.S. Dershowitz, J.C. Kafritsas, H.C. Chan	DAA G29-83-K-0016

9. PERFORMING ORGANIZATION NAME AND ADDRESS	10. PROGRAM ELEMENT, PROJECT, TASK AREA & WORK UNIT NUMBERS
Department of Civil Engineering Massachusetts Institute of Technology Cambridge, Massachusetts 02139	

11. CONTROLLING OFFICE NAME AND ADDRESS	12. REPORT DATE
U. S. Army Research Office Post Office Box 12211 Research Triangle Park, NC 27709	February 1986
	13. NUMBER OF PAGES 95

14. MONITORING AGENCY NAME & ADDRESS (if different from Controlling Office)	15. SECURITY CLASS. (of this report)
	Unclassified
	15a. DECLASSIFICATION/DOWNGRADING SCHEDULE

16. DISTRIBUTION STATEMENT (of this Report)

Approved for public release; distribution unlimited.

17. DISTRIBUTION STATEMENT (of the abstract entered in Block 20, if different from Report)

NA

18. SUPPLEMENTARY NOTES

The view, opinions, and/or findings contained in this report are those of the author(s) and should not be construed as an official Department of the Army position, policy, or decision, unless so designated by other documentation.

19. KEY WORDS (Continue on reverse side if necessary and identify by block number)

Rock Joints, Joint Geometry, Flow in Fractured Media, Stochastic Models, Numerical Models, Coupled Flow-Deformation, Fracture Propagation

20. ABSTRACT (Continue on reverse side if necessary and identify by block number)

The research project "Rock Mass Persistence" funded by ARO under Grant No. DAAG-29-83-K-0016 started December 1, 1982 and ended November 30, 1985. Its objectives were to first develop analytical models which can describe joint geometries as they occur in real rock masses. The analytical descriptions have to be derivable from data as obtained in usual field exploration. These geometric models were then to be used to develop methods

(over)

DD FORM 1 JAN 73 1473 EDITION OF 1 NOV 65 IS OBSOLETE

UNCLASSIFIED

SECURITY CLASSIFICATION OF THIS PAGE (When Data Entered)

for describing flow through jointed rock masses and for describing the fracturing, i.e., the strength and deformability of jointed rock masses.

The objectives were achieved. Basic knowledge on jointed rock mass description and behavior, was expanded. Practically applicable methods were developed. The basis for future fundamental and applied research was created.

The complete research results are presented in a separate set of three volumes: I Rock Joint Systems, II Coupled Flow Deformation Analysis, and III Fracture Propagation in Jointed Media. This Final Technical Report and Executive Summary presents these results in a concentrated form.

The most significant results are:

- Two and three dimensional stochastic joint system models; with computer code
- Stochastic fracture flow models through a combination of the joint system models and a finite element model; with computer code
- Simplified expressions for joint geometry
- Scale effect, anisotropy and three dimensional character significantly affect flow in fractured media
- Two dimensional coupled flow/deformation analysis using the distinct element method; with computer code
- Coupling is particularly important when joint apertures vary in rock mass
- Wedge/block analysis for translation, rotation and time dependent effects; with computer code
- Hybrid boundary element/displacement discontinuity element method for fracturing of jointed media; with computer code
- Mode I and II fracturing, as well as sliding in slip weakening mode can be modeled
- Verification/validation with analytical and experimental results

These results are important for the practical advances and for the basis of further research they provide.

Table of Contents

List of Figures

List of Tables

1. Introduction

The research project "Rock Mass Persistence" funded by ARO under Grant No. DAAG-29-83-K-0016 started December 1, 1982 and ended November 30, 1985. Its objectives were to first develop analytical models which can describe joint geometries as they occur in real rock masses. The analytical descriptions have to be derivable from data as obtained in usual field exploration. These geometric models were then to be used to develop methods for describing flow through jointed rock masses and for describing the fracturing, i.e., the strength and deformability of jointed rock masses.

The objectives were achieved. Basic knowledge on jointed rock mass description and behavior was expanded. Practically applicable methods were developed. The basis for future fundamental and applied research was created.

In addition to the originally defined research objectives significant additional work was performed. This consisted of the final development of a coupled flow deformation analysis method based on the distinct element procedure and particularly of its use in parametric studies.

This final technical report presents the research results in three volumes:

Vol. I Rock Joint Systems

Vol. II Coupled Flow - Deformation Analysis

Vol. III Fracture Propagation in Jointed Media

Each volume was developed from a Ph.D. thesis. Given their extent the most important results are summarized in this Executive Summary. Each of the following Chapters 2 to 4 is therefore devoted to a summary of

Volumes I to III respectively. This is followed by general conclusions and recommendations for further research, a listing of personnel who have been working on the project and acknowledgements. A listing of papers which have been or will be produced based on this research will conclude the Executive Summary.

2. Rock Joint Systems

2.1 Background

Geometric and mechanical characterization of rock joints is the basis for most of the work of engineering geologists, and civil and mining engineers when dealing with rock masses. Also, such a characterization plays an important role in investigations on joint genesis. Joints are usually characterized by the parameters listed in Table 2.1; in addition joint termination and autocorrelation have been considered in this research. However, given their pervasive and three-dimensional nature on the one hand and their limited exposure in outcrops, borings and tunnels on the other hand makes complete descriptions of joints difficult. Such an ideal characterization would involve the specific description of each joint in the rock mass, exactly defining for instance its location, shape, size, planarity, aperture and shearing resistance. This is not possible for a number of reasons: 1) the visible parts of joints are limited (for instance to joint traces only), thus preventing a complete description; 2) joints at a distance from the exposed rock surfaces cannot be directly observed; 3) direct (visual or contact measurements) and indirect (geophysical) observations have limited accuracies.

For these reasons joints in a rock mass are usually described as an assemblage rather than as individual features. The assemblage has stochastic character in that joint characteristics vary in space. Such variations may be minute as in the case of the orientation of a set of approximately parallel joints or they may be large if a particular property has substantial variability. It is important to note that spatial variability can but does

Table 2.1 -- Joint Parameters

Parameter	Descriptionn
Attitude (orientation)	Strike and Dip, or Dip Direction and Dip or Pole Orientation with spherical coordinates.
Location	Coordinates of points on joint planes (usually spacing and location is measured).
Spacing	Distance between intersection points produced by intersecting a line perpendicular to the joint mean attitude and the joints of a set. A set of joints consists of joints that are parallel or subparrallel to each other.
Size	Extent of jointing generally expressed as length of traces on two-dimensional outcrops or as the area of jointed segments in a joint plane (see also persistence).
Persistence	The proportion of actual jointed parts a_i of a joint plane A, 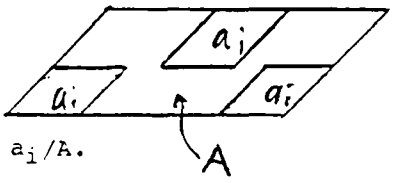 "Persistence" = $\sum a_i/A$.
Aperture	Width of open joint measured perpendicularly to joint walls (only joints filled with air or water are considered open, while joints containing filler between the wall rock are considered closed.
Joint Filler	Material weathered from wall rock, material sedimented in joint, material precipitated in joint.
Planarity	Three dimensional shape of joint surface; generally either planar, or with regular or irregular deviations from a plane.
Roughness	Deviation from the ideal planar surface on the microscale usually with wavelength < 1 cm.
Waviness	Deviation from the ideal planar surface on the macroscale usually with wavelengths > 1 cm.
Shape	Shape of joint boundaries, generally either circular, elliptical, polygonal or irregular.

not have to imply random underlying mechanisms; spatial variability may just as well be the result of a number of simultaneous or sequential but very specific mechanisms.

Two major approaches have emerged to describe the assemblage of joint characteristics in a rock mass: the traditional disaggregate characterization and the more recent aggregate characterization. In the former, each joint characteristic is described separately, for instance through orientation distributions (pole diagrams), spacing distributions and others. In the latter the interdependence of joint characteristics is captured through the formulation of joint system models. A particular joint system model represents a typical geometry. The individual characteristics are still stochastic but their interdependence is specified; for instance, in an orthogonal model the mean orientations of three joint sets are at right angles to each other, but some variability of orientation about these means exists.

Table 2.2 summarizes the rock joint system models. Each of the five models consists of a particular combination of the rock joint system characteristics in Table 2.1. Joint planarity is specified as planar for all joint system models, and any joint location or autocorrelation process is permissible within any model. Any component specified as stochastic may also be deterministic.

The orthogonal model was developed by Irmay* (1955), Childs (1957) and Snow (1965). They applied the model as did Schwartz et al. (1980) to hydrologic problems. Figure 2.1 shows a regular orthogonal joint system model. The Baecher model (Baecher et al. 1978) represents joints as circular or

---

* Literature references are listed in Appendix I. Note, however, that only a very limited number of references are used in this Executive Summary. Complete literature references are given in Volumes I to III.

Table 2.2

JOINT SYSTEM MODELS

MODEL NAME	JOINT SHAPE	JOINT SIZE	TERMINATION AT INTERSECT.	CO-PLANARITY	ORIENTATION OF SETS
1. Orthogonal	Rectangle	Bounded	no	---	Parallel
		Unbounded	yes	yes	Parallel
		Unbounded	no	yes	Parallel
2. Baecher	Circle Ellipse	Bounded	no	no	Stochastic
3. Veneziano	Polygon	Bounded	in joint planes only	yes	Stochastic
4. Dershowitz	Polygon	Bounded	yes	yes	Stochastic
5. Mosaic Tesselation	Polygon	Bounded	yes	yes	Regular Stochastic

For all models, joints are planar, and any location or autocorrelation process is possible. Joint locations are usually stochastic. Bounding of joints implies that joints which are smaller than the region under consideration can be represented. This means, with reference to the sketch in Table 1, that A is the region and a_i are bounded joints; if the joints were unbounded a_i would be $\geq$ A. Joint sizes are usually stochastic either specified directly or indirectly through stochastic location or orientation.

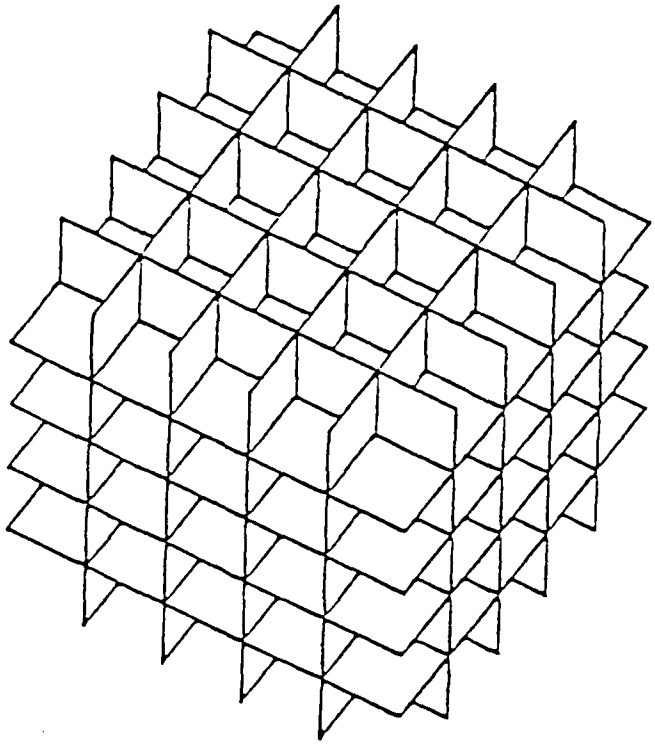

FIGURE 2.1 THREE DIMENSIONAL ORTHOGONAL MODEL

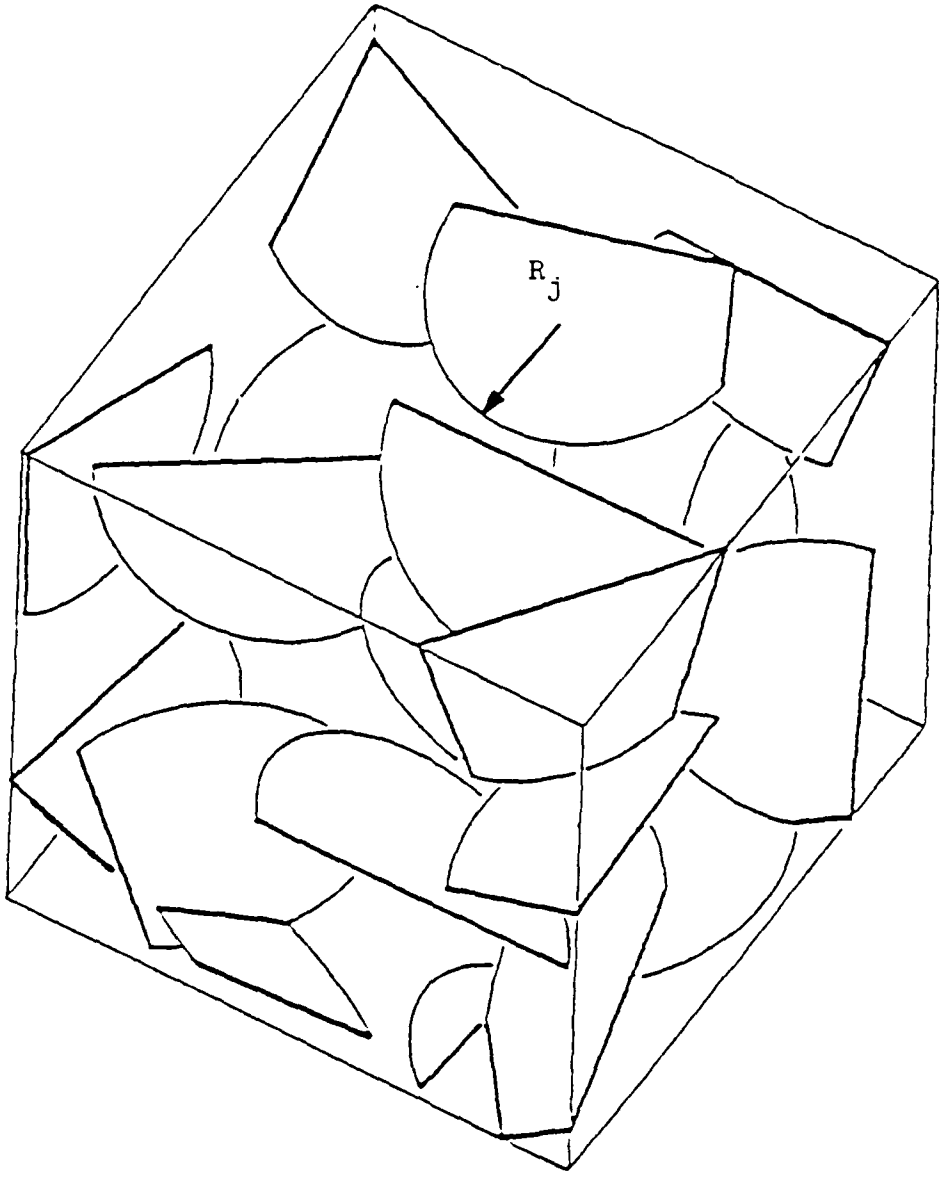

FIGURE 2.2 BAECHER JOINT SYSTEM MODEL

elliptical disks (Figure 2.2). The joint radii can be regularly or stochastically distributed (lognormal or exponential distribution). Similarly, joint orientations can be regular (e.g. exactly parallel) or represented by any orientation distribution (Fisher, bi-variate Fisher, Bingham, uniform, or bivariate normal); also joint location can be regular or stochastic (usually by a Poisson process).

The Veneziano model (Veneziano 1979) describes joints as polygons. It is based on Poisson plane and Poisson line processes as shown in Figure 2.3. Orientation distributions are as in the Baecher model.

The Dershowitz model is also based on Poisson plane and Poisson line process but such that joint plane intersections produce joints (Figure 2.4). The Dershowitz, Baecher and Veneziano models have been developed in this and previous MIT research.

A variety of two-dimensional and three-dimensional Mossaic Tesselation models (Figs. 2.5 and 2.6) represent other possible joint system models.

2.2 Joint System Modelling and Simplified Expressions

Joint System models can be expressed by numerical procedures which represent the two or three-dimensional deterministic (regular) and stochastic character of the particular model. The computer code JINX has been developed for this purpose. It includes the Orthogonal, Baecher, Veneziano and Dershowitz models with the corresponding deterministic and stochastic characteristics in two and three dimensions. It is thus the first three-dimensional stochastic joint geometry code. JINX consists of 6 basic components which can be linked together in any combination as desired. Each of the components consists of one or more programs for specific applications. The components are as follows:

- Common Variable Storage: For reallocation of storage for different models.

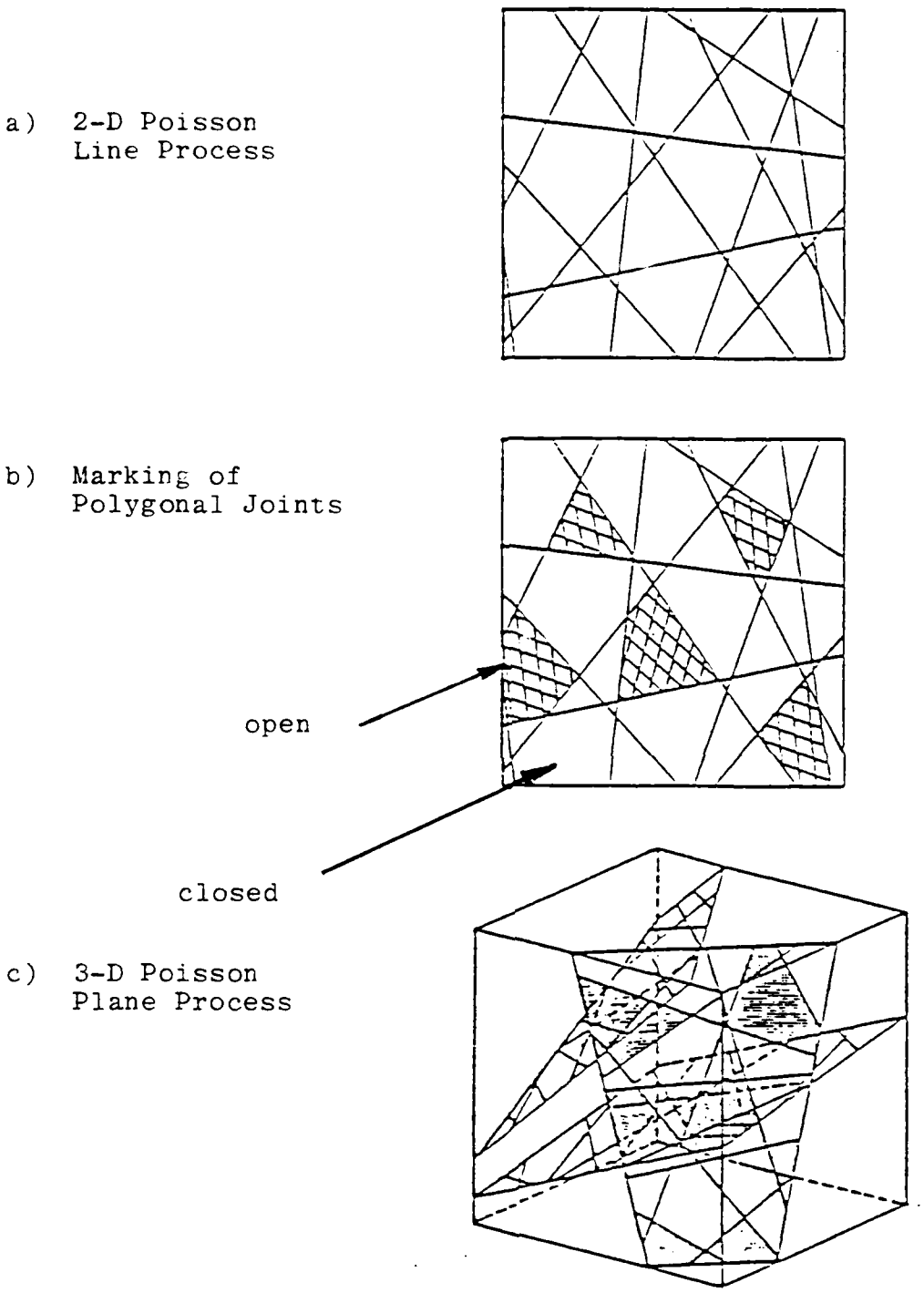

FIGURE 2.3 GENERATION OF VENEZIANO (1979) JOINT MODEL

a) 3-D Poisson Plane Process

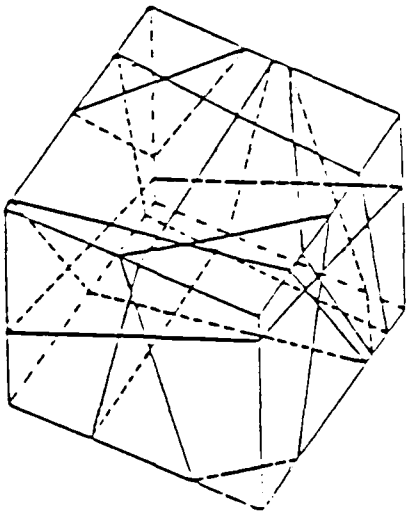

b) Poisson Line Process Formed by Intersections

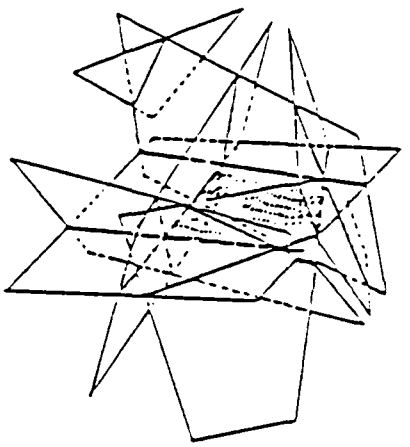

c) Marking of Polygonal Joints

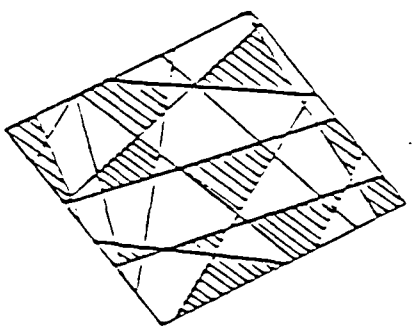

FIGURE 2.4 GENERATION OF DERSHOWITZ JOINT MODEL

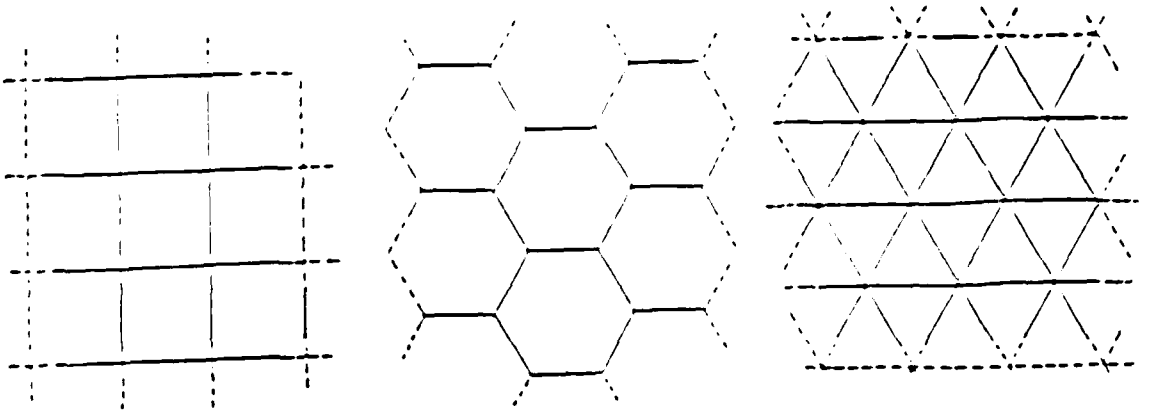

Orthogonal Hexagonal Triangular

a Regular (Deterministic) Tesselation

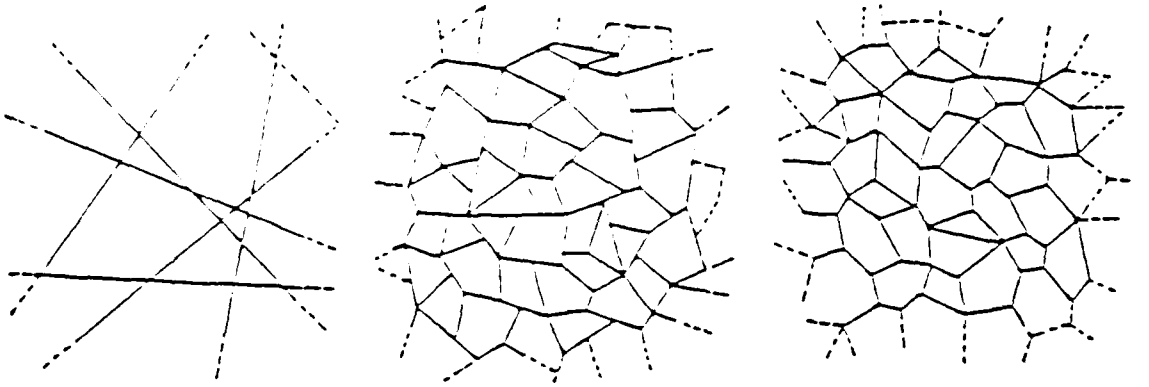

Poisson Lines Regular Homogeneous Isotropic Process Homogeneous Isotropic Process (No T Intersections)

(see Cowan, 1980)

b) Stochastic Tesselation

FIGURE 2.5 TWO DIMENSIONAL MOSAIC TESSELATION

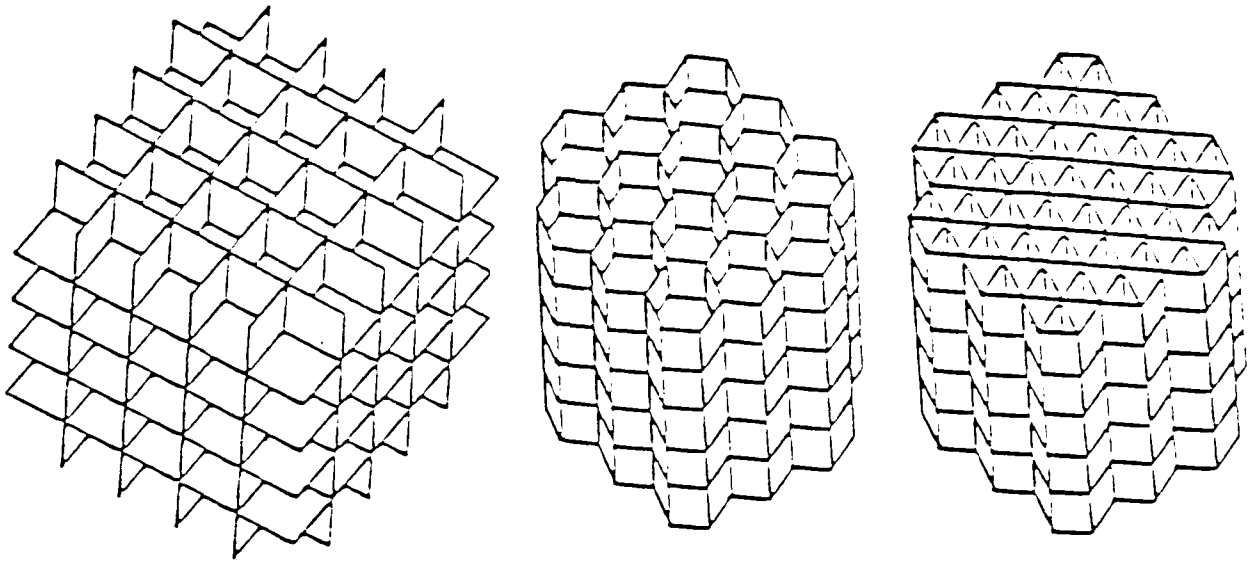

Orthogonal Hexagonal Triangular

a. Regular (Deterministic) Tesselations

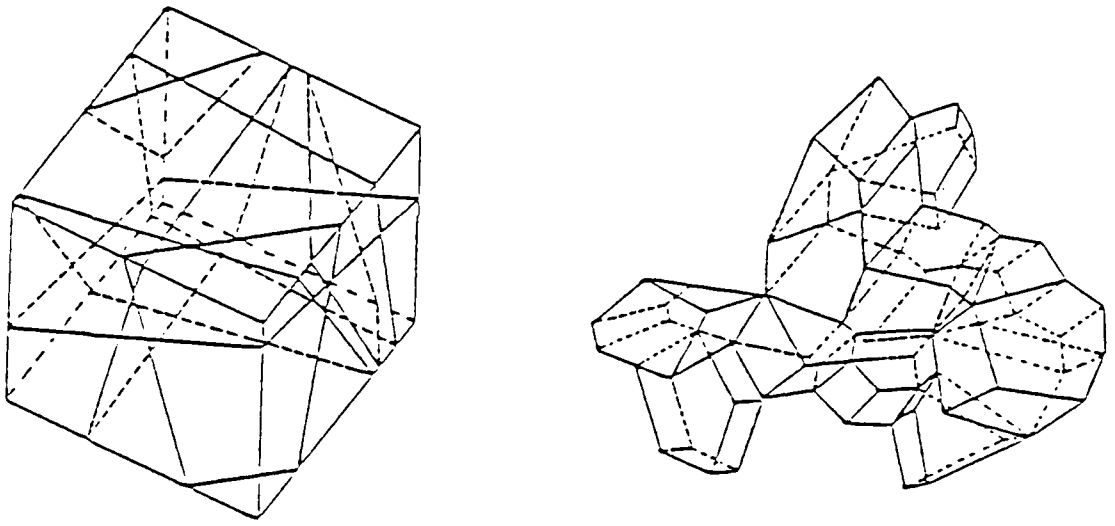

Poisson Planes Polyhedra

b. Stochastic Tesselations

FIGURE 2.6 THREE DIMENSIONAL MOSAIC TESSELATION

- Input and Control: Controls execution of simulation, analysis, and finite element preprocessor packages.
- Simulation: Generation of Baecher model, Veneziano model and Dershowitz model. The usual joint characteristics as listed in Table 1 serve as input parameters.
- Analysis: Calculation of joint intersections and sample statistics (RQD, fracture frequency) for two and three dimensional networks, of joint network connectivity measures and definition of connected joint units for two and three dimensional models. Calculation of block size measures for two and three dimensional networks. Statistics and output for Monte Carlo simulations.
- Graphics: Graphical display of two dimensional rock joint networks and projection of an individual 3-D Dershowitz model joint plane on the horizontal (x-y) plane. Stereoplotting of generated joint orientation distributions.
- Finite element flow programs and preprocessors (see Section 2.4,

The computer program package JINX is of great significance:

- Practically, it serves as a basis for hydraulic flow modelling (see Section 2.4) in jointed media and for fracture propagation models of jointed media.
- It is an essential research tool for the comparisons conducted in this research (see below) and for future work on joint genesis.

Comparisons between a large number of joint maps and photographs were made. They showed that the different joint system models are necessary to cover the variety of real joint geometries. While the joint system models represent a wide range of real geometries they still do not cover all of them. Notably, they do not cover geometries with non planar joints.

The stochastic representations involve simulation with a number of realizations of the particular model. It is often desirable for engineering purposes but also in many research applications to express joint geometry with simpler measures rather than to use the computer simulation. Extensive work in this direction was perfomed:

- A number of so-called persistence measures were created. They involve expressing joint density as joint area per volume or by number of joints per volume.
- Several so called connectivity measures were also developed. These involve geometric expressions which are related to hydraulic conductivity of the jointed medium or which directly express this conductivity (see also Section 2.4).
- Finally, several block size measures were created in which block shape and size are expressed in a simplified manner.

These simplified measures have been developed both for two and three dimensions. Wherever possible analytical expressions were derived, otherwise the measures were numerically obtained by performing a number of simulations with the complete models.

2.3 Comparisons

Extensive parametric studies were conducted to compare the different models. A number of interesting results which were obtained, will be summarized here. By running simulations with the complete models and simultaneously deriving the simplified measures one can assess how represenative each of these measures is. This makes it possible to select the more representative measures for engineering application, and further research. From these investigations one can conclude

that the persistence measure P_2 (P_{32} in three dimension), which is the joint trace length per area (joint area per volume), the connectivity measures C_7 (which is the equivalent hydraulic conductivity) and C_8 (equivalent joint network length, see Fig. 2.7) provide the best simplified measures.

Another interesting result is the importance of joint connectivity. The Baecher and Veneziano models with essentially independent joints and the Dershowitz model with joint termination at joint intersections provide extremes for such a comparison.

The models were compared in both two and three dimensions using analytical techniques and computer simulations. Figure 2.8 illustrates the relationship between intersection intensity C_1 (number of joint intersections per unit volume) and persistence measure P_{32} (area of joints per unit volume) for disk (Baecher) and Polygon (Dershowitz) joint system models. Clearly, the intersection intensity of the Dershowitz model is higher than that in the Baecher model.

This difference can be seen in terms of engineering parameters in Figure 2.9 which plots effective hydraulic conductivity K against joint size for two-dimensional models. Substantial flows occur at much lower levels of intensity in the Dershowitz model than in the Baecher model. Figure 2.10 shows a similar result for three-dimensional hydrological modeling. In addition, this figure shows that the behavior is significantly different in two and three dimensions.

This points out the importance of both the geometry of the joint system model and the dimensionality of modeling: The use of two rather than three-dimensional models may have dramatic effects on predictions of engineering behavior.

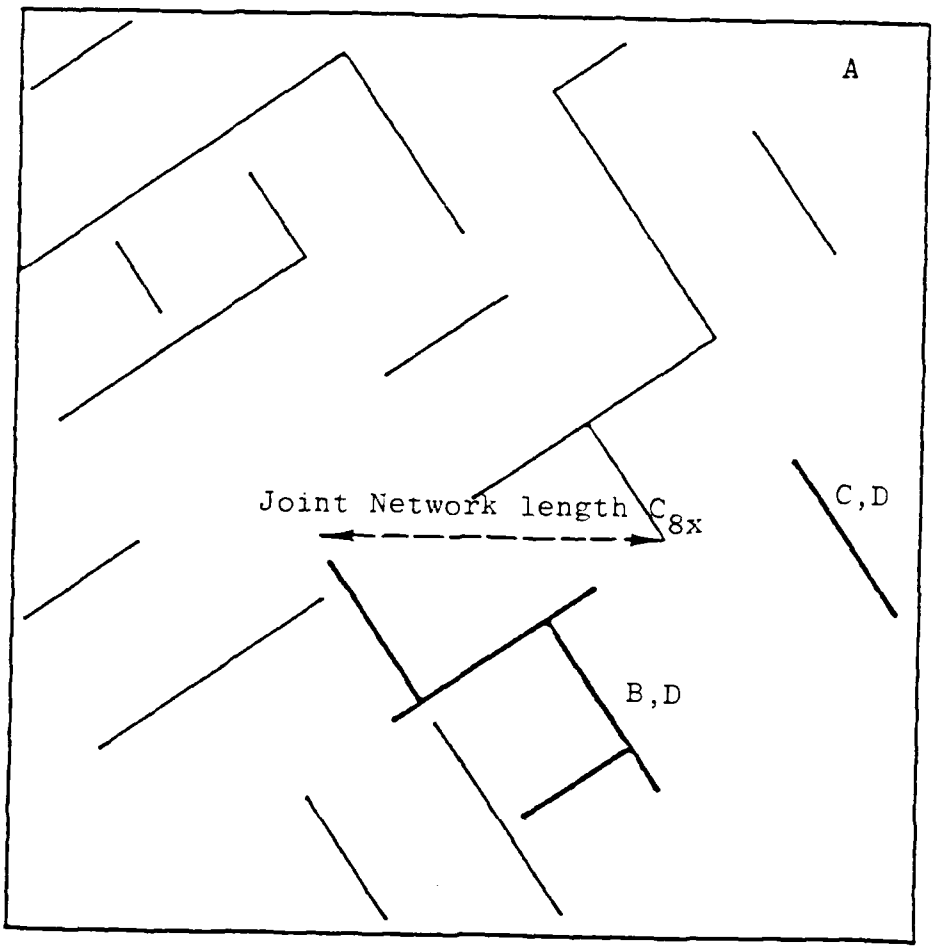

(A) all joints form the "joint system"
(B) two or more interconnected joints form a "network"
(C) joints with no intersections are "isolated joints"
(D) joint networks and isolated joints are "joint units"

Note: C_{8} can be in any direction. In this figure, C_{8x} is in the x direction as shown.

FIGURE 2.7 EQUIVALENT JOINT NETWORK LENGTH C_{8x}

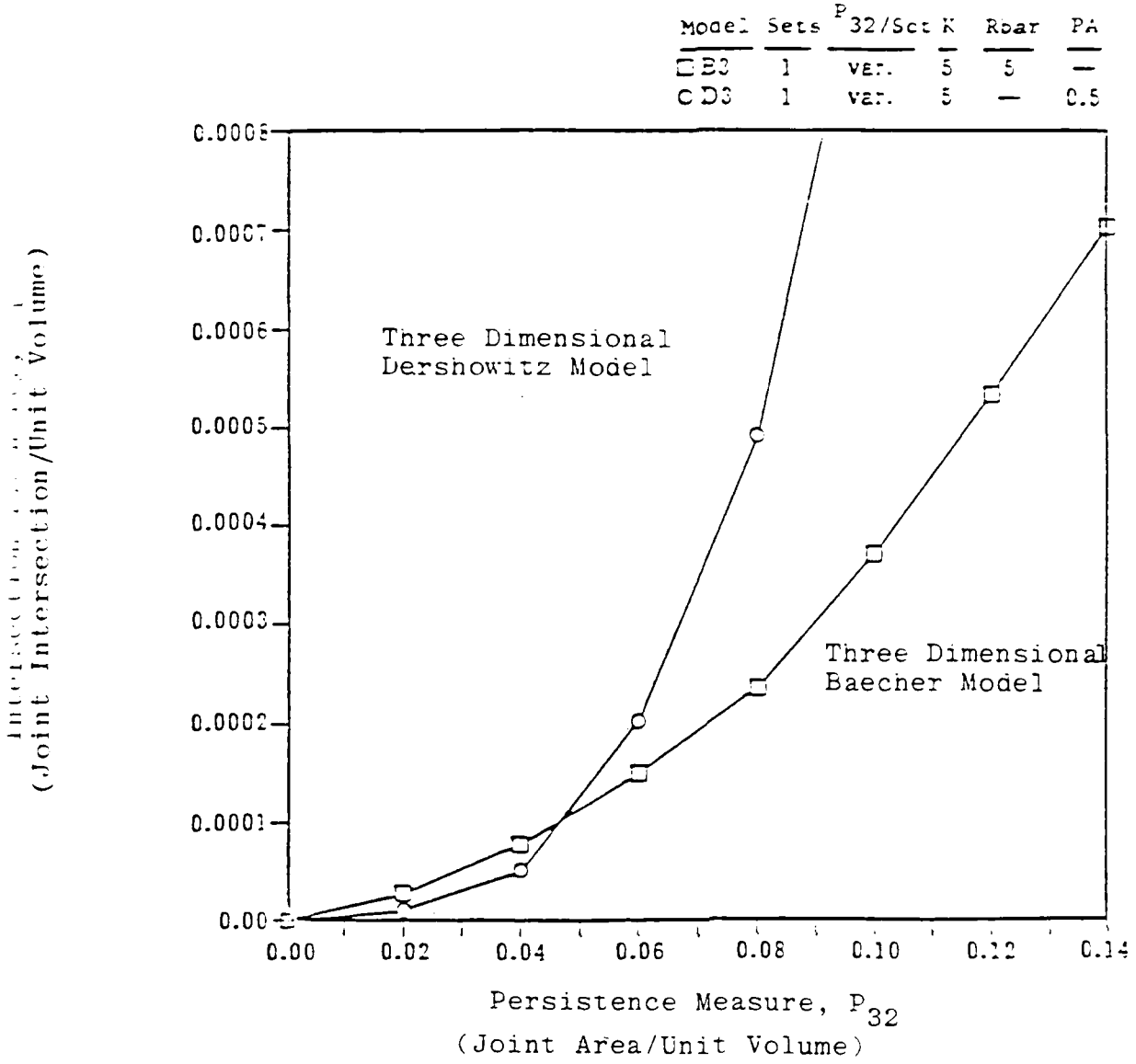

Sets = number of joint sets

P_{32}/Set = persistence (joint area/vol.) per set

K = dispersion factor for Fisher distribution

Rbar = mean radius (or equivalent)

PA = area persistence (joint per joint plane)

FIGURE 2.8 RELATION BETWEEN INTERSECTION INTENSITY C_1 AND PERSISTENCE MEASURE P_{32}

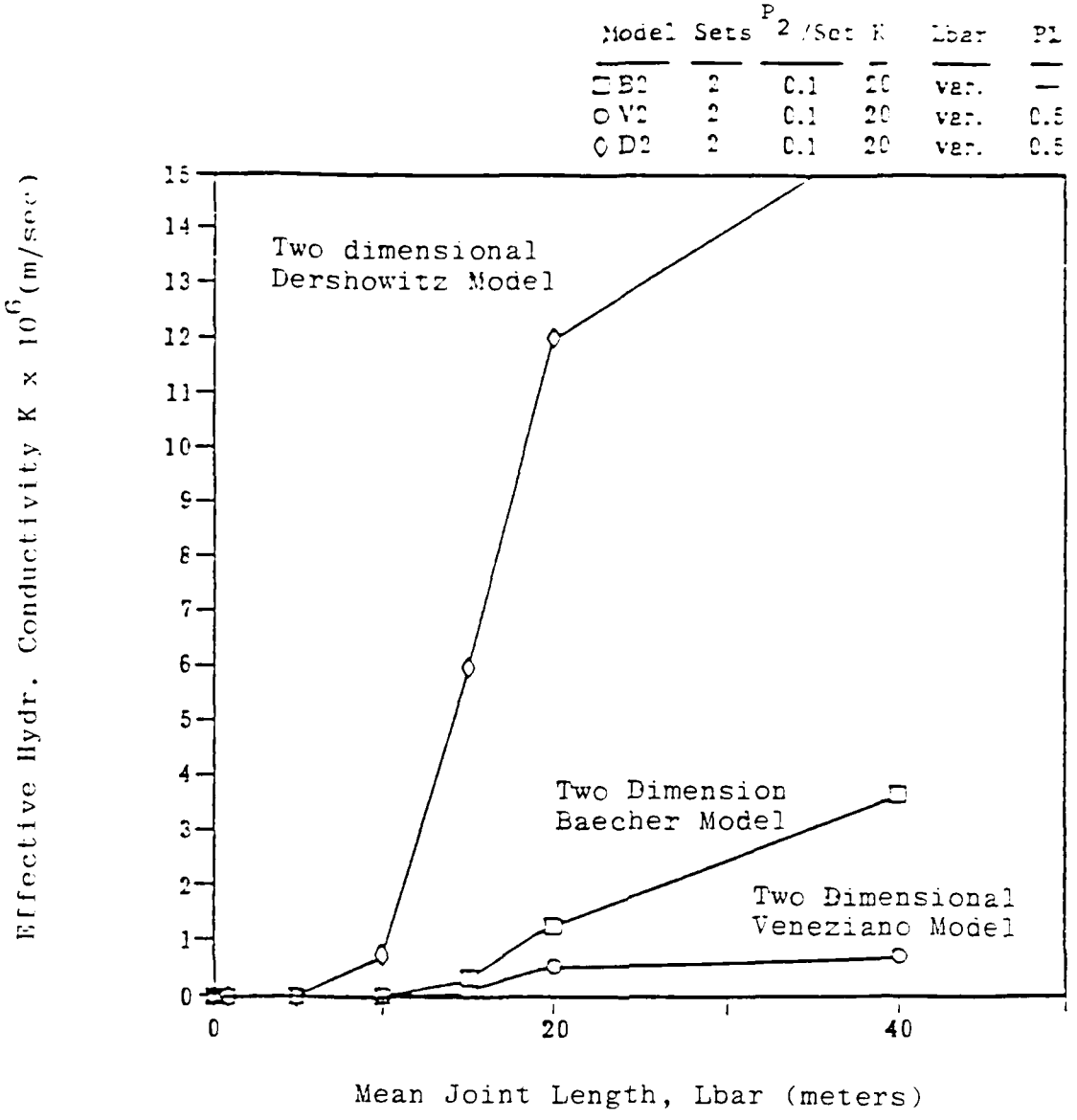

sets = number of joint sets

P_2/sets = persistence (trace length/area) for the set

K = dispersion factor for Fisher distribution

Lbar = mean joint length (or equivalent)

PL = length persistence (trace length/ total joint length)

FIGURE 2.9 RELATION BETWEEN EFFECTIVE HYDRAULIC CONDUCTIVITY AND JOINT SIZE: TWO DIMENSIONAL MODELS

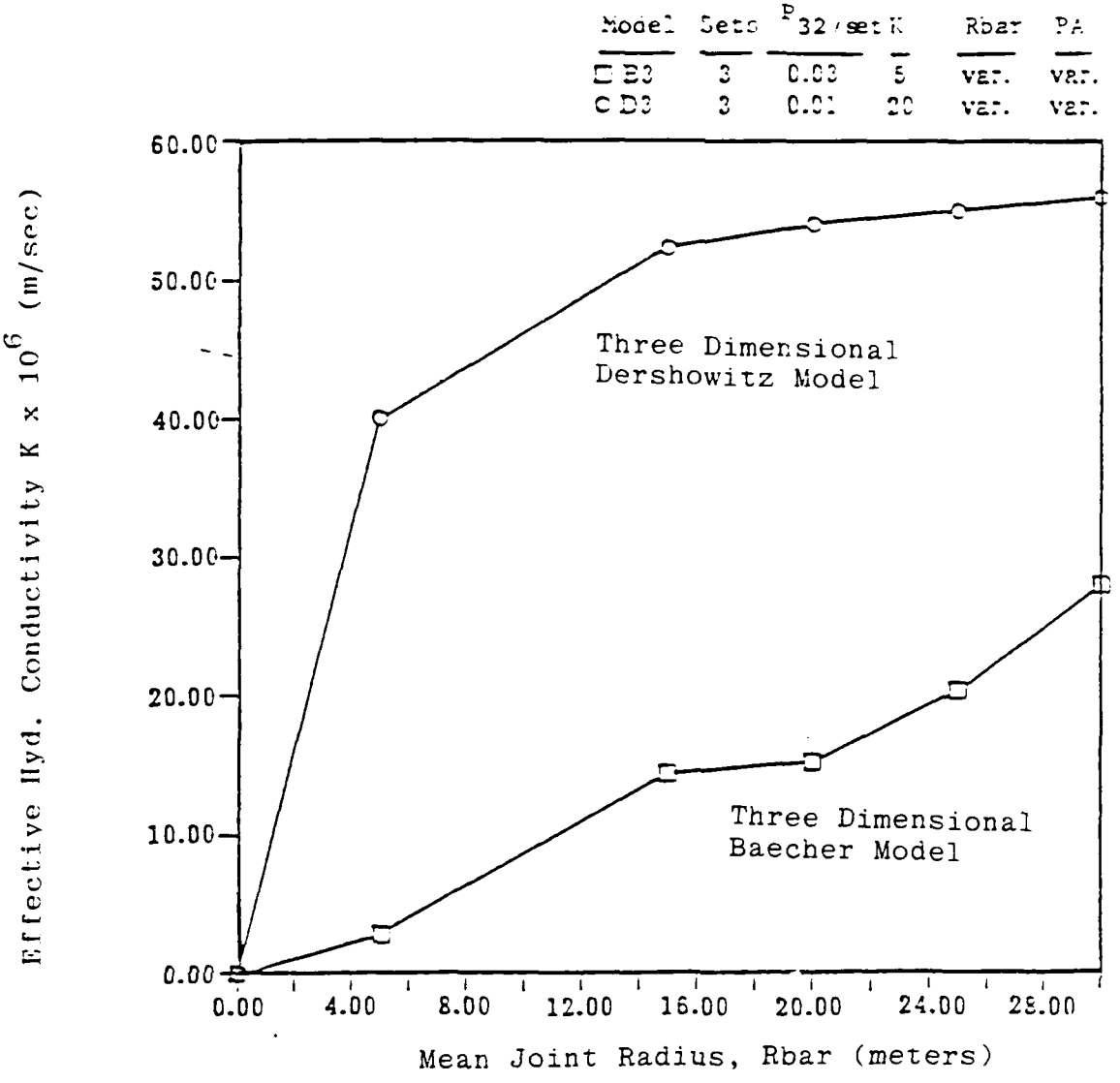

Sets = number of joint sets

P_{32}/Set = persistence (joint area/vol.) per set

K = dispersion factor for Fisher distribution

Rbar = mean radius (or equivalent)

PA = area persistence (joint per joint plane)

FIGURE 2.10 RELATION BETWEEN EFFECTIVE HYDRAULIC CONDUCTIVITY AND JOINT SIZE: THREE DIMENSIONAL MODEL

2.4 Hydrologic Applications of Joint System Models

By combining the joint geometry models whith a suitable model representing flow in jointed media one can determine the hydraulic performance of such media.

The flow of water through a system of joints is determined when the head along each individual joint is known and such that:

a) Laplace's equation is satisfied within each joint.

b) There are no jumps in total head along the intersections of two or more joints (i.e., where two or more jonts meet they have the same head).

c) Continuity is satisfied along the intersections of two or more joints (i.e., the sum of the influxes into two or more intersecting joints is zero along any segment of their line of intersection).

d) The conditions of no-flow through the free surface and zero piezometer head (assuming the atmospheric pressure to be zero) at the free surface are satisfied.

Such a distribution of heads throughout a system of joints can be found using a Finite Element approach.

A computer program for three-dimensional laminar flow through jointed rock was developed. It uses Finite Element discretizations of joints such that the Finite Element meshes of two or more intersecting joints share all nodes that lie on the line of intersection. The unknowns in this formulation are the heads at the nodes. The head at any point inside an element is obtained by interpolation from the heads at the nodes of the element. Laplace's equation is satisfied inside each element for any values of the head at the nodes, given an appropriate selection of element type (e.g., four node quadrilateral elements). The heads at the nodes are determined from the imposition of the requirement of continuity at the edges of the elements. If the problem involves a free

surface, iterations are necessary to determine the position of the free surface. Revising the Finite Element mesh in each iteration, as is commonly done for the solution of two-dimensional problems of free-surface flow through porous media, is inconvenient because here the elements are tied to the geometry of the joints. A scheme that does not involve mesh revisions is therefore used. The Finite Element joint flow model and the geometric joint system models were combined in the computer program package JINX. This was then used to develop some of the connectivity measures (Section 2.2 and 2.3) and to develop a number of hydrological applications. These applications can be summarized as follows:

- Scale effect: Groundwater can flow in individual joints only as far as the size of the joint. This results in a scale effect in which hydraulic conductivity is proportional to the intergral of the joint size distribution over all joints which are larger than twice the scale of interest (Figure 2.11). When the intersection of joints to form joint networks is considered, it is the size distribution of these networks (C_8) rather than the size of individual joints which controls flow at any scale (Figure 2.7). Figures 2.9 and 2.10 showed effective hydraulic conductivity for networks of disk (Baecher) and polygon (Dershowitz) joint system models. For both models, the effect of scale is pronounced: As the scale of the problem under consideration increases, the effective hydraulic conductivity rapidly decreases.

  The result shown in Figure 2.9 and 2.10 has practical applications for performance modeling of jointed rock. A major objection to the use of flow models is the difficulty of measurement of effective hydraulic apertures for joints. The shape of the curve in Figure 2.9, however, can be established from statistics of joint orientation, trace

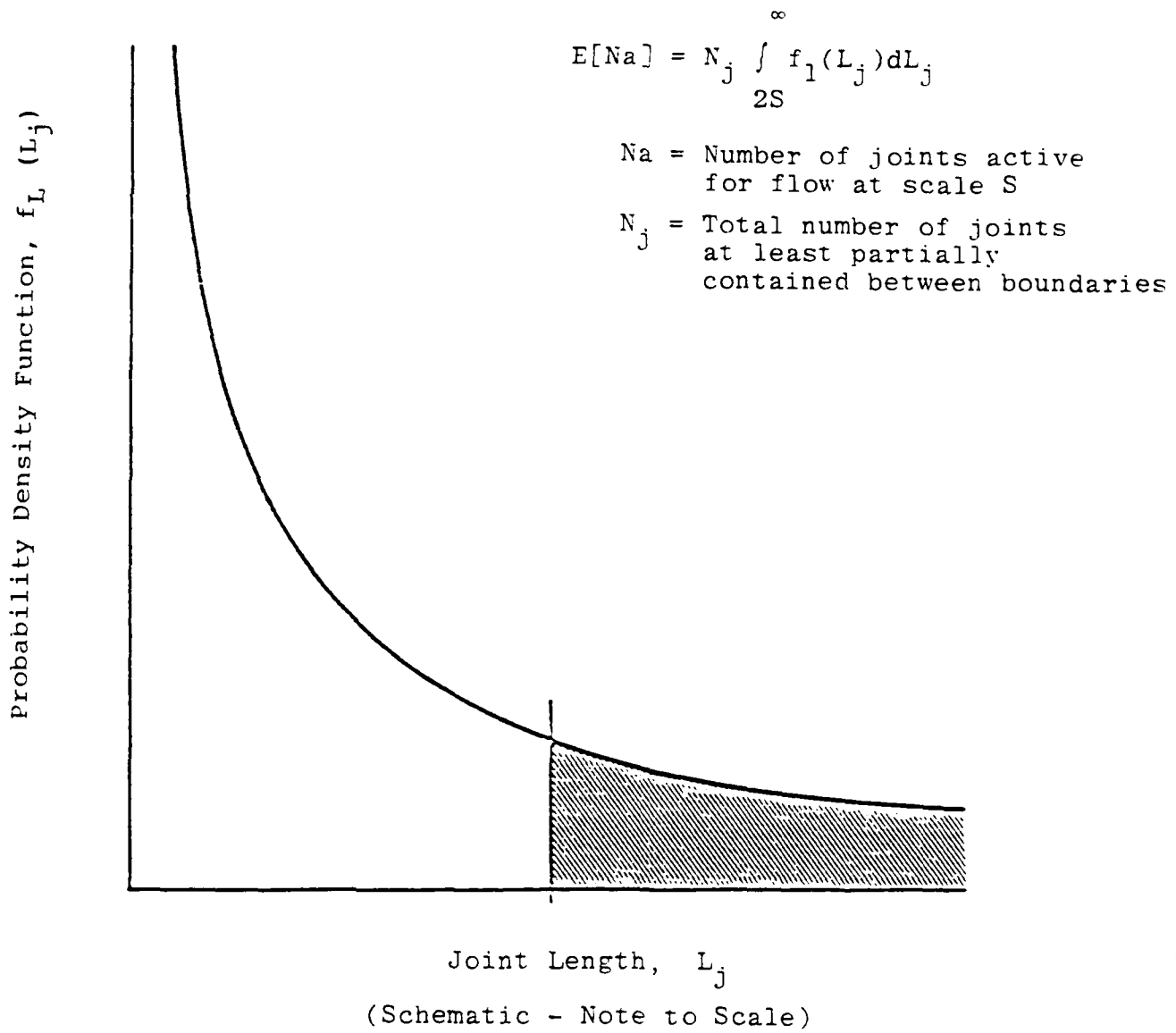

FIGURE 2.11 NUMBER OF JOINTS CONTRIBUTING TO FLOW IN RELATION TO SCALE

length, and intensity, which can readily be obtained from boreholes and mapping in outcrops and adits. The actual values on the ordinate (effective hydraulic conductivity) can then be obtained by performing hydrological tests at two or more scales and thus normalizing the curve. This allows one to make projections about the effective hydraulic conductivity at much larger scales.

- Anisotropy Effect: Just as the distribution of trace lengths of individual joints controls the scale at which flow can occur in individual joints, the distribution of joint orientation determines the anisotropy of flow in individual joints (Figure 2.12a). Similarly, for networks of interconnected joints, the anisotropy of joint system geometry determines the hydrological anisotropy (Figure 2.12b).

Figure 2.13 shows the first quadrant of permeability ellipses at scales of 2.5, 10 and 20 times the mean joint length for the Dershowitz joint system model with individual joint orientations distributed according to a Fisher distribution with very low dispersion. As a result, at a small scale, corresponding to the influence of individual joints, the effective hydraulic conductivity is highly anisotropic. At larger scales, however, joint networks control flow and the permeability ellipse indicates much less anisotropy.

This result has significant implications for the assessment of the hydrological anisotropy of jointed rock. The hydrological anisotropy of joint systems is scale dependent and depends strongly upon the formation of joint networks of interconnected joints. In situ tests used to evaluate anisotropy can only be used to predict anisotropy at the scale

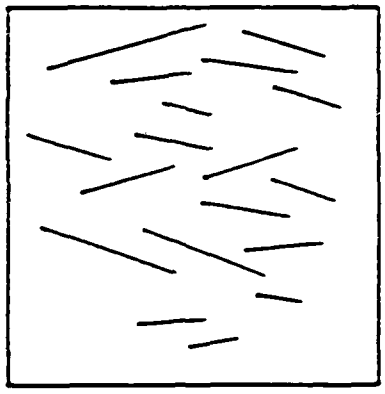

A) At scale of individual joints, anisotropy of flow is directly related to anisotropy of joint orientations

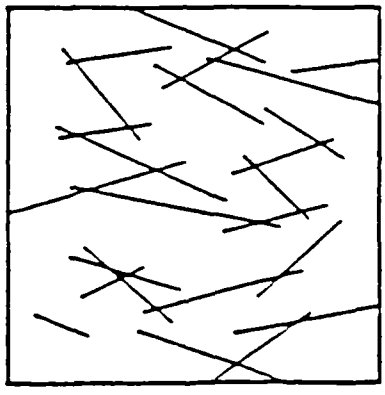

B) At scale of joint networks, joint orientation anisotropy may have less effect on flow anisotropy

FIGURE 2.12 SCALE EFFECTS ON JOINT SYSTEM ANISOTROPY

Model	Sp	Sets	P_2/Set	K	PL
D2	20	1	0.2	20	0.5
D2	5	1	0.2	20	0.5
D2	2.5	1	0.2	20	0.5

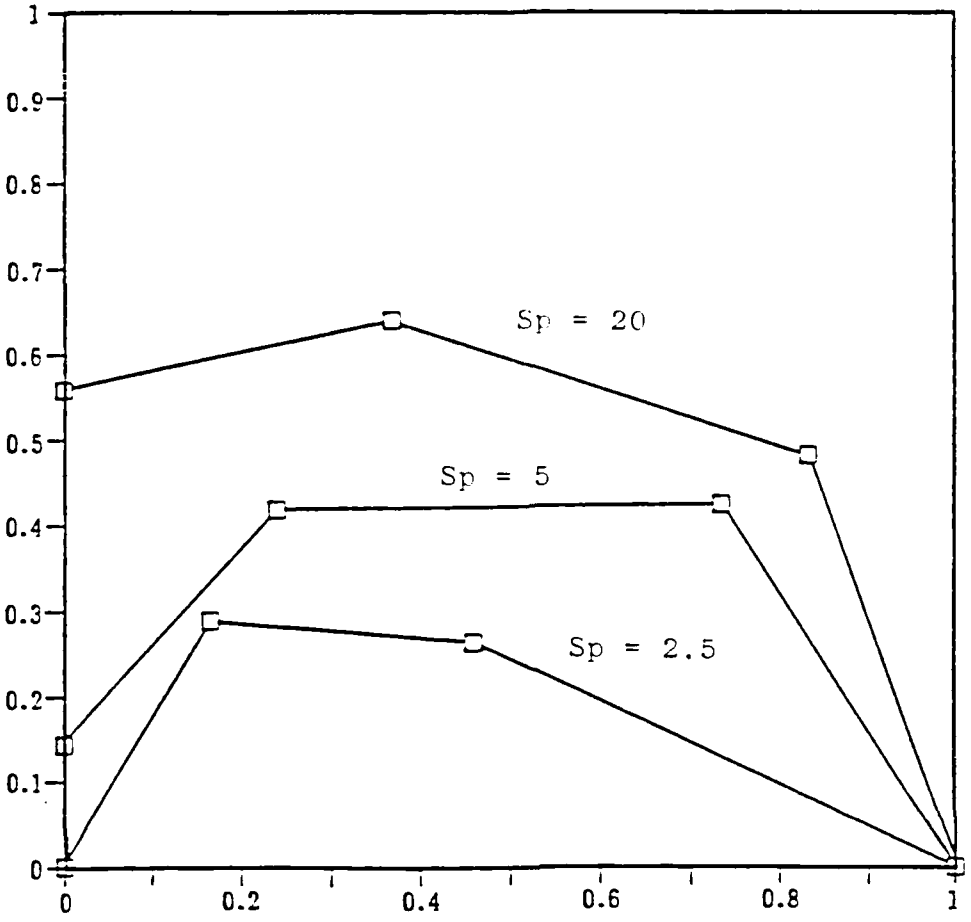

Ratio of Effective Hydraulic Conductivity to Effective Hydraulic Conductivity in x-Direction

Sp = ratio of the problem scale to the mean joint length

Sets = number of joint sets

P_2/Set = persistence (trace length/area) for the set

K = dispersion factor for Fisher distribution

PL = length persistence (trace length/total joint length)

FIGURE 2.13 PERMEABILITY ELLIPSES FOR 2-DIMENSIONAL DERSHOWITZ MODEL

at which they were run. In order to extrapolate these results to larger scales, joint system models must be developed and evaluated as in Figure 2.13.

- Aperture Effects: Many researchers (e.g. Long et al., 1983, Snow, 1968) have noted that since effective hydraulic conductivity is proportional to joint aperture cubed and the distribution of aperture is generally assumed to be lognormal, aperture uncertainty and variability tends to dominate all other effects in determining joint system hydrological properties.

  While this is correct for the case where all flow occurs in individual joints, it is not necessarily so for flow through networks of interconnected joints. At large scales, where flow occurs in series through interconnected joints with independent apertures, the variability of aperture has much less influence on hydrological properties than would be assumed based upon flow in single joints. This result is illustrated by the distribution of effective hydraulic conductivities for flow through joint systems of n joints with a lognormal aperture distribution (Figure 2.14).

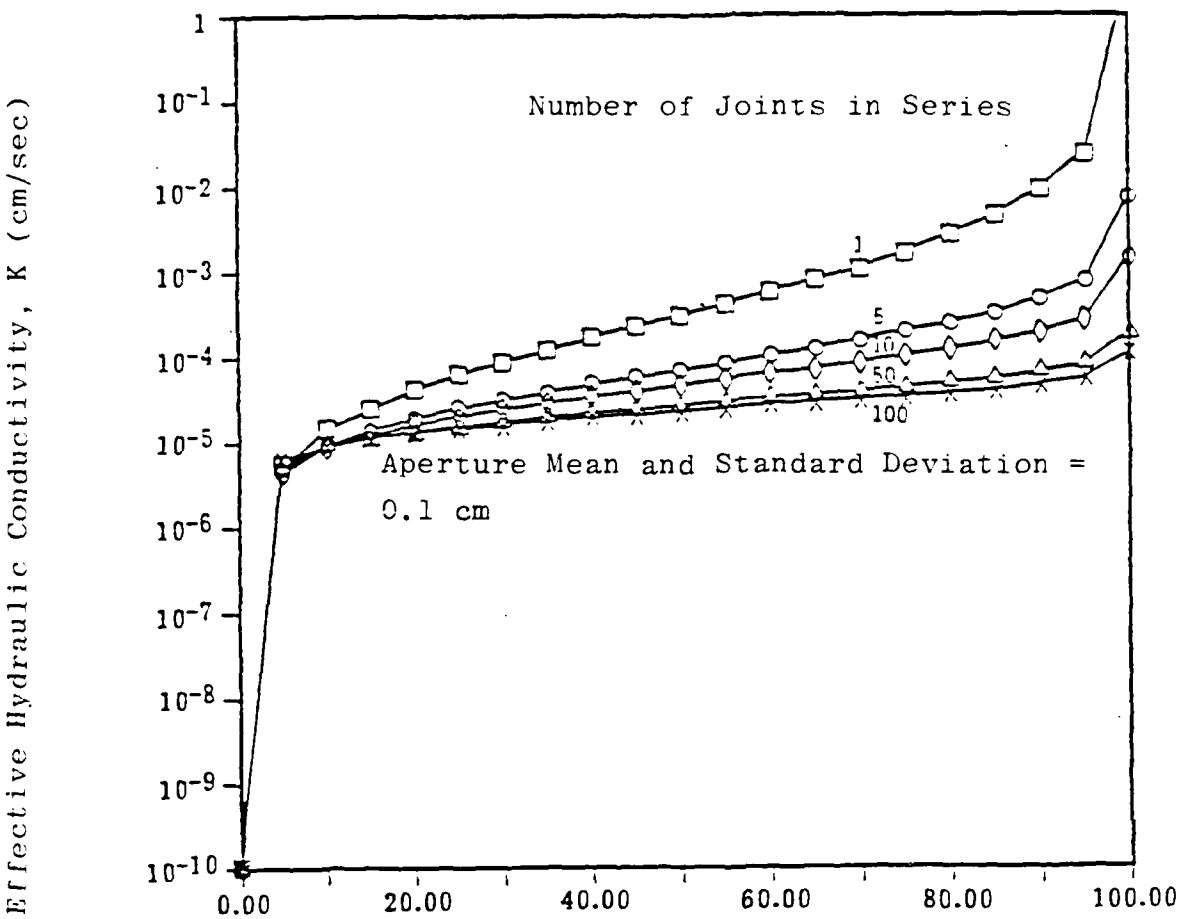

FIGURE 2.14 CUMULATIVE DISTRIBUTION OF EFFECTIVE HYDRAULIC CONDUCTIVITY, EFFECT OF INCREASING NUMBER OF JOINTS REDUCES EFFECT OF APERTURE VARIATION (APERTURES ASSUMED LOGNORMALLY DISTRIBUTED)

3. Coupled Flow-Deformation Analysis for Jointed Media

3.1 Background

In many engineering problems in jointed rock, deformation and, eventually, instability (failure) involve interaction between cleft water pressure in the joints and deformation of the joints. Closure or opening of the joints perpendicularly to their surface influences water flow and pressure in the joints. Similarly, increases and decreases of the water pressure in joints affect joint apertures. This interaction becomes more complex if joints displace along their surface (in shear); the usual associated asperity interaction and dilatancy effects can affect joint aperture. Also, joint fillers add to the complexity of the problem.

A method of analysis which can treat the interaction of joint deformation, cleft water pressure, and flow is needed when designing structures in and on rocks and also for gaining a more basic understanding of jointed rock mass behavior from a geologic point of view. The method should also be useful when interpreting monitoring instrumentation. For instance water pressure and deformation in rock masses can be measured. With an appropriate analysis method inferences on the state of the rock mass, particularly in relation to instability, can be drawn from the data. This will make it possible to integrate monitoring into design which is required in the application of advanced "observational" or "adaptable" design methods; in such approaches the design is optimally adapted to encountered conditions, eliminating unnecessary conservatism.

A variety of continuum and discontinuum methods exist for rock mass deformation and failure, and flow. In an initial phase of the research it was decided, based on an extensive review of available approaches, that discontinuum methods had to be used for both the deformation and the flow analysis.

Continuum approaches are ill suited to treatment of large relative displacements as they occur in joints. Equivalent porous media approaches are often unrepresentative when analyzing jointed media as was explained in Chapter 1 of this Executive Summary. Consequently the so called rigid block or distinct element method (Cundall 1971, 1974) was chosen to model deformation and it was decided to couple it with a discontinuous flow model.

3.2 Coupled Flow Deformation Analysis

3.2.1 Deformation Analysis

In the Rigid Block Method, the rock mass is assumed to consist of separate blocks touching each other at a discrete number of contacts where elastic, frictional and viscous forces are applied.

Two types of initial, i.e. before any displacement, block configurations are possible in the computer code developed here, as shown in Fig. 3.1. The configuration in Fig. 3.1a simulates two fully persistent joint sets of arbitrary (but constant for each joint) orientations and spacings. The configuration in Fig. 3.1b simulates two joint sets of arbitrary (but constant for each joint set) orientations and spacings, one joint set being fully persistent and the other having a persistence of fifty percent. From these basic assemblies any shape of a real jointed rock mass, e.g., a slope or the rock mass around a tunnel can be created. Larger or irregularly shaped blocks are also possible, provided that they can be formed by combining elementary blocks configured as shown in Fig. 3.1.

In the distinct element method the blocks are considered rigid, but the joints are considered deformable, i.e. all deformations are represented as joint deformations. This is a reasonable assumption for most rock mass applications. Deformations of the rock may occur by relative displacement of the rock blocks as shown in Fig. 3.2. Reactions (forces) at the contacts are

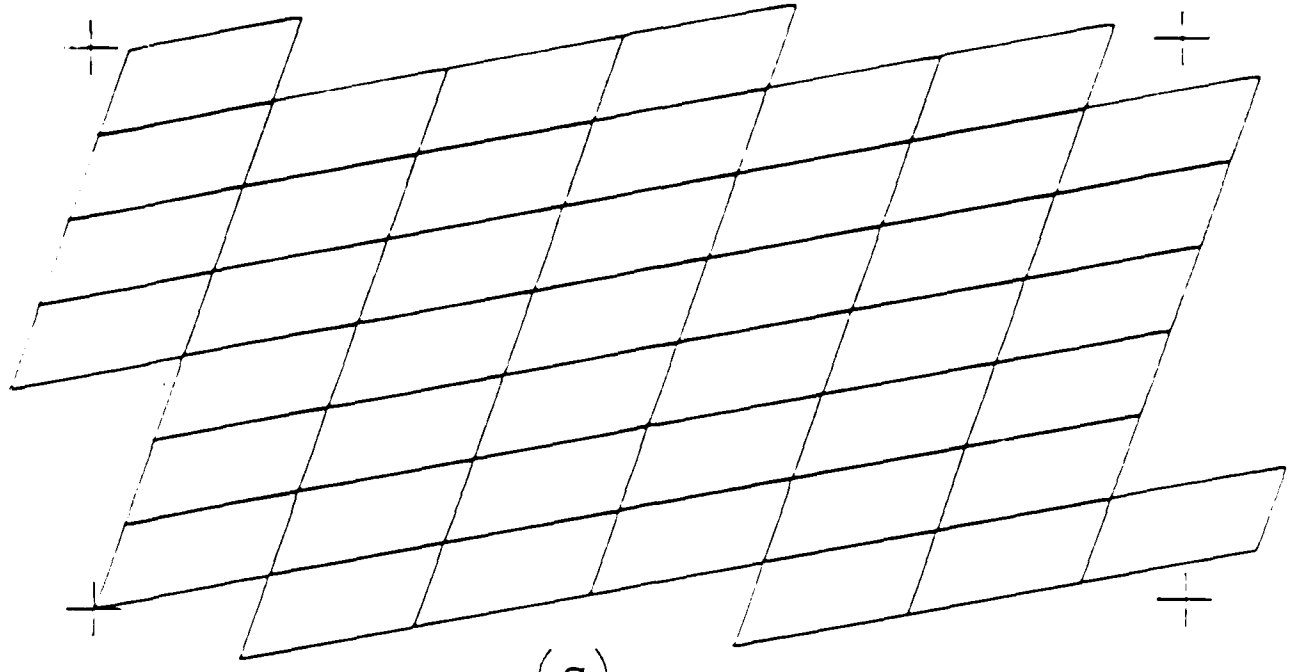

(a)

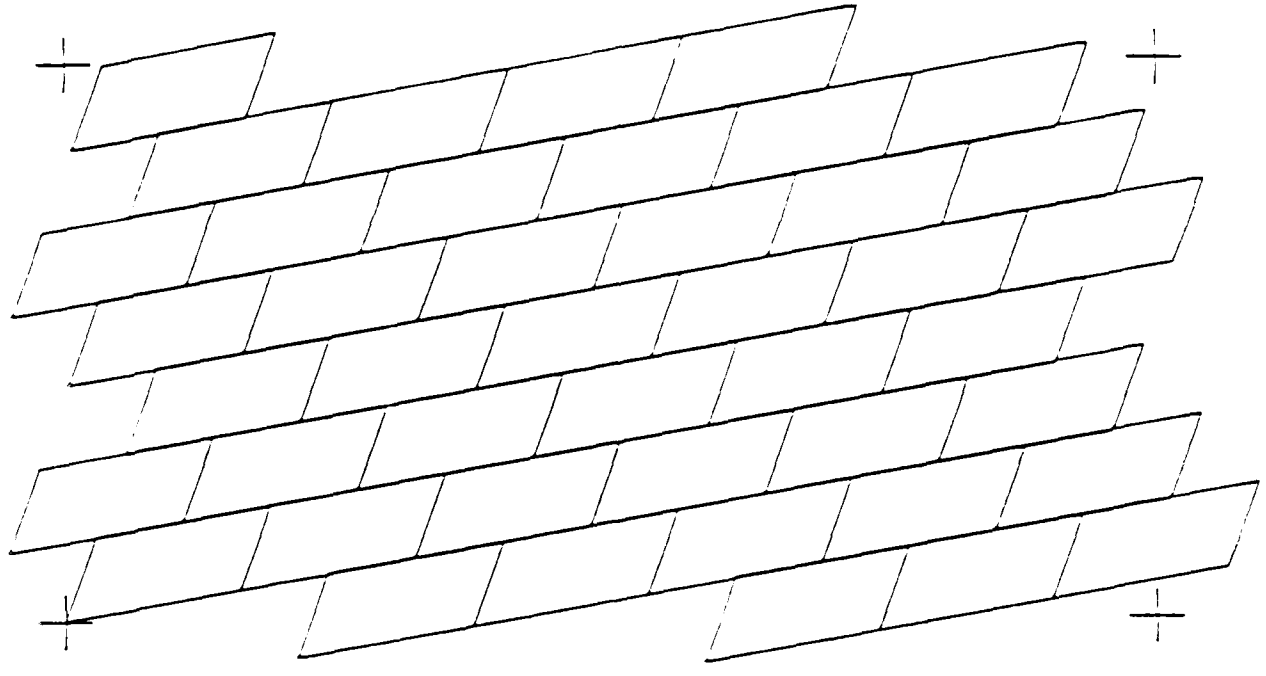

(b)

FIGURE 3.1 BLOCK CONFIGURATIONS THAT CAN BE MODELLED. BLOCKS CAN BE COMBINED TO FORM LARGER AND IRREGULARLY SHAPED BLOCKS.

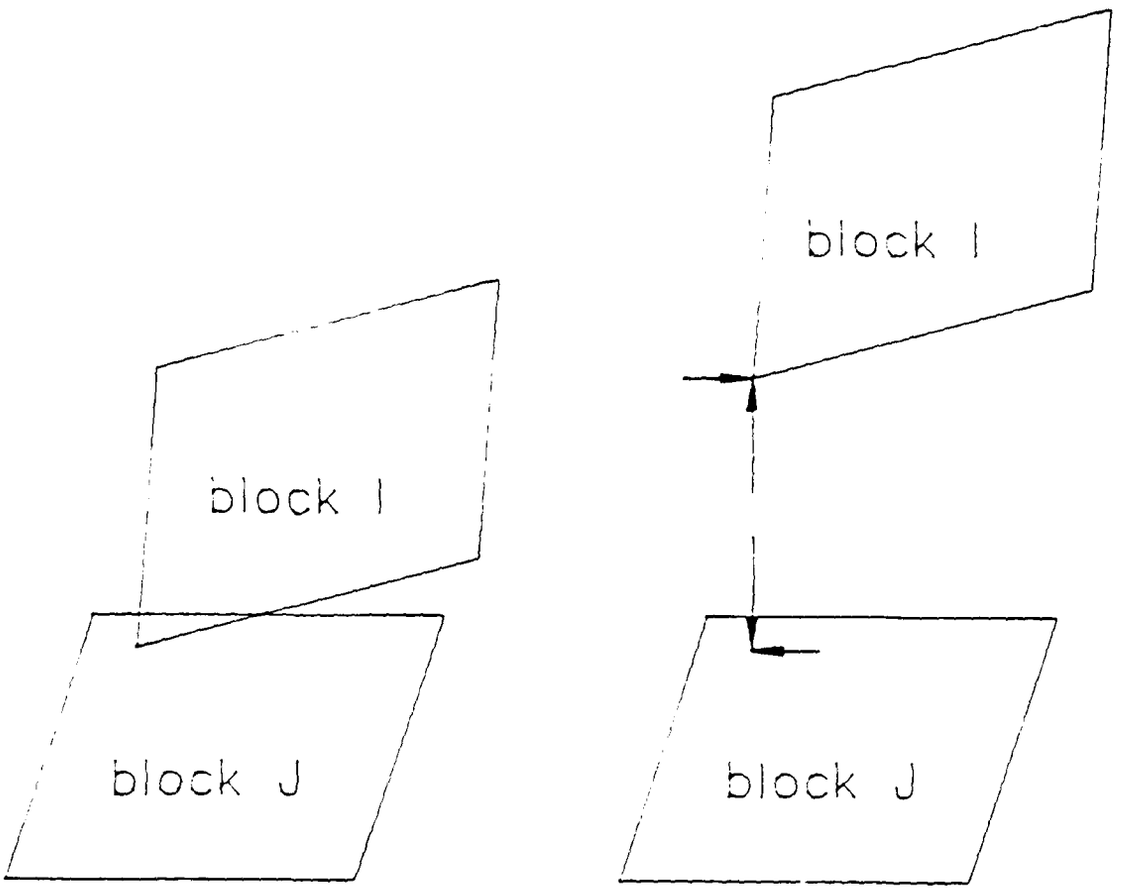

FIGURE 3.2 RELATIVE DISPLACEMENT OF ROCK BLOCKS

obtained from the penetration or separation at contacts through the application of appropriate deformation laws. These can include time dependent behavior or the interaction with fillers. Deformation analysis by dynamic relaxation proceeds in time steps, evaluating at a series of successive instants the forces acting on each block (its own weight, the reactions of neighboring blocks, and water forces). These forces determine the acceleration of each block, which is then integrated to find the displacement increment during the time step under consideration. This procedure is essentially that of Cundall (1974) with the modifications described in 3.3.2 and 3.3.3 below.

3.3.2 Flow Model

Flow is modeled as taking place within a network of conduits corresponding to block sides (which can be thought as pipes) meeting at a number of 'nodes' corresponding to block corners. In modeling flow the changes in the joint apertures that are produced by the deformation model are taken into account. However, except for changes in apertures, the flow algorithm assumes that the geometry does not change during deformation. This is equivalent to assuming that flow takes place in a network of conduits of varying cross-sections but of constant lengths and positions in space. Therefore, the geometry of this flow network depends on the initial position of the blocks, and subsequent changes affect only apertures. This apparent disparity between the flow and the deformation algorithm is justified by the fact that the flow variables (e.g., heads, pressures) are much more sensitive to aperture changes than to changes in the locations of nodes.

The solution of the flow problem is standard. Laminar flow is assumed; flow in joints with fillers described by Darcy's law and for open joints by the

Poiseuille relation

$$q = \frac{a^3 g}{12\nu} i$$

(where q = flow per unit width, a = aperture, g = acceleration of gravity, ν = kinematic viscosity, i = head loss per unit length). Flow in joints is obtained from heads at the nodes and by satisfying continuity conditions at the nodes. To make the problem determinate, heads of some nodes need to be given as boundary conditions.

This procedure is complicated if a free surface is involved. In the model solution procedure, an assumption is made as to which nodes are included in the flow region. Given the heads at some of them, it is possible to solve the set of equations obtained by applying the condition of continuity at nodes where head is unknown and thus to determine these unknown heads. Based on these heads it is possible to check, and if necessary, update the assumption about which nodes participate in the flow. After making these corrections, heads at nodes included in the flow are computed again. The same procedure is repeated until the assumed position of the nodes relative to flow does not change.

While the flow problem is solved iteratively in this manner, block positions remain unchanged. Figure 3.3 shows how a joint's aperture used for flow computations is related to the joint deformation as described by the Block Method. Clearly, raw deformation data from the Rigid Block Method are inappropriate for studying flow, since the Rigid Block Method accepts overlapping of a joint's faces. Therefore, "rigid block" apertures, which can be positive or negative, are converted to "real" apertures, which are always positive and can be used in modeling flow in jointed rock.

3.2.3 Coupling

Coupling is handled through an iteration of:

1. Obtain joint apertures from deformation analysis.

MODELLING OF DEFORMATION

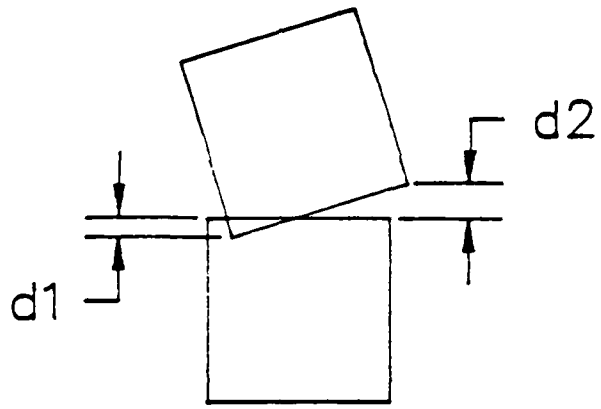

(here $d1<0$, $d2>0$ by convention)

CONVERT d TO a:

$$a = a_{inf} + (a_0 - a_{inf})\, e^{\frac{d}{a_0 - a_{inf}}}$$

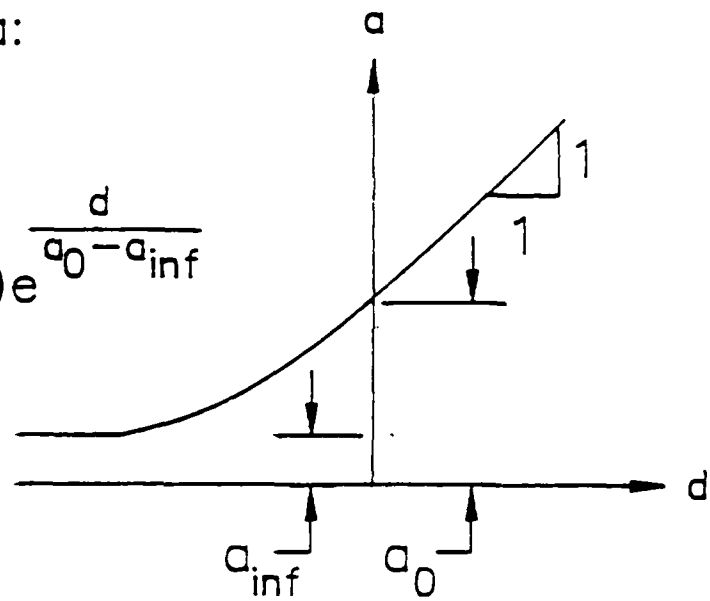

MODELLING OF FLOW (blocks in initial position, aperture adjusted for deformation)

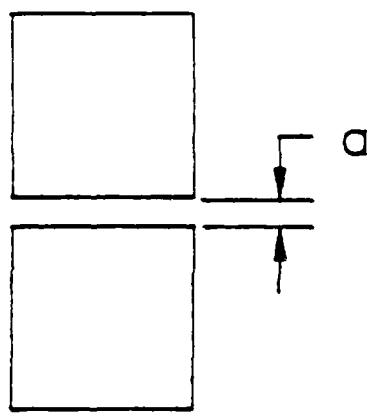

FIGURE 3.3 RELATIONSHIP BETWEEN RIGID BLOCK DEFORMATIONS AND FLOW APERTURES

2. Determine flow and pressure in joints from flow model.

3. Modify forces acting on blocks based on Step 2.

4. Step 1.

3.2.4 Computer Code

The Computer Code RGDBLK was developed for the coupled flow-deformation anlaysis.

Emphasis was placed on making the computer program user-friendly; it incorporates routines for automatically setting up the geometry of a problem (e.g. a rock slope) and its boundary conditions for flow with a minimum of information from the user (e.g. joint orientation and spacing, position of the water table, etc.). The program is interactive, making use of a video screen, and lets the user intervene in the solution process. For example: one can model the initial state of stress under no-flow (hydrostatic) conditions prevailing before a rock slope is excavated, followed by modeling the "excavation" of the slope by removing some of the blocks, and finally, modeling the coupling of flow and deformation as the rock slope deforms. The user can control the iterative solution procedure through several parameters such as the size and number of time steps and the degree of coupling between flow and deformation (that is, the frequency with which updated information about deformation should be used to update flow forces or vice versa). The output of the program is in the form of plots of block displacements at various instants, of information about the water-head field at various instants, and of information about forces and displacements at particular blocks.

Due to its considerable flexibility, this computer program can be used either for modeling particular situations occuring in practice and thus serving

as a design tool, or to simulate the behavior of jointed rock masses in a more general manner, thus serving as a research tool.

3.3 Case Studies

The flow deformation model is applied to three typical cases of rock mass behavior, a rock slope, a well in a jointed mass and a dam and reservoir on a jointed mass. In all three cases extensive parametic studies were conducted. In the Sections below only one typical example will be presented, followed by a summary of the parametric study results, the details of which are presented in Volume II.

3.3.1 Slope in a Jointed Rock Mass

The geometry of the problem is shown in Fig. 3.4 After excavation, the water levels are assumed to be in the positions marked A and B, the position B representing an open crack. (It should be noted that simultaneous excavation and lowering of the water table can also be investigated.) The phreatic surface and water pressure distribution between these two points was then determined using the coupled model and other approaches. The coupled model provides displacements in addition to flow results. In addition to calculating the displacements and water pressure distributions, the latter were used for a comparison study. "Standard", triangular, trapezoidal or rectangular water pressure distributions are assumed in the critical joint. The stability of rock mass above this joint was determined using limit equilibrium analysis with these pressure distributions and those obtained from the coupled model.

Three different cases have been studied with the coupled model. The first two allow one to compare the model with other models. The third makes full use of the coupled model's capabilities:

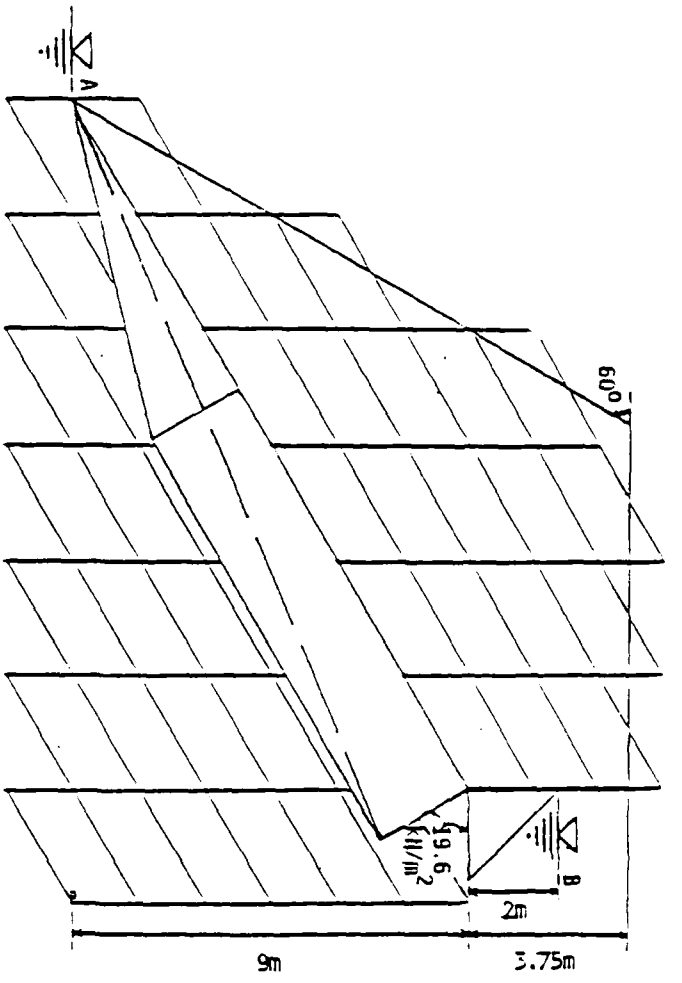

FIGURE 3.4 GEOMETRY AND ASSUMPTIONS FOR ANALYSIS OF SLOPE IN JOINTED ROCK MASS

1. Assume joints of identical aperture throughout the slope, and model flow. (This is equivalent to a pipe network approach).
2. Assume deformation due to excavation takes place and different joint apertures result (smaller in zones of higher stresses). Flow is then modeled through these joints but no coupling is introduced. This, in essence, represents a study that one could do using two separate models, first one to determine displacements and then a discrete flow model to determine water pressures in the deformed model.
3. Assume coupling of apertures and flow.

Figure 3.5 shows the deformed mass after excavation, but without flow. The joint overlaps indicate that aperture changes will have a significant effect on flow patterns and thus pressures. Figure 3.6 presents water pressure distributions in the "critical joint" that were obtained in the three above mentioned cases studied with the coupled flow model.

These pressure distributions should be compared with the "usual" assumptions in Fig. 3.4. (The critical joint is that used in the standard limit equilibrium analysis.) The pressures with the equal size pipe network in case 1 are greater than with the usual assumptions (Fig 3.4) but smaller than in deformed joints in case 2 (different size pipe network). This pressure increase was to be expected given that joints close under increased stresses. When coupling is introduced in case 3 the water pressure tends to open the joints and thus causes a pressure decrease compared to case 2. These results are specific to the case studied and should not be generalized.

The effect of these differences in pressure distribution on slope stability was quite significant. The required friction angles for the slope in Fig. 3.4 to be stable are:

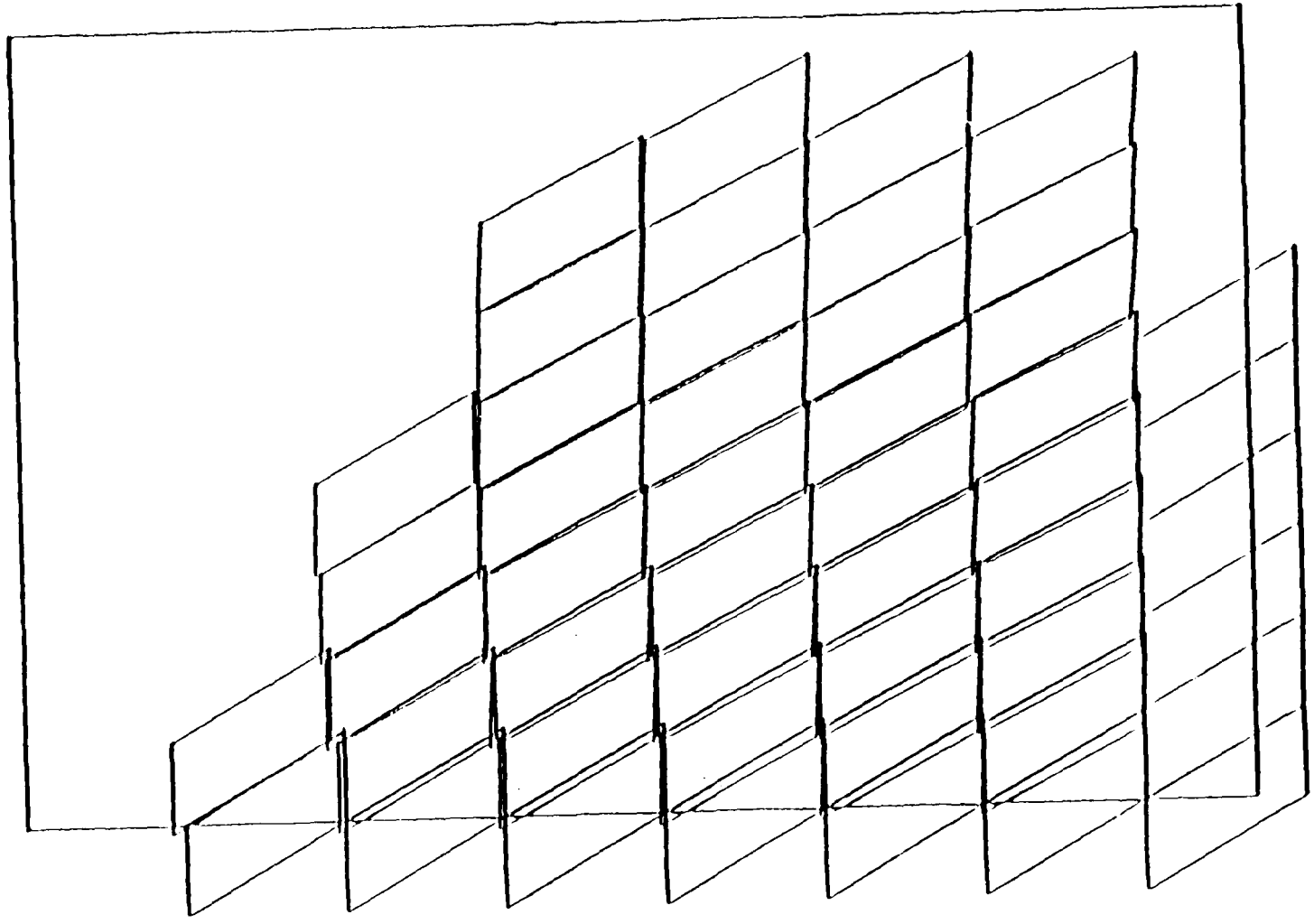

FIGURE 3.5 DEFORMATION (EXAGGERATED) OF ROCK MASS AFTER EXCAVATION WITHOUT FLOW

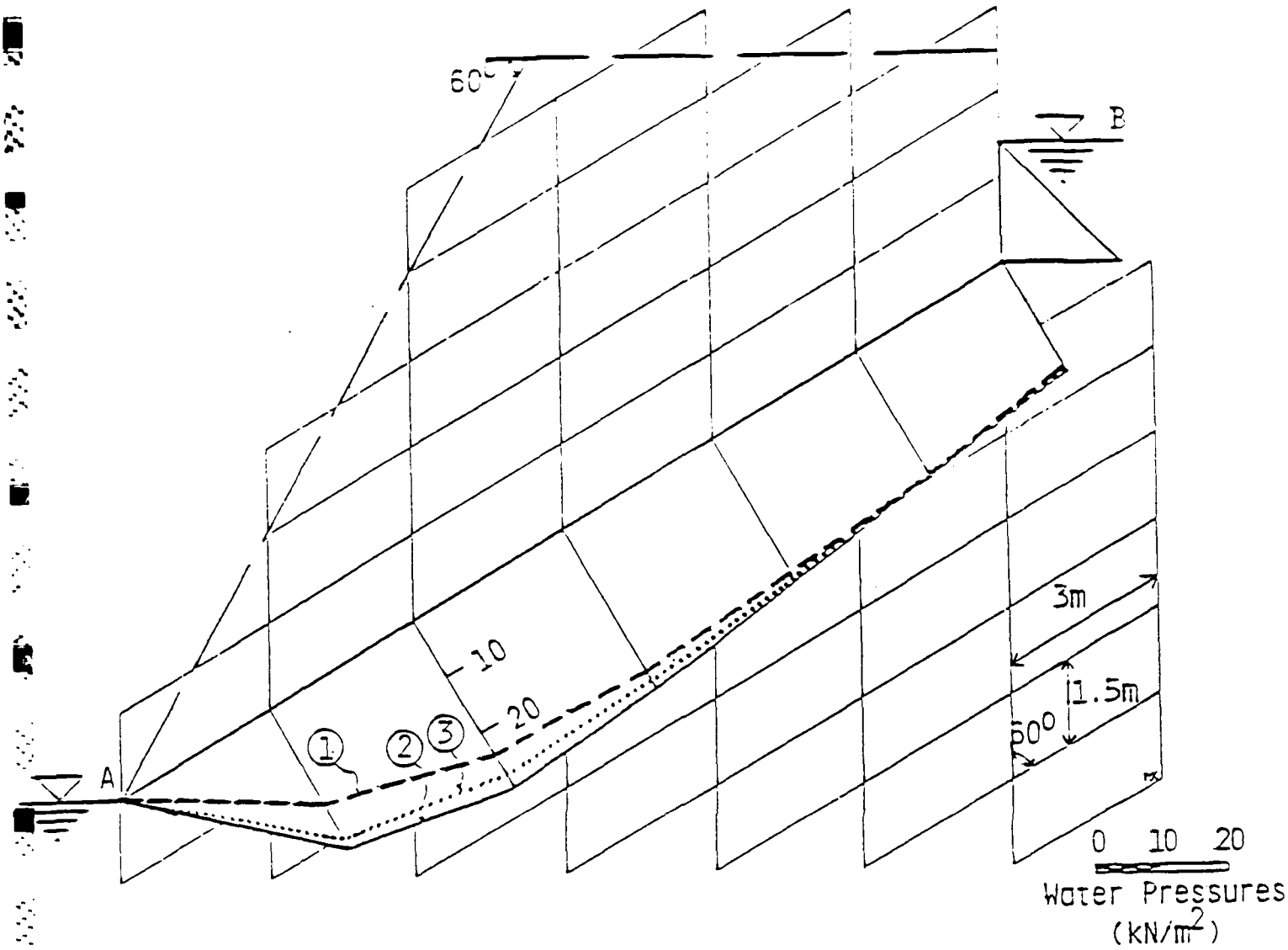

Key:

1. Joints with equal apertures
2. Joints with apertures changed by deformation
3. Coupled case

FIGURE 3.6 WATER PRESSURE DISTRIBUTIONS IN "CRITICAL JOINT" FOR CASES REFERRED TO IN THE TEXT

Triangular Pressure Distribution: 34°
Trapezoidal Pressure Distributon: 37°
Distribution in equal size pipe network: 39°
Distribution in different size pipe network: 41°
Distribution in coupled case: 40°

These results show that the usual assumptions may be unconservative in some cases. This is especially true for local instability where individial blocks become unstable.

A series of parametric studies was also carried out in which the friction angle and the joint parameters relevant to conductivity of water were varied. By considering different friction angles, the appropriateness of the method for predicting failure was established; moreover, patterns of numerical behavior corresponding to stable or failing cases were identified. By considering different values for the parameters affecting conductivity it was possible to study situations where coupling is more or less important. As might have been expected, the less uniform the apertures of the joint network were, the more pronounced was the effect of coupling. Although in real cases there may be considerable uncertainty regarding the conductivity properties of the joints, it is usually possible to estimate an upper bound of coupling influence for particular cases.

3.3.2 Well in a Jointed Rock Mass

Injection or withdrawal of water in a jointed rock mass causes displacements of blocks, increasing and decreasing joint apertures and water pressures. This is again a case where coupling of flow and deformation seems to be necessary. Fig. 3.7 shows the displacements of blocks caused by an injection in the center. Again the comparison of pressures along the center joint reveals important information. Fig. 3.8 shows pseudo-equipotentials (also lines of constant pressure in this case) under the assumption of uniform apertures (a), and when changes in

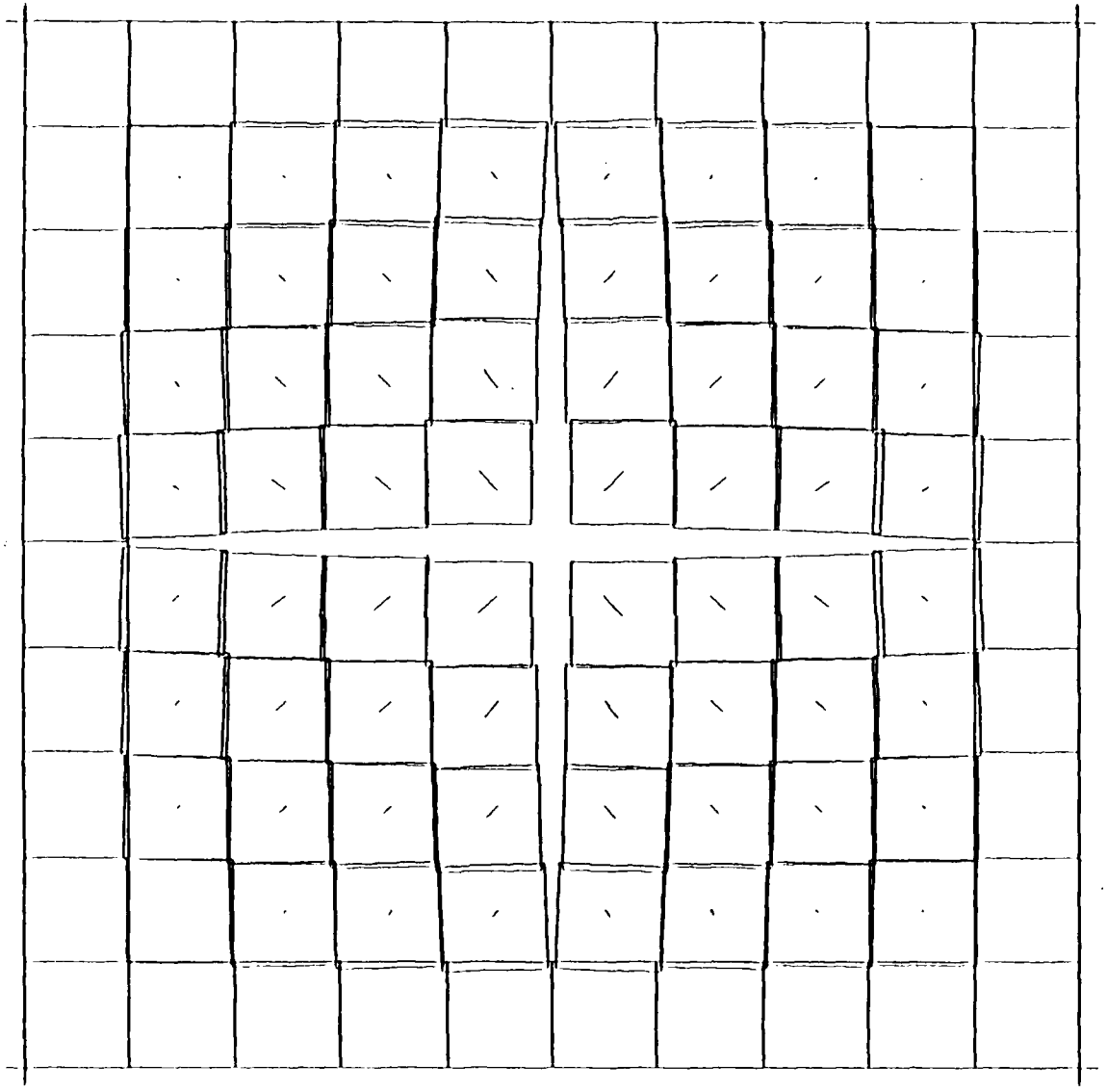

FIGURE 3.7 BLOCK DISPLACEMENTS (EXAGGERATED) ACCOMPANYING INJECTION OF WATER IN A WELL AT THE CENTER OF A HORIZONTAL ORTHOGONAL JOINT SYSTEM

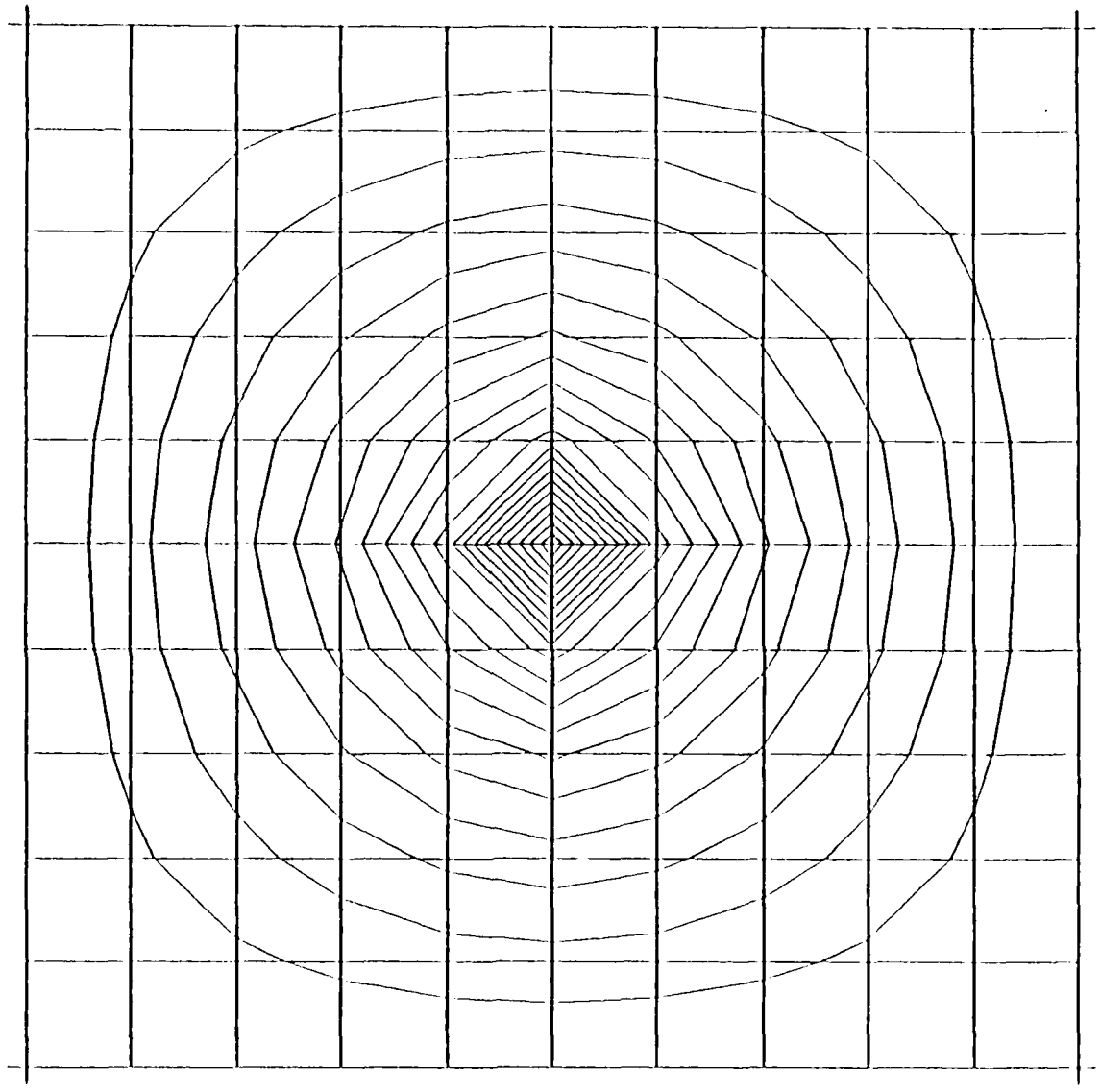

FIGURE 8A PSEUDO-EQUIPOTENTIALS AROUND WELL IN NETWORK OF JOINTS OF EQUAL APERTURES

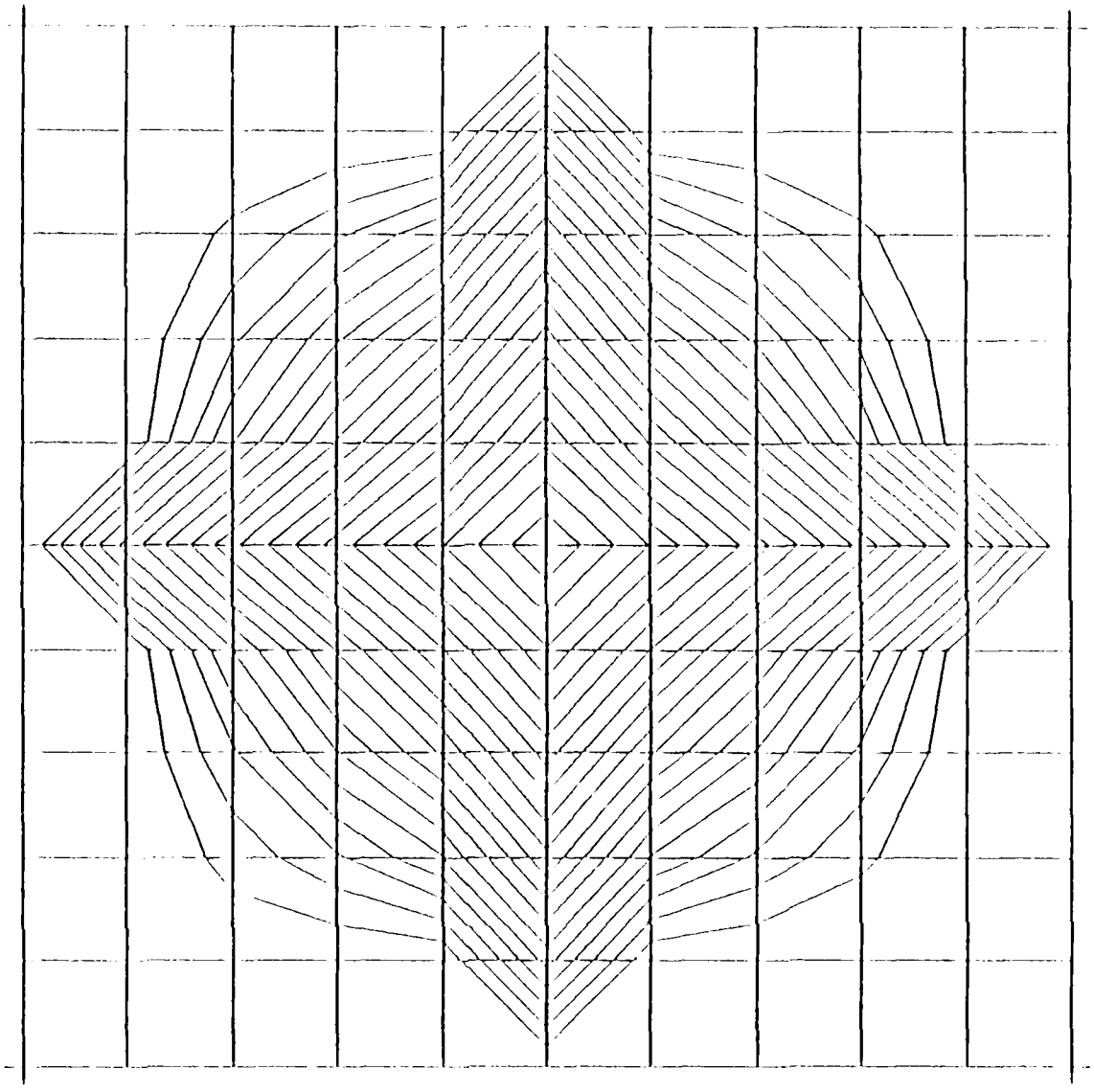

FIGURE 3.8B PSEUDO-EQUIPOTENTIALS AROUND WELL IN NETWORK OF JOINTS DEFORMED BY FLOW/DEFORMATION COUPLING

apertures due to coupling are considered (b). Corresponding flow rates are 0.95 x 10^{-5} m^3/sec and 4.53 x 10^{-5} m^3/sec. In this example, taking into account joint deformations has a pronounced effect and a coupled analysis gives different results from an uncoupled one.

As in the case of the slope, parametric studies were carried out varying the parameters affecting joint conductivity. More pronounced coupling effects correspond to parameter values associated with less uniform apertures in the joint network. It was also attempted to simulate observed behavior of well tests. In particular, the coupling of the response of the head at the well to the application of flow rates that are step-wise functions of time were simulated. This was accomplished with good results.

3.3.3 Dam and Reservoir on Jointed Rock Mass

Flow of water from the reservoir through jointed rock under the dam (Fig. 3.9) contributes to water loss and has therefore negative economic consequences. Water pressure distribution under a dam has significant effects on dam stability. Drainage and grout curtains are used to control pressure buildup and flow.

While a number of seepage flow and water pressure measurements under dams have been conducted, there is a lack of analytical approaches for flow and pressure prediction. This is true for jointed rock (see Chapter 2 of this Executive Summary), particularly for cases where water pressure and joint deformation strongly interact. This situation has become acute through the recognition that in many concrete dams the joints open up on the upstream side leading to pressure increases both at depth and possibly under the dam itself. This opening of joints is caused by the downstream displacement of the dam. This same displacement can also close joints downstream of the dam and effectively lead to high water pressures in the downstream ground with negative consequences on stability.

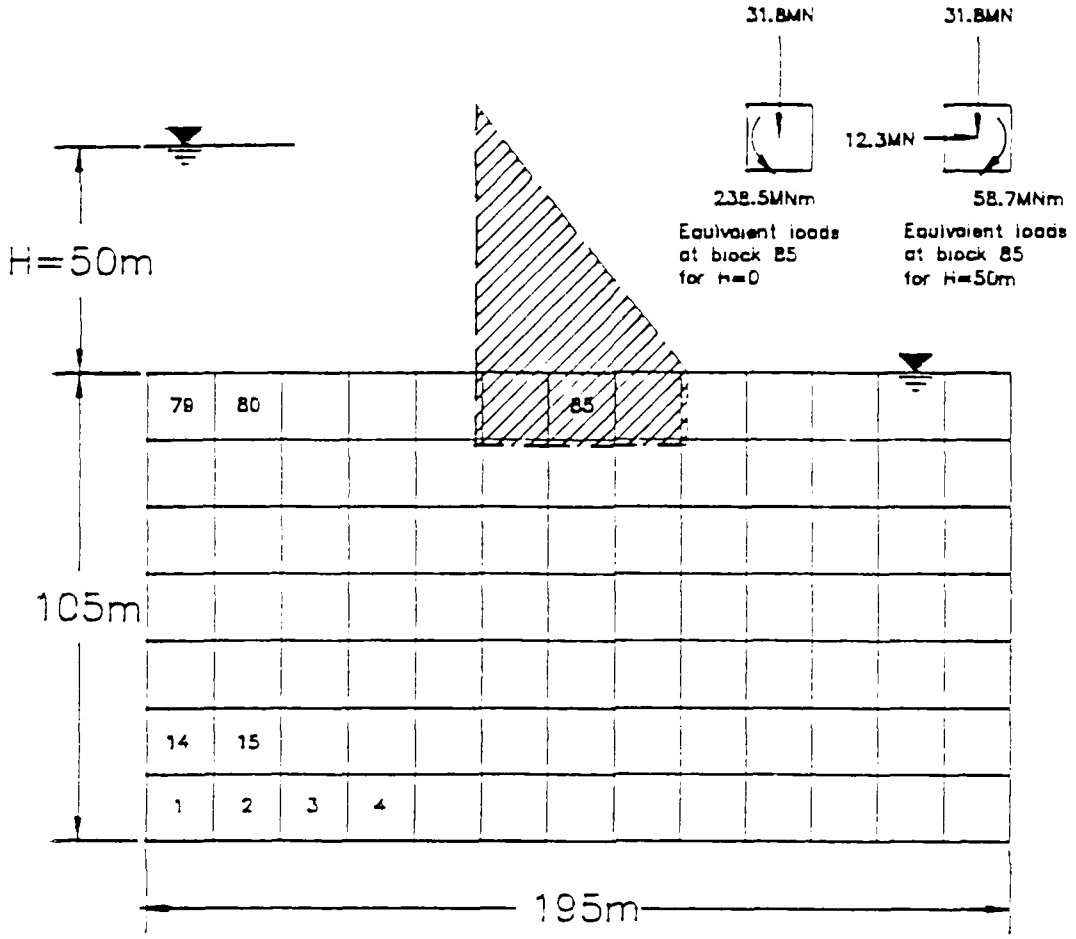

FIGURE 3.9 DAM GEOMETRY

The dam parametric study was conducted to shed light on these issues. The following variables were studied:

- Existence (or non existence) of grout curtain or drainage curtain.
- Effect of length of these curtains.
- Joint filler existence and characteristics.
- Joint aperture.

and as before,

- Uniform pipe network flow, deformed pipe network flow, coupled flow-deformation.

In Fig. 3.10 and 3.11 a case without drains or grout curtain is shown for the uniform apertures (pipe network) and coupled conditions respectively. Clearly coupling effectively opens the upstream joint and this leads to full reservoir pressure under the upstream corner of the dam. The displacements (Fig 3.10, 3.11) reveal that such a joint opening does indeed occur, it is also apparent in the "uniform pipe network" case but is much more pronounced when coupling is introduced.

In Fig. 3.12 the no drain - no grout situation is compared to a grout curtain case (for coupled conditions). A grout curtain pushes the pressures to higher values at depth where a greater pressure gradient occurs. It is basically advantageous to have larger gradients (and higher absolute values) at greater depth. Also the pressure under the toe (tail end) of the dam is less than in the no grout -no drain case. With a drainage curtain (not shown) the expected complete pressure drop (to the tailwater level) occurs at the upstream corner of the dam, where the drainage curtain is in contact with the dam.

While the upstream joint opening has important effects, the closure of downstream joints is such as to not greatly affect the downstream pressure distribution and magnitudes.

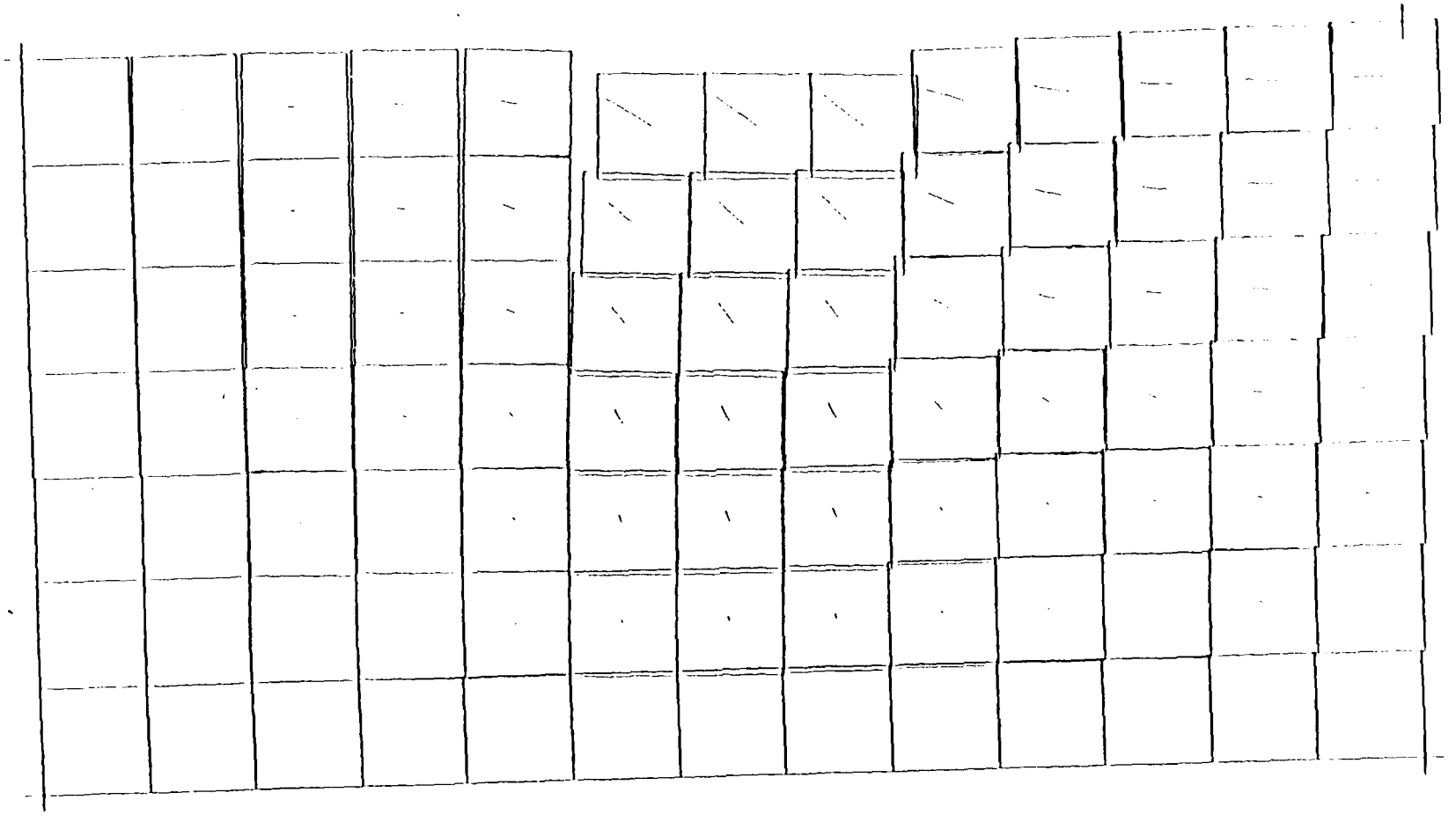

FIGURE 3.10 DISPLACEMENTS (EXAGGERATED) UNDER DAM WITHOUT COUPLING

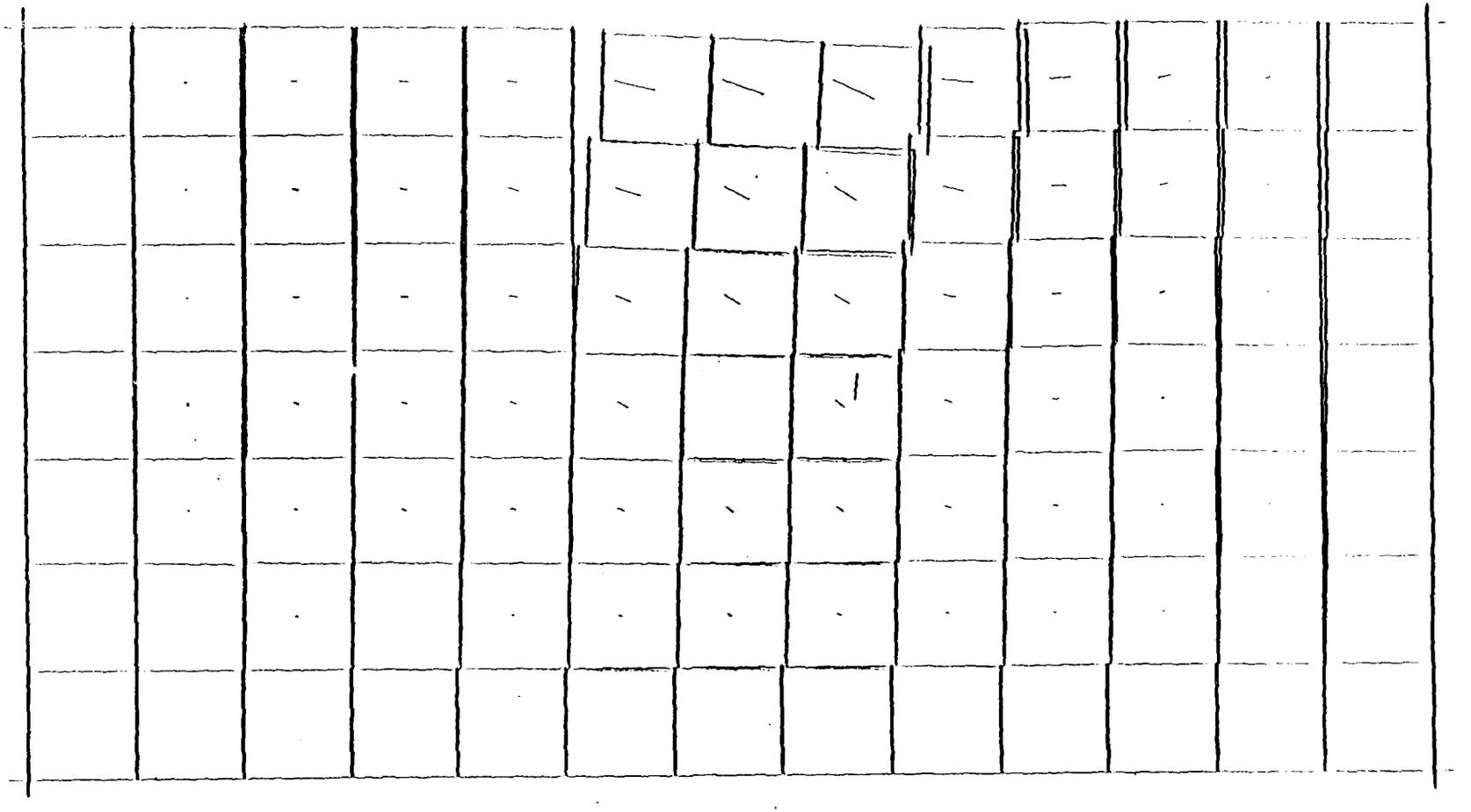

FIGURE 3.11 DISPLACEMENTS (EXAGGERATED) UNDER DAM WITH COUPLING

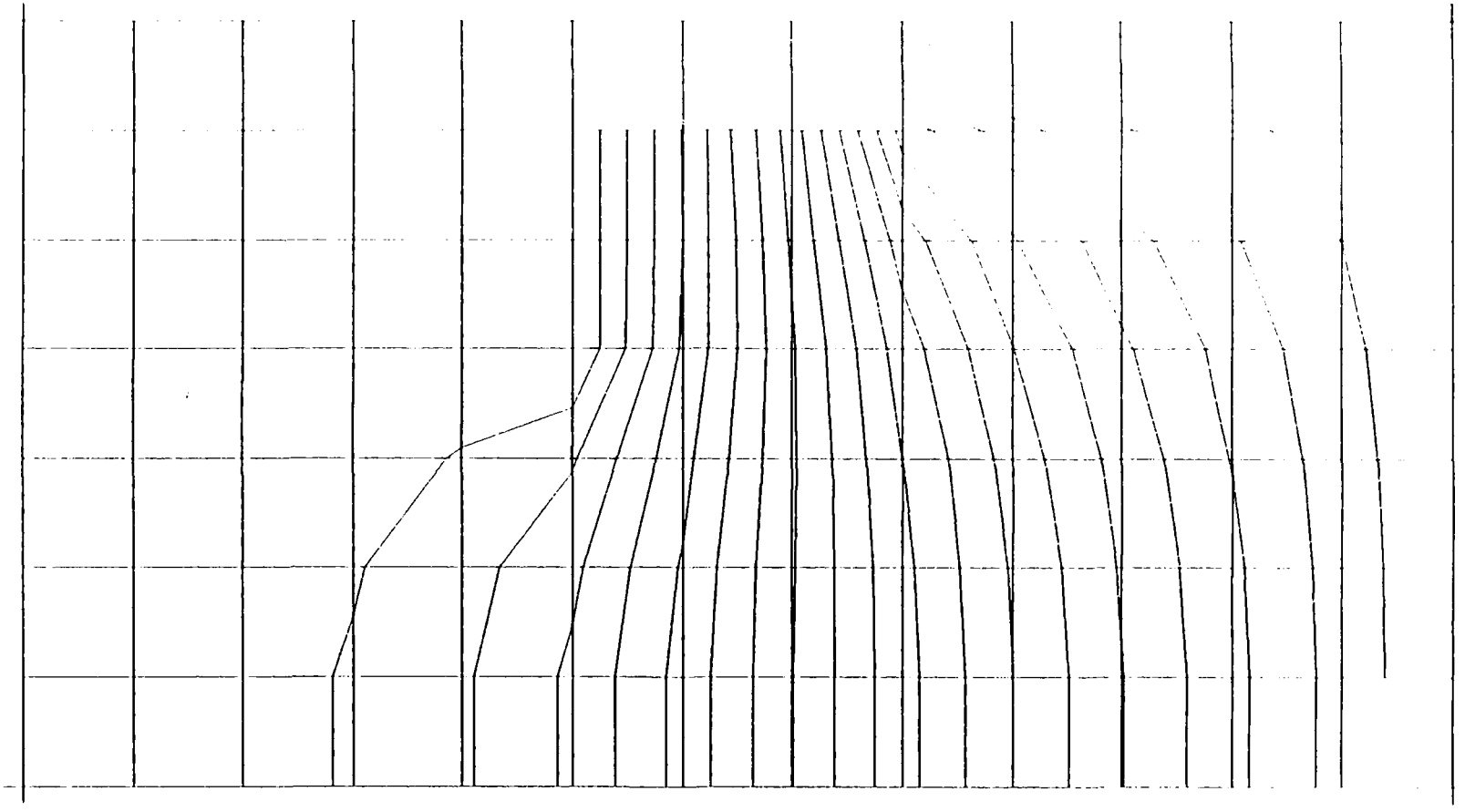

FIGURE 3.12A PSEUDO-EQUIPOTENTIALS IN THE COUPLED CASE (NO GROUT CURTAIN)

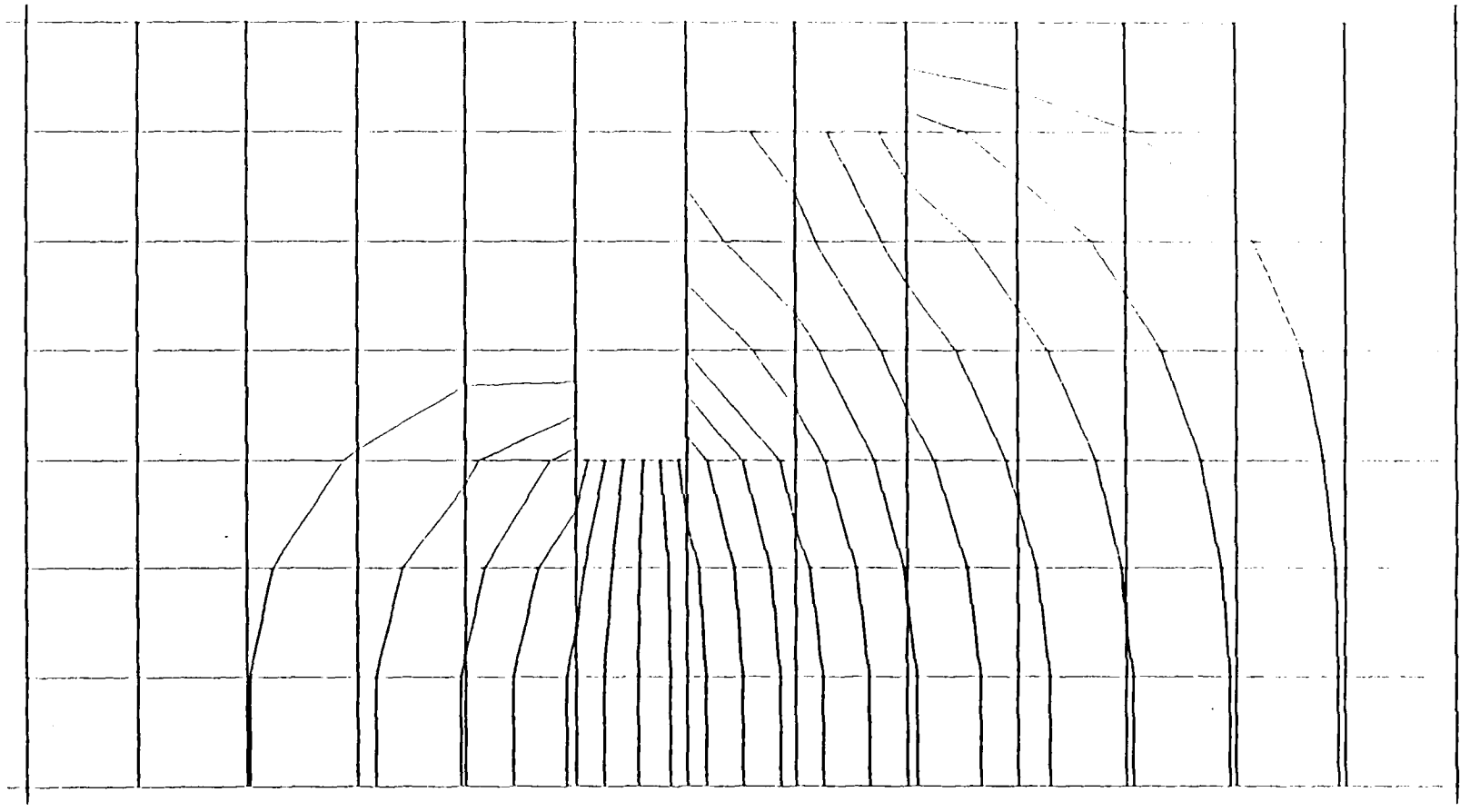

FIGURE 3.12B PSEUDO-EQUIPOTENTIALS IN THE COUPLED CASE (WITH GROUT CURTAIN)

The parametric studies consisted of varying the parameters listed in Fig. 3.13. Coupling proved to be significant in the cases without drains (drains essentially isolate the dam foundation from the flow region). The effect of coupling was studied in terms of the water pressure diagrams under the dam, the factor of safety of the dam as it can be derived from such diagrams, and the rate of flow of reservoir water underneath the dam. Ignoring coupling was seen to lead to an underestimation of water-pressure under the dam. In comparison to the equal-aperture assumption, this underestimation reached approximately 25%, leading to even more significant overestimation of the factor of safety. Estimates of the losses of reservoir water were seen to depend significantly on whether coupling is recognized and also on the hard to measure conductivity properties of the joints.

3.4 Wedge or Block Stability Analysis with Rotation and Time Effects

3.4.1 Basic Considerations

Failure of rock slopes often involves study of wedges or blocks as shown in Fig. 3.14. In the examples shown in Fig. 3.14 the wedge can either slide on one or two planes. Cases with blocks constrained by more than two planes are also possible. In the one plane case the motion of the wedge is constrained only by the requirement that the wedge stays on the plane of sliding. Such two-dimensional motion will, in general, also involve rotation of the wedge. In the two (or more) plane case the wedge can move only in the direction of the intersection of the two planes on which it slides and the motion is one-dimensional.

In addition to modelling of unidirectionl or rotational sliding it is also desirable to include time effects. The failure (instability) of rock slopes usually evolves over time where "time" can be very short (seconds) or extend over many years. Ideally, one would like to model wedge/block instability in a way that allows one to consider the entire range of time dependent effects.

JOINTS: with filler - without filler

APERTURES: small - medium - high

GROUT CURTAIN: absent - 1 block deep - 2 blocks deep - 3 blocks deep

DRAINS: absent - 1 block deep - 2 blocks deep - 3 blocks deep

UPSTREAM WATER LEVELS: low - high

K_o: low - high

FIGURE 3.13 PARAMETERS USED IN THE DAM CASE STUDIES

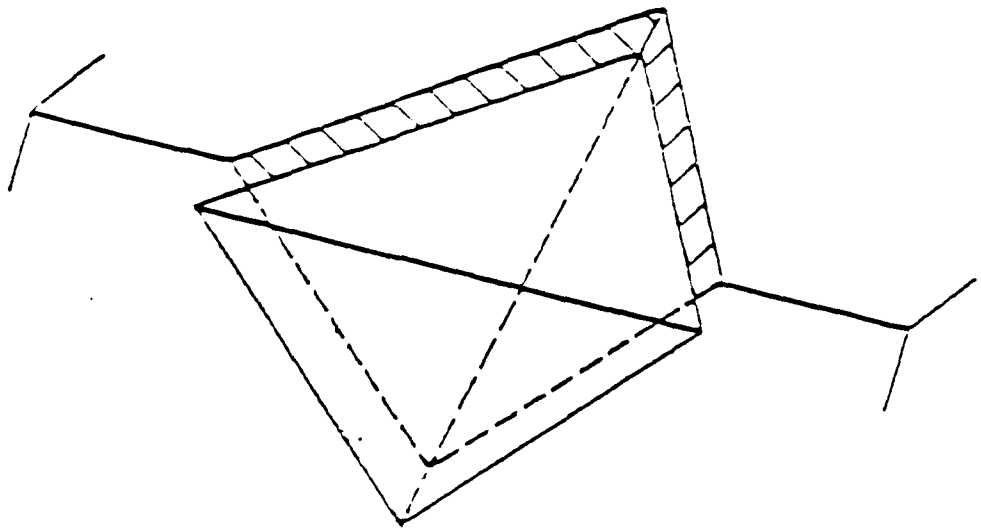

a. Failure of a wedge by sliding on two planes

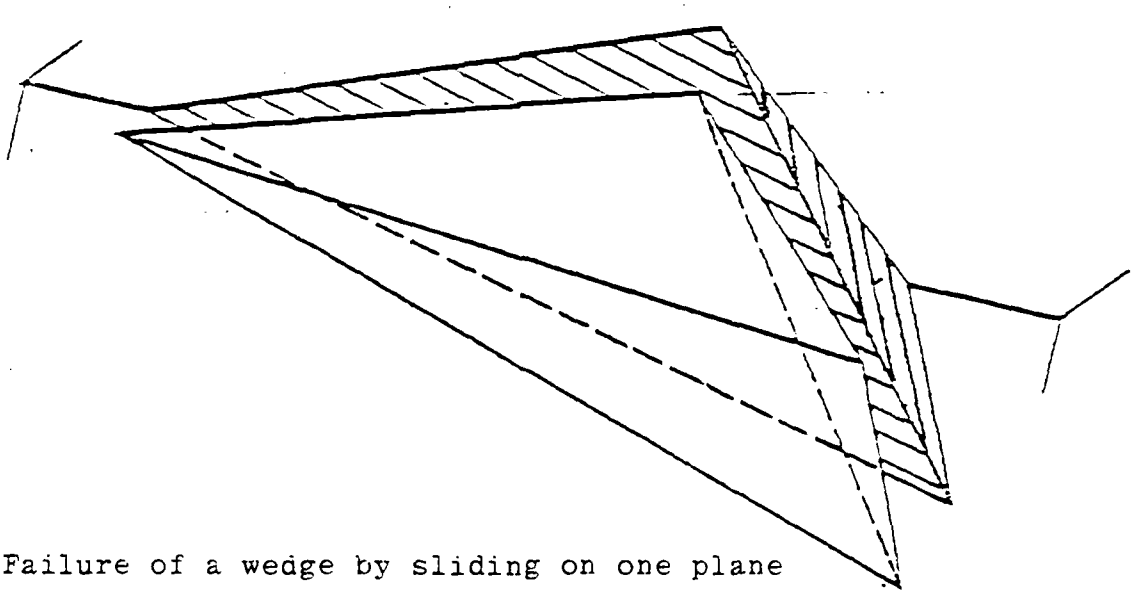

b. Failure of a wedge by sliding on one plane

FIGURE 3.14 WEDGE SHAPES

A rigid block type analysis and computer code has been developed to model wedge/block rotation with time dependence. The assumption of a rigid block for the intact rock wedge (block) bounded by joints is a good approximation as discussed in Section 3.1. The rigid block procedure is essentially the same as discussed in Section 3.2 with the following differences:

- The wedge/block is a single block but the joint surfaces are subdivided into elements (this will be shown in 3.4.3 Implementation).
- A model for time dependent joint behavior was developed (Section 3.4.2)

3.4.2 Joint Behavior Model

A model for joint behavior in a strain-controlled loading is postulated in which shear strain increases monotonically as a function of normal stress, shear displacement and rate of shear displacement. Shear stress is divided into two additive components. Both compondents depend on the normal stress, one being also a function of displacement and the other of displacement and displacement rate. The second term disappears when the displacement rate is small, but becomes dominant when the displacement rate is large. Shear stress on the failure surface is then expressed as

$$\tau = \tau_s(\sigma,\delta) + \tau_d(\sigma,\delta,\dot{\delta}) \ , \qquad (3.1)$$

where τ is shear stress; τ_s its 'spring' component, depending on normal stress σ and shear displacement δ ; τ_d its 'dashpot' component depending on σ, δ and on shear-displacement rate, $\dot{\delta}$.

The 'spring' component of shear stress, (i.e., the rate-independent component), depends on shear displacement in a form like that of Figure 3.15a. Figure 3.15b shows the assumed constant-peak-displacement type of dependence of shear stress behavior on normal stress, while Figure 3.15c presents an alternative

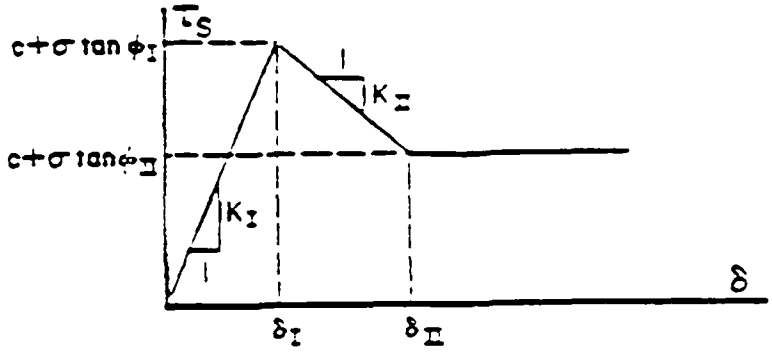

a. The τ_s versus δ diagram for a certain value of the normal stress, σ .

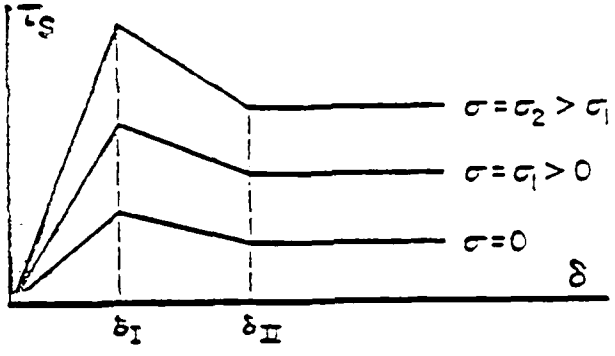

b. The effect of the normal stress, σ , on the τ_s versus δ diagram in the adopted constant peak displacement model

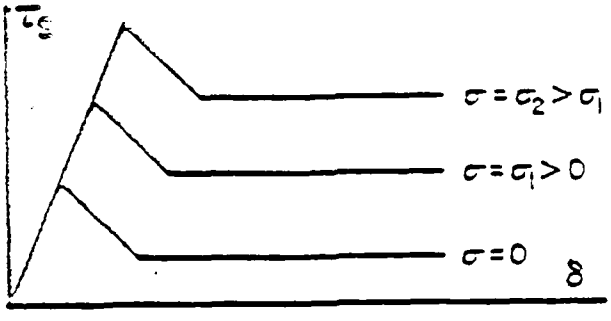

c. An alternative model displaying constant stiffness behavior

FIGURE 3.15 SHEAR STRESS-DISPLACEMENT BEHAVIOR OF ROCK JOINTS (RATE INDEPENDENT COMPONENT OF SHEAR STRESS)

model displaying constant stiffness behavior. Both types of behavior are supported by examples of direct shear test results in the literature.

The displacements δ_I and δ_{II} are parameters of the model. When the displacement is less than δ_I, asperities of the joint surfaces deform without breaking or sliding. Their movement is constrained by asperitites with which they interlock and by friction forces between the joint surfaces. In the region $0 < \delta < \delta_I$ the shear 'modulus' (relating stress to displacement) of the joint is

$$K_I = \frac{c}{\delta_I} + \sigma \frac{\tan\phi_I}{\delta_I} \qquad (3.2)$$

that is, it increases with normal stress.

As long as $\delta < \delta_I$ the displacement is entirely due to the deformation of the asperities. When a displacement of δ_I is reached, the asperities are on the verge of breaking or sliding. The shear stress at this point is

$$\tau_S = c + \sigma \tan\phi_I \qquad (3.3)$$

i.e., it is equal to a component proportional to normal stress plus a cohesion intercept.

As the displacement increases beyond δ_I, asperities start to break or slide. Breaking is associated with a drop in shear stress, and the higher the normal stress, the more extensive is the breaking of asperities and the larger the drop in shear stress. Under zero normal stress, sliding is predominant and there is almost no breaking of asperities, hence no drop in shear stress. In the region $\delta I < \delta < \delta_{II}$, shear stress and displacement are related by the 'modulus'

$$K_{II} = \sigma \frac{\tan\phi_{II} - \tan\phi_I}{\delta_{II} - \delta_I} \leq 0 . \qquad (3.4)$$

By the time the displacement reaches δ_{II}, the breaking of asperities has ceased as all asperities constraining relative displacement of the two sides of the joint

have been eliminated. For displacements larger than δ_{II} , the shear stress is given by

$$\tau_s = c + \sigma \tan\phi_{II} \quad . \tag{3.5}$$

The 'dashpot' component of shear stress, τ_d , is described as a function of δ_I and δ_{II} in Figure 3.16. It is proportional to the normal stress. In the range $0 < \dot{\delta} < \delta_I$, τ_d depends on the rate of displacement $\dot{\delta}$ but not on displacement and is equal to zero when $\dot{\delta} > \delta_{II}$. This behavior is not based on experimental results, as creep along discontinuities has received very little attention until now. However this assumed behavior seems plausible if one associates viscous behavior with deformation of intact rock that forms the asperities. Viscous effects should decrease in importance as the relative displacement of the two faces of the joint becomes larger, as the displacements increase sliding over asperities or breaking of asperities rather than viscous deformation of the asperities will occur.

3.4.3 Implementation of the Model

The computer program WEDGE has been prepared to apply the procedures outlined above. It can accomodate any wedge geometry and any loading history. In its present form it computes normal stresses based on the assumption that the wedge is rigid and that the underlying rock has a Winkler-type behavior, i.e., the normal stress at any point on the failure surface is proportional to the normal displacement at that point, given that the coefficient of proportionality is the same for all points on the failue surface. However, if desired, values for the normal stresses as computed by a Finite Element program can be used as input. The joint behavior model is that of Section 3.4.2 including the cohesion term.

The program determines the factor of safety of the wedge by an incremental application of the loads and predicts the motion of the wedge in time. Rotational effects are fully taken into account.

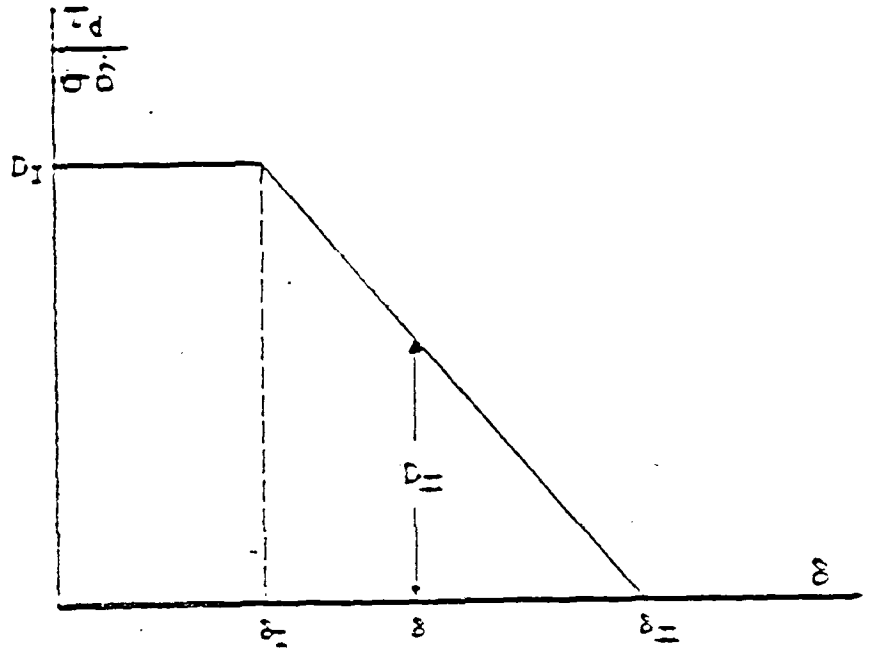

$$D_{II} = D_I \frac{\delta_{II} - \delta}{\delta_{II} - \delta_I}$$

FIGURE 3.16 SHEAR STRESS-DISPLACEMENT BEHAVIOR OF ROCK JOINTS (RATE DEPENDENT COMPONENT OF SHEAR STRESS)

Figure 3.17 shows the geometry of a wedge considered in this example. Two cases were examined. In the first, joints exhibit only strength that is proportional to normal stress, i.e., there is friction but no cohesion. In the second, joints exhibit strength that is independent of normal stress, i.e., there is cohesion but no friction. Figure 3.18 shows the loads acting on the base of the wedge and Figure 3.19 the elements into which the base of the wedge is divided.

The results from the first case (friction only) are presented in Figure 3.20 as a plot of displacements of the wedge versus time. There is no rotation, as is always the case if the external loads acting on the wedge can be reduced to a single force and if there is no cohesion. This is so because shear stress, shear deformability and shear resistance, being proportional to normal stress, vary in the same way over the failure surface, thus resulting in a translational motion of the wedge.

The results from the second case (cohesion only) are shown in Figure 3.21 as plots of the displacements of the wedge versus time. In this case there is rotation of the wedge, because shear resistance is uniform over the failure surface whereas shear stresses are not. Note, however, that under different external loading conditions, rotation effects may be present even in the absence of cohesion.

In both cases the loads were applied instantaneously at $t = 0$. Under a very slow incremental application of the loads (equivalent to ignoring time effects), both cases have factors of safety equal to 0.47.

The wedge/block analysis developed in this research makes it possible to represent the behavior of joints, the displacements of rock wedges and the evolution of displacements in time. With these features it is possible to predict and assess stability as well as the state of incipient failure.

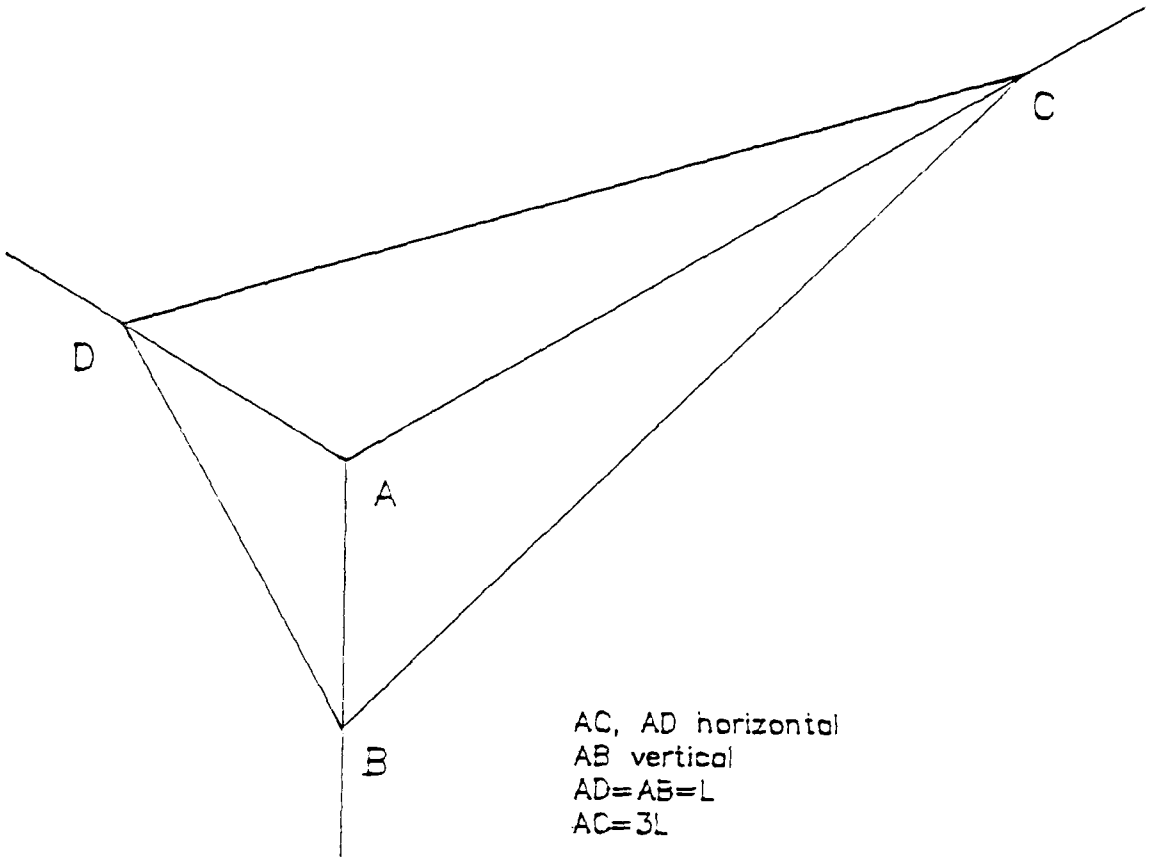

FIGURE 3.17 WEDGE GEOMETRY OF EXAMPLE CASE

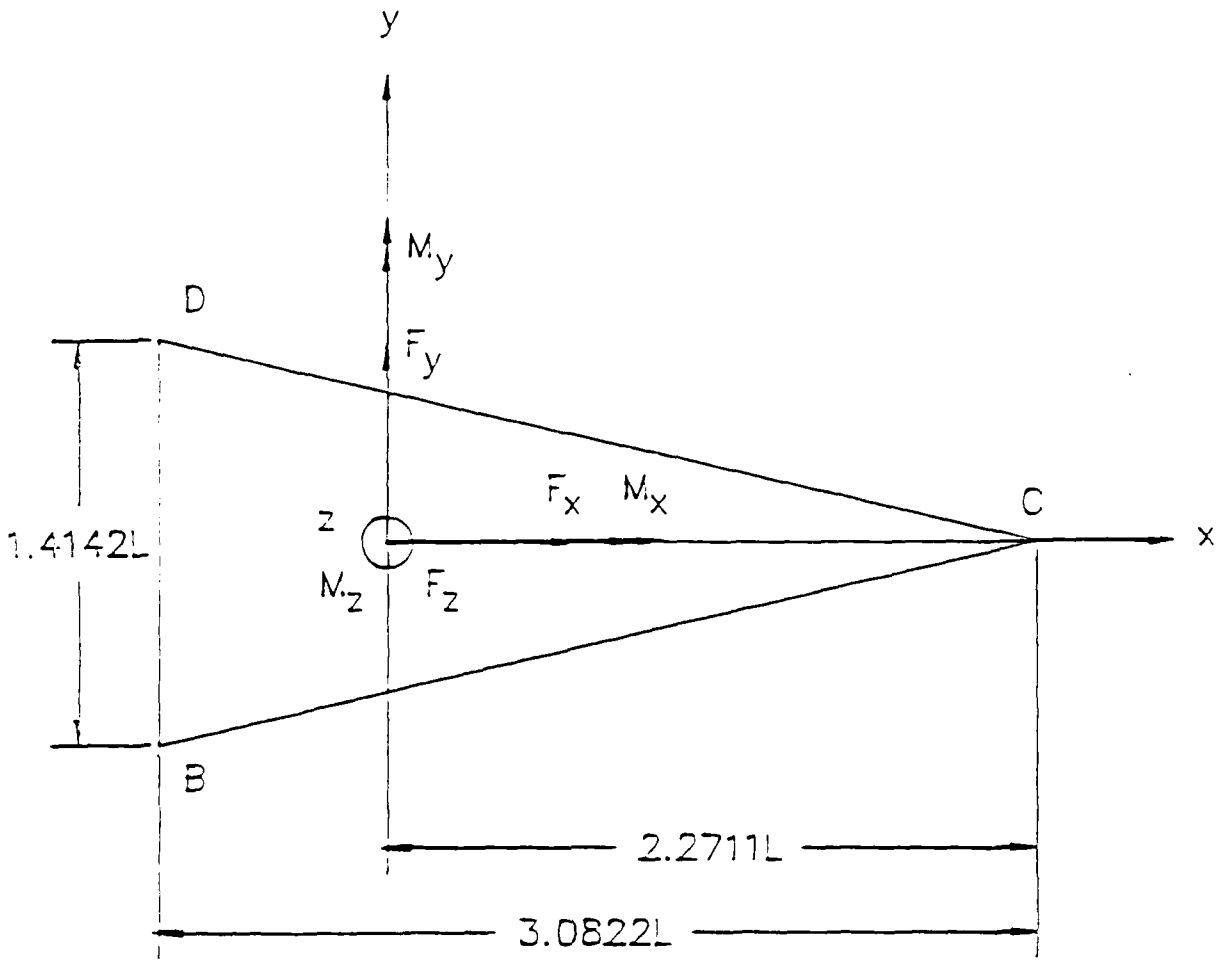

$F_x = -.3244\ F$ $\qquad M_x = .2434\ FL$

$F_y = -1.4142\ F$ $\qquad M_y = .0558\ FL$

$F_z = -1.3644\ F$ $\qquad M_z = 0$

Joint Properties:

case 1: $\delta_I = 0.5S$, $\delta_{II} = 2S$, $\tan\phi_I = 0.8$, $\tan\phi_{II} = 0.5$,

$c = 0$, $D_I = 1.T/S$

case 2: $\delta_I = 0.5S$, $\phi_{II} = 2S$, $\tan\phi_I = \tan\phi_{II} = 0$,

$c = 0.313\ F/L^2$, $D_I = 1.T/S$

FIGURE 3.18 LOADS ACTING ON WEDGE OF FIGURE 3.17

Forces, lengths and time normalized with respect to F, L and T respectively, which are arbitrary. Displacements normalized with respect to another arbitrary length, S.

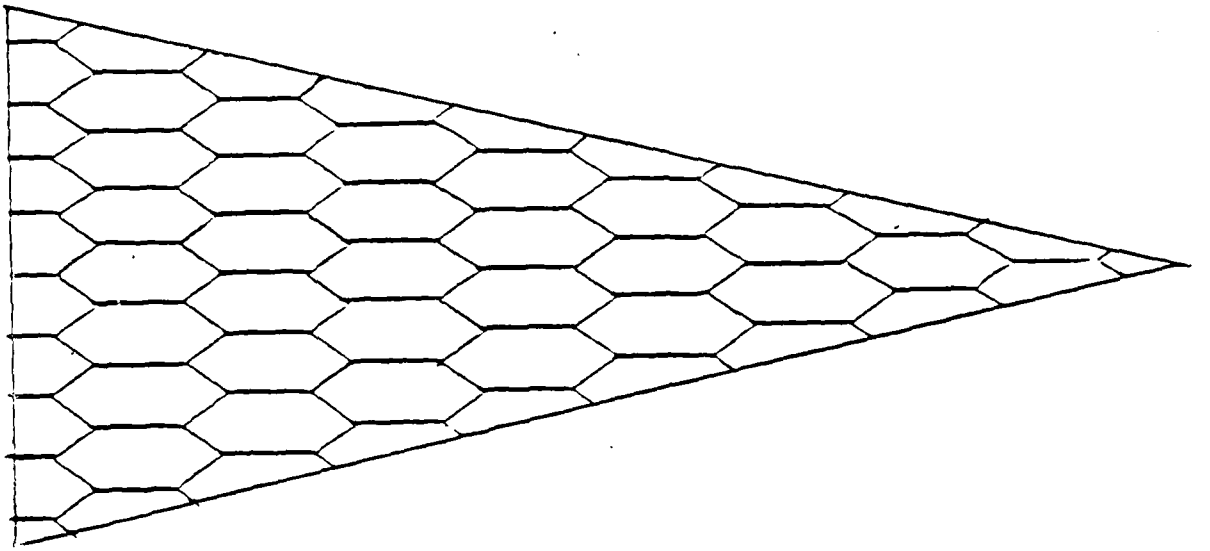

FIGURE 3.19 SUBDIVISION OF FAILURE SURFACE INTO ELEMENTS

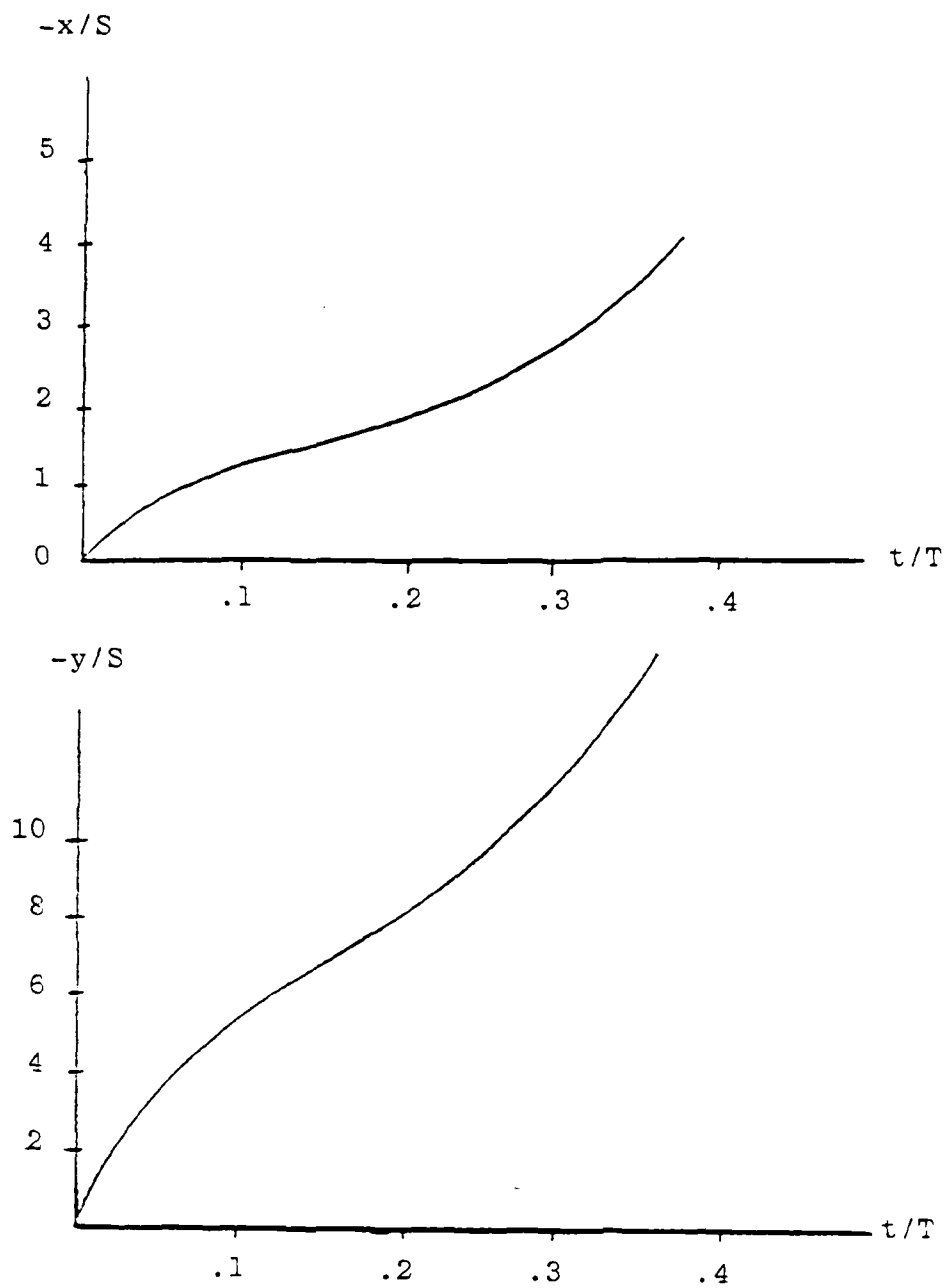

FIGURE 3.20 DISPLACEMENT TIME PLOTS (FRICTION-ONLY CASE) THERE IS NO ROTATION. ALL ELEMENTS SIMULTANEOUSLY REACH δ_I AT T = 0.88T AND δ_{II} AT T = 4.18T (AT THAT TIME FAILURE OCCURS).

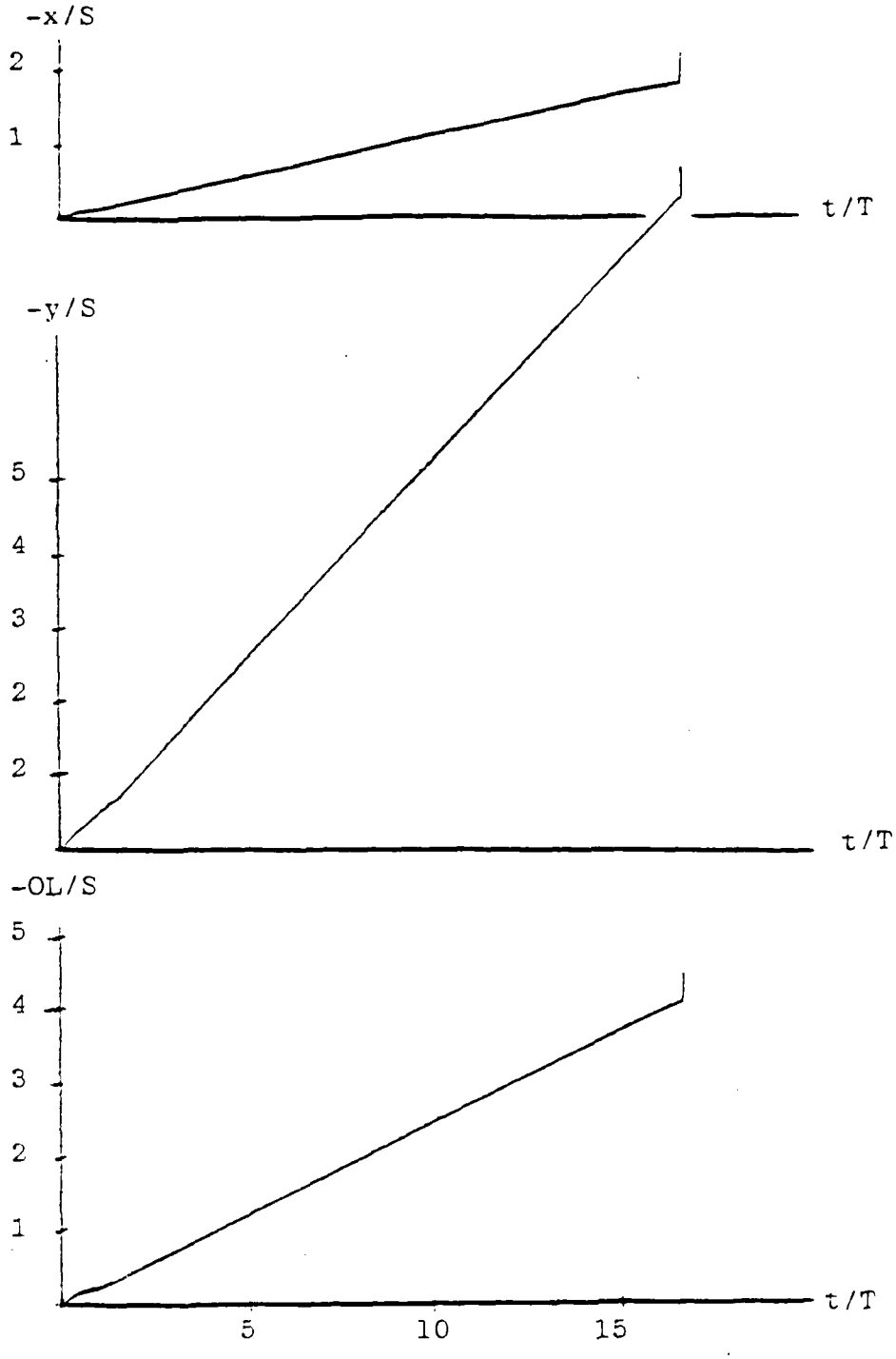

FIGURE 3.21 DISPLACEMENT TIME PLOTS. THE LARGER LINEAR PART OF THE PLOTS IS DUE TO THE FACT THAT $K = 0$ WHEN $\tan\phi_I = \tan\phi_{II}$ (SEE EQUATION 3.14). FAILURE OCCURS AT $T = 16.8T$.

4. Fracture Propagation in Jointed Media

4.1 Background

Displacements along or normal to joint surfaces are major contributors to rock mass deformability. Similarly, and as has been shown above, many failure modes of rock masses involve displacement along joints. Nevertheless, rock mass deformability and failure (strength) can also be caused by propagation of new fractures. Such fractures can propagate between existing joints located in the same plane or they can propagate from a joint in one plane to one in another plane. Various studies of this behavior have been conducted. For instance experimental studies on model rock masses show the different types of failure including propagation of new fractures (e.g. Einstein and Hirschfeld (1973). Lajtai (1969) showed that shearing under low normal stresses usually leads to tensile fracturing. This approach was incorporated in stochastic rock mass failure models of the MIT rock mechanics group (see e.g. Einstein, et al., 1981)).

The intent of the research reported here was to extend the preceding work. Specifically concepts and approaches of fracture mechanics were used to model the propagation of new fractures from existing joints*. Also, appropriate numerical methods were developed for modeling existing joints, the initiation and propagation of new fractures,and the remainder of the rock mass and its boundaries. These methods can be combined with the stochastic rock joint system models to represent fracturing of rock masses; initial work on this last aspect was also completed.

---

* Note that in the following text the term fracture is used most of the time rather than joint. This is done to indicate the generality of the procedure which is applicable to any "fracture like" discontinuity in rock.

4.2 Hybridized Displacement Discontinuity - Indirect Boundary Element Method

The Displacement Discontinuity Method uses only Displacement Discontinuity Elements and the Indirect Boundary Element Method uses Stress Discontinuity Elements. By incorporating the two types of elements in the same numerical procedure, the two methods are effectively hybridized. The Indirect Boundary Element Method can model a continuum better than the Displacement Discontinuity Method but the latter method can model fractures better. By modelling the external boundaries with Stress Discontinuity Elements, the advantages of both methods are utilized.

It has to be mentioned that both methods and thus the hybridized method are based on assumptions of linear elasticity. For the intact rock this is a simplified, but usually justified, assumption. For fracture propagation the assumption of Linear Elastic Fracture Mechanics (LEFM) can be used as a first approximation, but should often be replaced by more appropriate approaches (see Section 4.2.2).

4.2.1 Details on Elements

Analytical influence functions (induced stresses and displacements) of the Displacement Discontinuity Elements and the Stress Discontinuity Elements have been derived.

A Displacement Discontinuity Element has a positive and a negative surface which are separated by an arbitrarily small distance in the undeformed state (Fig. 4.1a). A separation and/or a slip can be applied to the two surfaces to model (part of) a fracture (Fig. 4.1b,c). The element shown in Fig. 4.1 has a constant displacement discontinuity along its axis and is called a Constant Displacement Discontinuity Element. Elements with square root, linear and parabolic

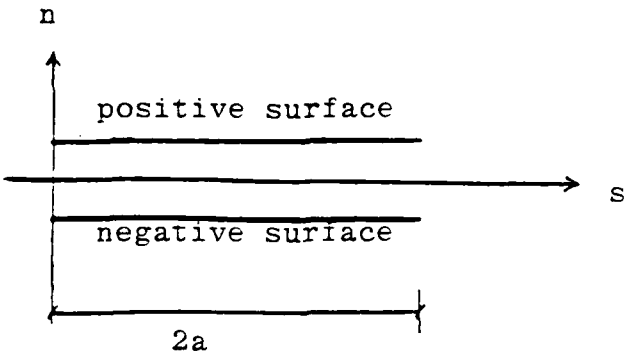

(a) undeformed state

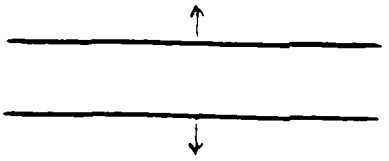

(b) separation

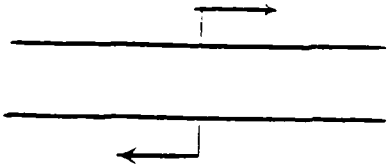

(c) slip

FIGURE 4.1 DISPLACEMENT DISCONTINUITY ELEMENT

distributions of displacement discontinuities are considered. Each of their influence functions are derived analytically by integrating the induced stresses/displacements due to the infinitesimal dislocations along the element axis. Except for the parabolic elements, these influence functions have been checked with published results and results by numerical integration.

A Stress Discontinuity Element has a positive and a negative surface which are separated by an arbitrarily small distance in the undeformed state (Fig.4.2a). Normal and/or shear stresses can be applied to the two surfaces to model external loads (Fig.4.2b,c). As a result of the applied stresses, jumps in the induced stresses across the element axis occur and are termed stress discontinuities. Elements with a constant and a linear distribution of stress discontinuities are considered. The influence functions of the Linear Stress Discontinuity Element have been derived analytically using Kelvin's point force solution for plane strain..

4.2.2 Fracture Propagation Criteria

For a closed fracture under compression and shear, uneven shear stresses exist at the fracture surfaces. The distribution of the shear stresses depends both on the distributions of the normal stresses and the slip across the fracture surfaces. Consequently, it is doubtful whether LEFM assumptions (i.e., a slip distribution proportional to the square root distance from the tip) are valid near the fracture tip. Thus a more realistic element type (the Parabolic Displacement Discontinuity Element) which does not give infinite stresses at the tip is used. The stress state at the tip can be calculated and the Maximum Tensile Stress criterion is used for modelling fracture propagation, i.e. the fracture propagates in that radial direction where the hoop stress reaches the tensile strength of the material.

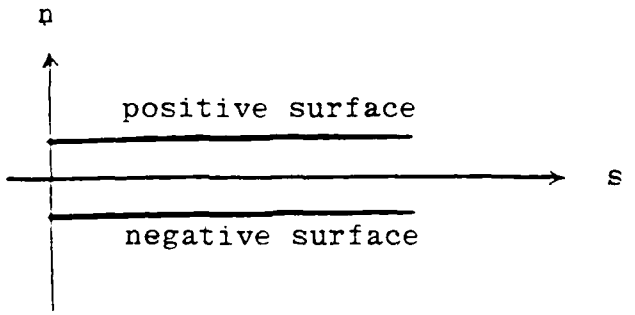

(a) undeformed state

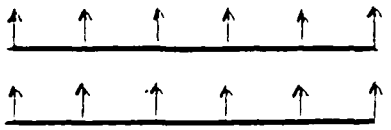

(b) applied normal stress

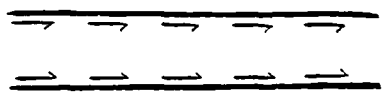

(c) applied shear stress

FIGURE 4.2 STRESS DISCONTINUITY ELEMENT

For an opened fracture it is assumed that no stresses act on the fracture surfaces. LEFM conditions are assumed near the fracture tip and the stress intensity factors are calculated. The Maximum Tensile Stress Factor criterion is used for modeling propagation.

4.3 Implementation

A Boundary Element program FROCK (Fractured Rock) utilizing the two types of elements discussed in 4.2 has been developed. It has the following advanced features:

(1) Any common type of linear elastic boundary conditions can be modelled. These include stress, displacement, mixed (e.g. roller) and spring boundaries.

(2) Automatic treatment of non-linear responses due to non-linear stress-slip relations (e.g. slip-weakening) of closed fractures, opening/closing of factures, and fracture propagation.

(3) Since analytical influence functions of the elements are used, only single precision is sufficient for the Fortran program FROCK.

(4) Optional acceleration of non-linear analyses.

(5) Optional iterations to achieve better accuracy. Usually a single additional iteration is sufficient.

(6) Modulized input commands - the user can modify different parts of the problem at will during the analysis.

(7) Mesh generation aids to facilitate input.

(8) The problem status can be stored and further analyses can be done at a later time.

(9) Realistic modelling of in situ conditions is obtained by incorporating gravity stresses as initial stresses.

4.4 Theorems

It was found that the influence functions of the Displacement Discontinuity Elements do have a number of interesting characteristics. The induced stresses/displacements due to the opening up of an element are approximately proportional to the total opening or "expansion" at distances far away from the element and are independent of the opening shape. Thus the "Theorem of Equivalent Expansions" was formulated which may have important potential applications such as the estimation of the expansion of underground fractures by surface or near-surface measurements. Similar observations were made on the relative slip of the elements. For Stress Discontinuity Elements the induced stresses/displacements at large distances are found to be approximately proportional to the total applied force on the element and to be independent of the pressure distribution on the element. The "Theorem of Equivalent Forces" was formulated which is in fact similar to Saint Venant's principle.

4.5 Case Studies

Many case studies were conducted to demonstrate the versatility of the program FROCK and to check the validity of the results. These cases are:

(1) Opened fractures in the infinite medium under tension and/or shear stresses. Various configurations have been tried (Fig.4.3). The stress intensity factors calculated by FROCK are compared with published results whenever available.

(2) Internally fractured rectangular plate under tension (Fig. 4.4). Different element types and boundary conditions are used in a number of cases. The K_I's calculated are usually within 15% of published results.

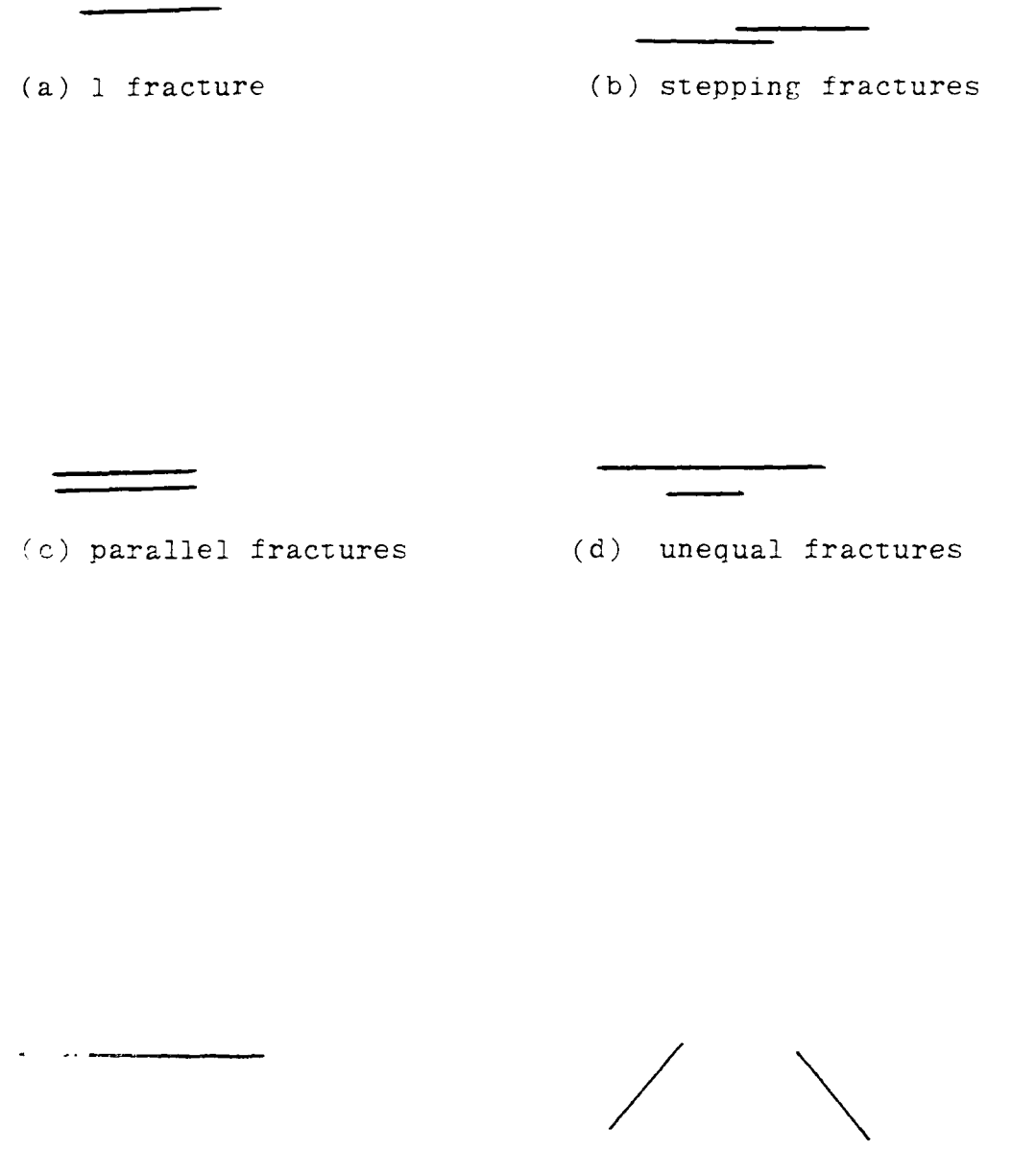

FIGURE 4.3 FRACTURE CONFIGURATIONS CONSIDERED

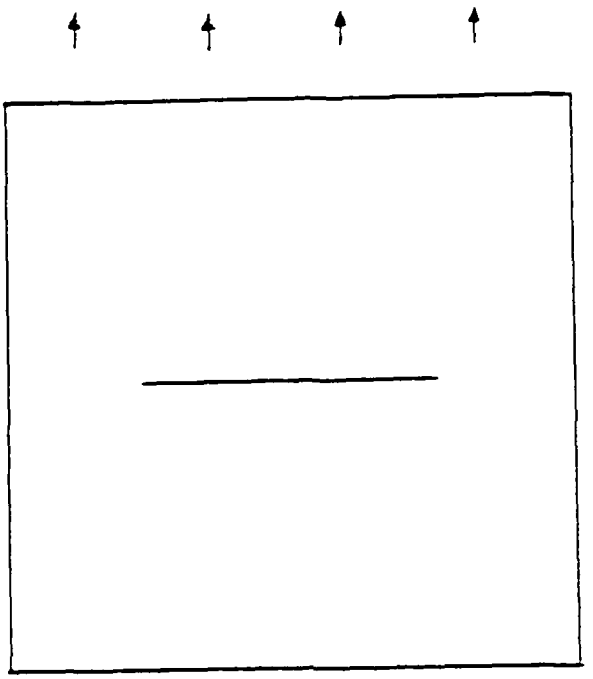

FIGURE 4.4 INTERNALLY FRACTURED RECTANGULAR PLATE UNDER TENSION

(3) Direct Shear Test. A Direct Shear Test on a rock joint which has a non-linear relation between the shear stress τ and the slip displacement δ is simulated (Fig. 4.5). The diplacement jump across the joint is shown by plotting the horizontal displacement u_x along a vertical section (Fig. 4.6). The shear stresses along the joint may not be uniform and are highest in the center part of the joint. Fig. 4.7 is a plot of the shear stress along the joint when the applied horizontal displacement is 6×10^{-4} (consistent units) at the top.

(4) Fracture propagation in a plate under compression: The propagation of a fracture in a rectangular plate under compression is simulated (Fig. 4.8). The propagation trajectories from the initially straight fracture seem to be consistent with experimental observations and theoretical stipulations.

(5) Fracture-fracture interaction and propagation under vertical tension in an infinite medium: Different configurations are considered (Fig. 4.9). For stepping fractures with small or no overlap the general pattern is that initially the inner tips have higher stress intensities than the outer ones and propagate first. After a while the propagations may or may not cause intersection of the two fractures. Then the outer tips start to propagate and approach the horizontal direction. Further on the outer tips open up essentially in Mode I with K_I's approximately equal to those of a horizontal crack with width equal to the horizontal distance beween the two fractures tips (Fig. 4.10).

(6) Fracture propagation in a plate under vertical tension: The propagation of an inclined fracture under vertical tension is simulated (Fig. 4.11). The trajectories compare well with published results from

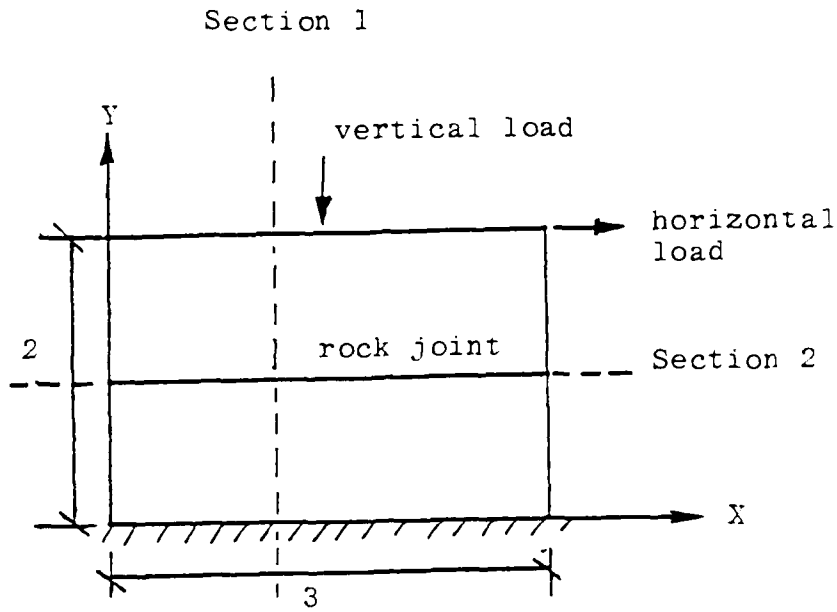

Shear Property of Joint: $\tau = \sigma.f(\delta) + 50$

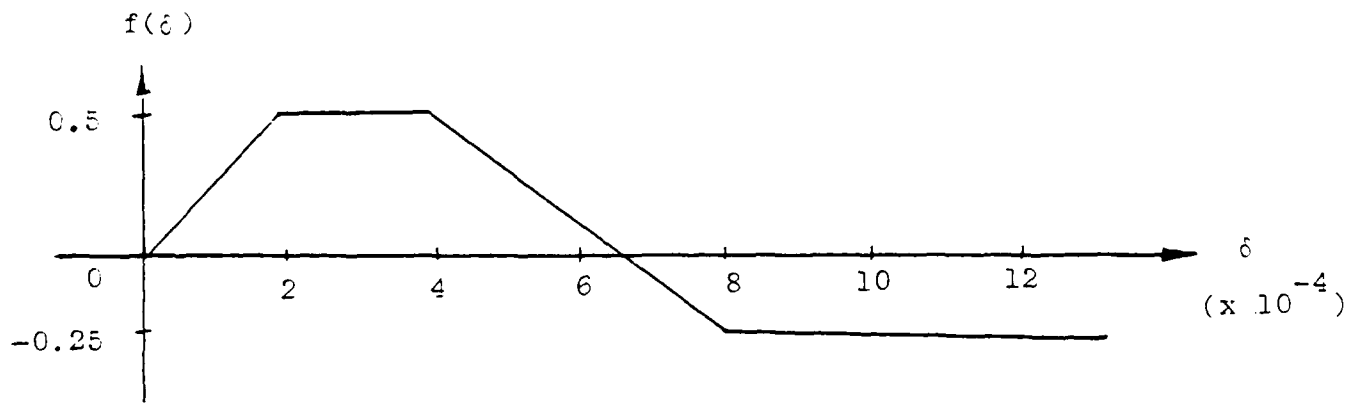

FIGURE 4.5 DIRECT SHEAR TEST

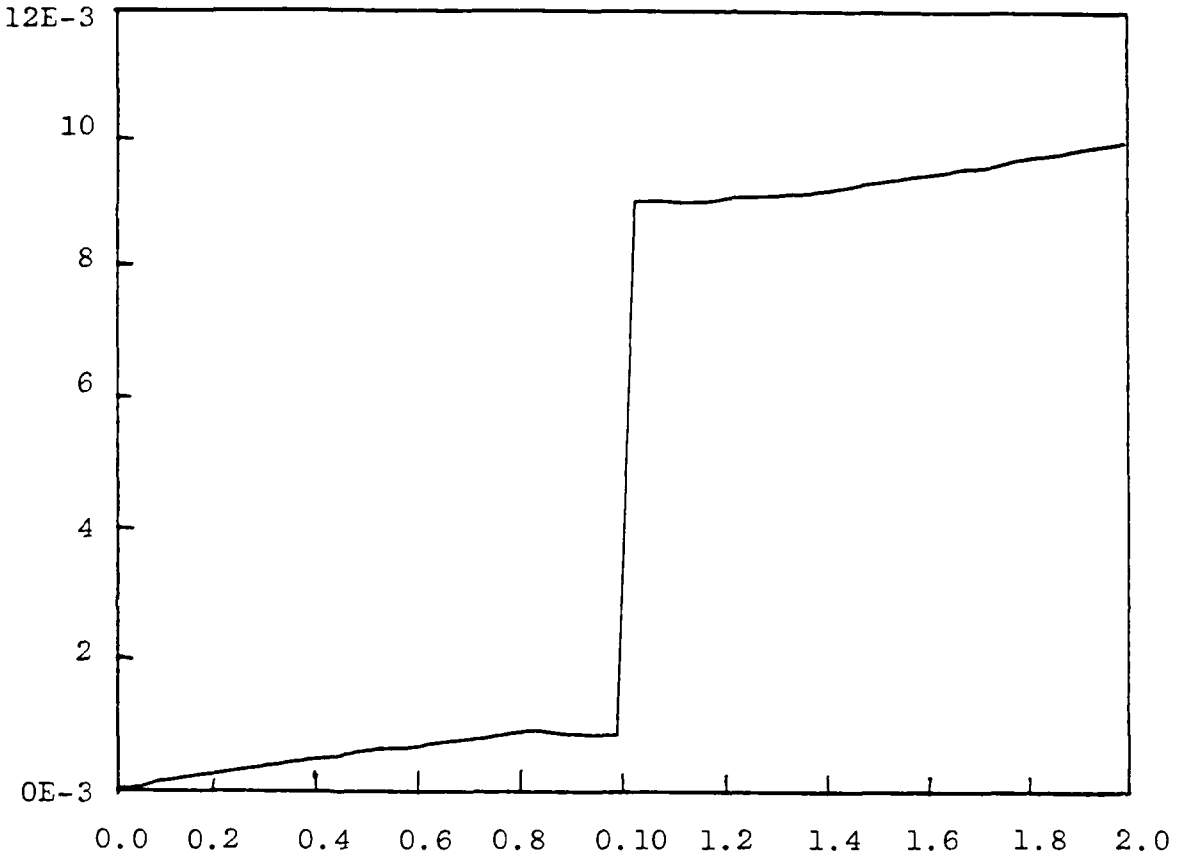

FIGURE 4.6 HORIZONTAL DISPLACEMENT JUMP (SECTION 1 OF FIG. 4.5)

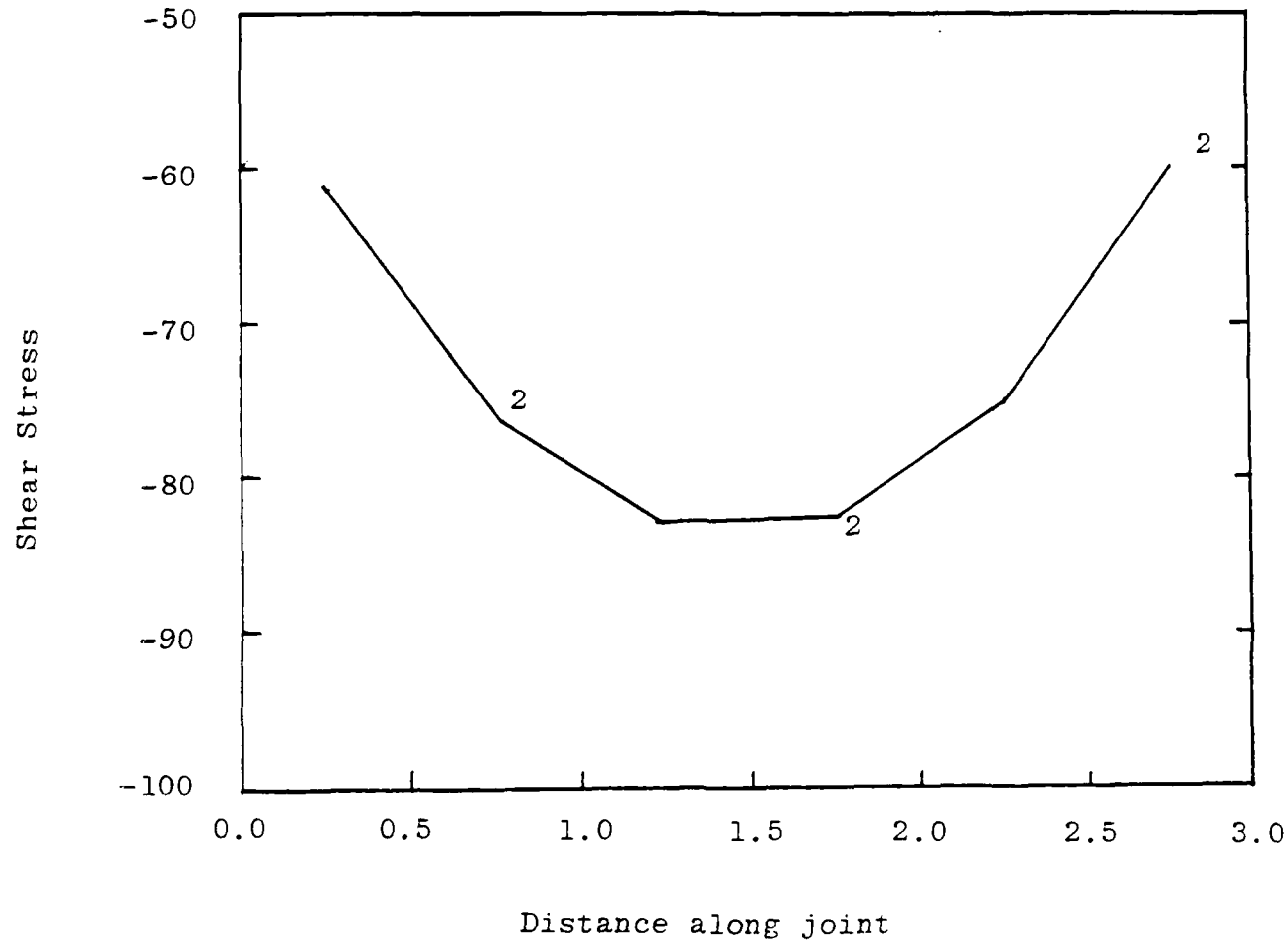

FIGURE 4.7 SHEAR STRESS ALONG FRACTURE (JOINT)

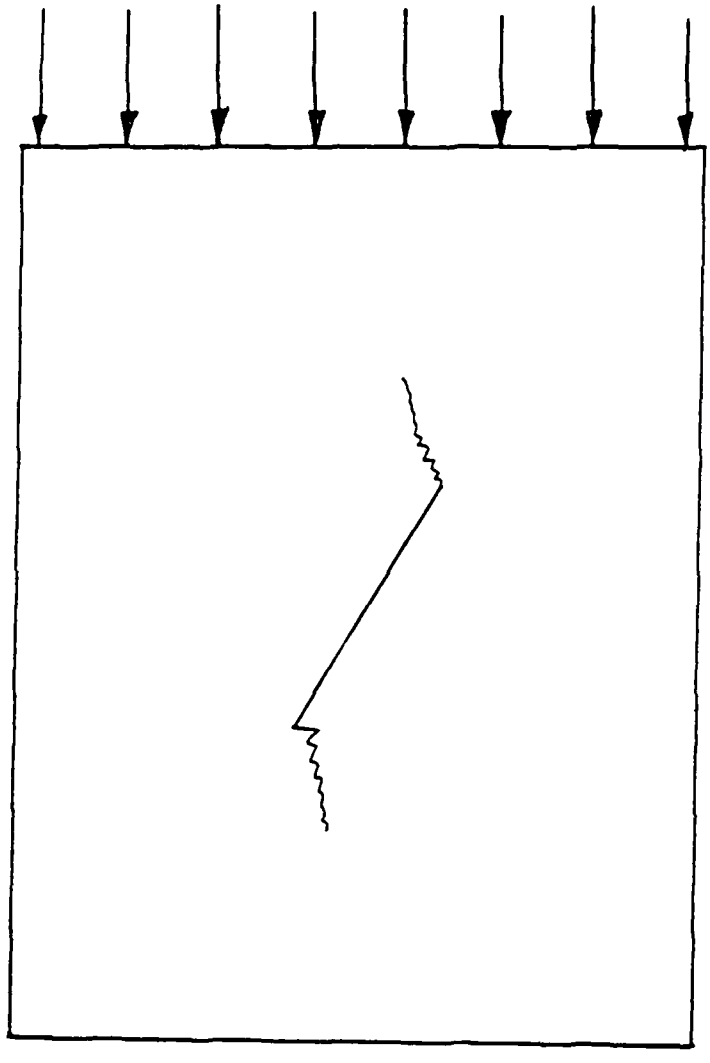

FIG. 4.8 FRACTURE PROPAGATION IN A PLATE UNDER COMPRESSION

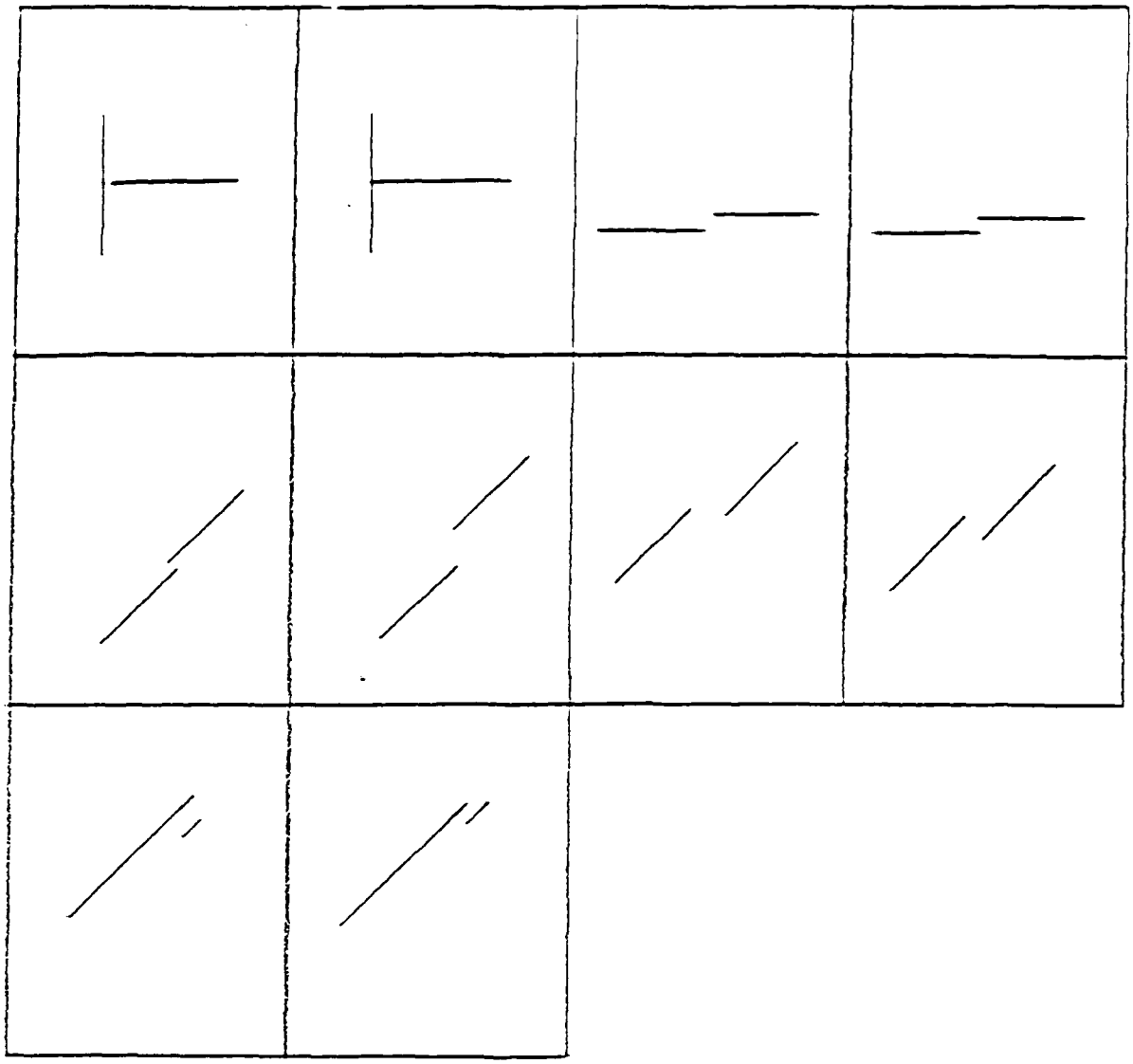

FIGURE 4.9 FRACTURE-FRACTURE INTERACTION AND PROPAGATION IN INFINITE MEDIUM UNDER VERTICAL TENSION

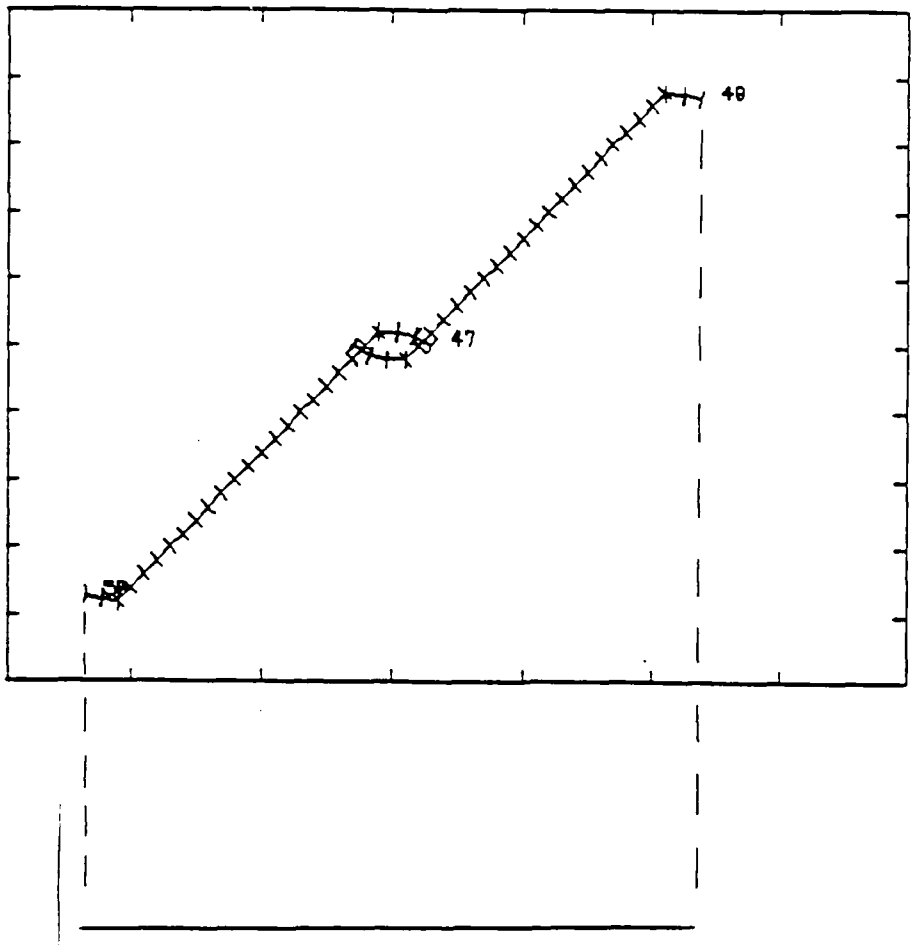

FIGURE 4.10 FRACTURE-FRACTURE INTERACTION AND PROPAGATION

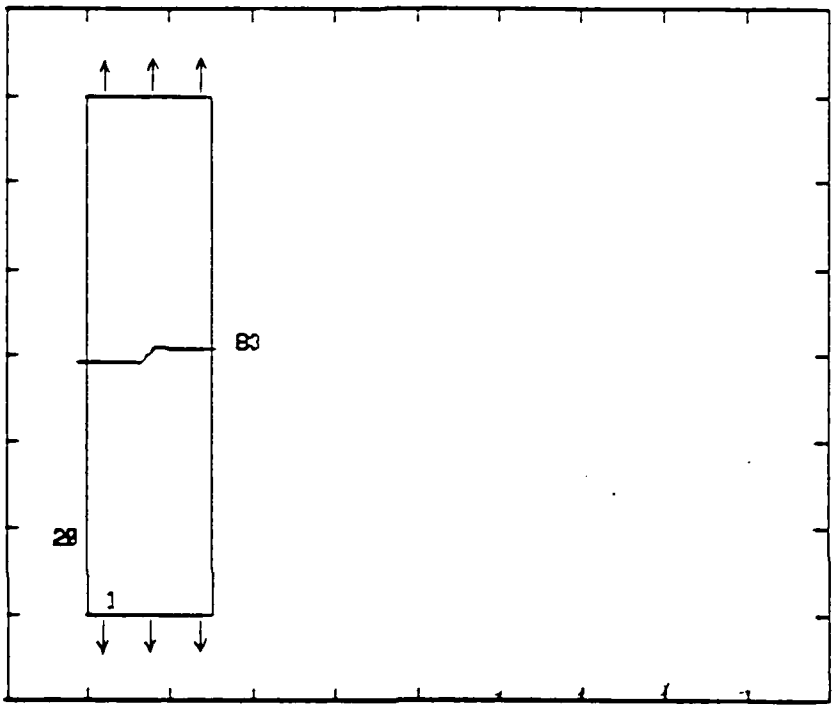

FIGURE 4.11 FRACTURE PROPAGATION IN A PLATE UNDER TENSION

a fatigue experiment on a titanium alloy (Fig. 4.12). The propagations of 2 stepping fractures in a plate is also simulated with satifactory results.

(7) Behavior of a joint in infinite medium under compression: Details of the behavior of an inclined joint in an infinite medium under vertical compression were examined, particularly the developements of sliding and tension at the tips with increasing compressive stress.

(8) Fracture propagation in a plate under compression: The effects of gravity, horizontal and vertical compressive stresses, and free ground surface on propagation were examined.

(9) Stability of an excavated slope: The possible propagation of new fractures from joints in an excavated slope leading to slope failure was examined. At first a slope without joints was considered and its stress distributions examined, followed by a slope with deterministic joints. Finally the uncertainty of the joint geometry was considered to some extent.

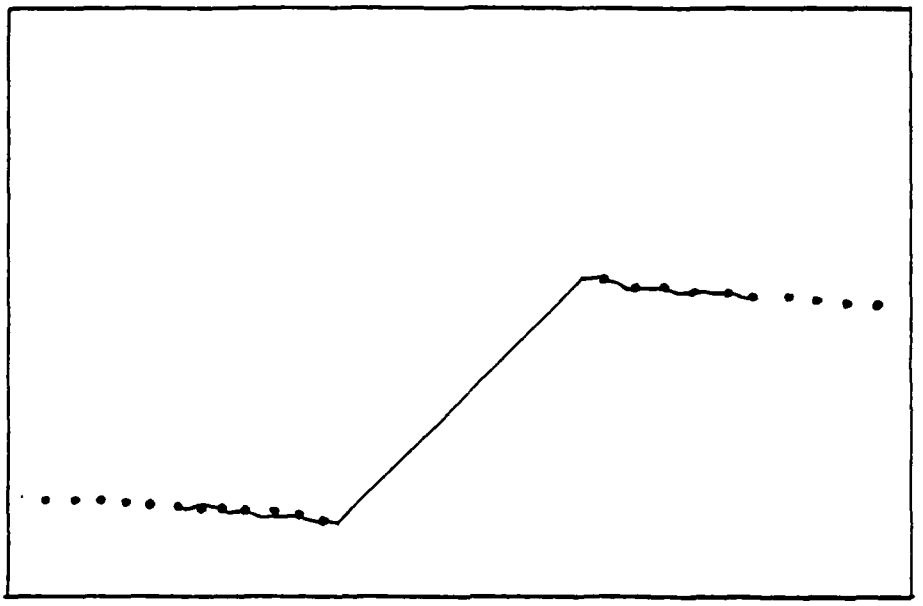

——— experimental trajectory

..... output from FROCK

FIGURE 4.12 COMPARISON OF NUMERICAL AND EXPERIMENTAL RESULTS (TENSION TEST ON TITANIUM ALLOY)

THIS PAGE IS INTENTIONALLY LEFT BLANK

5. Conclusions and Further Research

The research reported here has produced a number of significant contributions in the area of rock mass behavior:

- Joint geometry models. Two and, particularly, three-dimensional stochastic joint system models and associated computer codes have been created. They represent many actual rock mass geometries, relying on standard statistical sampling methods, and providing the basis for flow and fracture analysis.
- Flow through jointed media. The stochastic joint system models have been combined with pipe network and Finite Element flow models to represent flow through jointed media in two and three dimensions. The associated computer codes have been developed. Realistic flow analysis in rock is thus possible which is needed for engineering design (cut slopes, tunnels, dams, waste storage) and for hydrogeologic applications. Use in resource extraction can be foreseen.
- Simplified expressions for joint geometry and hydraulic characteristics of jointed rock masses have been created. Initial parametric studies show that "joint area per volume" (persistence measure P_{32}) and "connectivity" are simplified measures which can represent rock mass behavior and thus replace the complete models.
- Parametric studies with the flow in jointed media models have shown that joint system size relative to the domain (scale effect) and anisotropy (isotropy) of the joint systems have significant effects. Also three dimensional approaches lead to results that differ significantly from two dimensional approaches. Finally, joint aperture does not seem to have always the overriding effect that was stipulated previously.

- By combining the distinct element method and an analysis method for flow in joints of variable aperture a flow/deformation analysis for jointed rock masses was created. Associated interactive computer programs have been developed. The method couples deformation and flow, i.e. the effect of seepage pressure changes joint apertures, and changes in joint apertures affect flow. This analysis method is an essential tool for designing slopes, tunnels, wells and other structures in jointed rock. It is also essential for interpreting monitoring observations on water pressure and movements in these engineering projects.
- Extensive parametric studies with the flow/deformation analysis have been conducted for slopes in jointed rock, injection/withdrawal wells in jointed rock, and dams on jointed rock (with and without grout and drainage curtains). The results show that coupling is significant if the joint apertures vary within the rock mass. Ignoring the effect of coupling may lead to unconservative designs.
- A wedge/block analysis and computer code was developed with which the complete movement of wedges (blocks) in translation and rotation can be modeled, and which can represent the prefailure time dependent behavior.
- A numerical method for fracturing of jointed media has been developed based on displacement discontinuity elements of different types and boundary elements. Bounded and unbounded domains can be represented, as can fracture in mode I and II, and sliding of joints or newly propagated fractures in a slip weakening mode. This analysis method is essential to represent the deformation and possible failure of rock masses in which a combination of joint sliding and fracture of intact rock takes place. This method has been combined with the joint geometry models.

- The fracture model for jointed media produces the experimentally observed propagation of new fractures into a direction parallel to the major principal stress. It also produces fracturing in between joints and between joints and free surfaces which are important in rock mass failure. Of particular interest are:
  - Opening of fractures (joints) in tension for both infinite and bounded fields produces stress intensity factors which are close to the theoretically predicted ones.
  - Fractures (joints) in compressed stress fields propagate into the direction of the major principal stress as theoretically predicted and experimentally shown. Interaction of several fractures (joints) and different inclinations to each other and to the stress field can be modeled. The sequence of propagation is intricate and switches from one end of the existing fracture (joint) to the other.
  - A number of theorems expressing the effect of existing joints (fractures) on the behavior of the jointed rock mass under different stress fields have been developed.

Although the research results are significant and represent major advances further work is necessary in a number of areas:

- The joint geometry models need to be thoroughly validated in the field
- Modelling of nonsaturated flow, multiphase flow and transport would be of interest.
- The simplified measures need to be verified for flow applications and further developed for deformation (failure) applications.

AD-A168 949 ROCK MASS PERSISTENCE EXECUTIVE SUMMARY(U) 2/2
MASSACHUSETTS INST OF TECH CAMBRIDGE DEPT OF CIVIL
ENGINEERING H H EINSTEIN ET AL. FEB 86 R86-12-786
UNCLASSIFIED ARO-19291.4-GS DAAG29-83-K-0016 F/G 8/7 NL

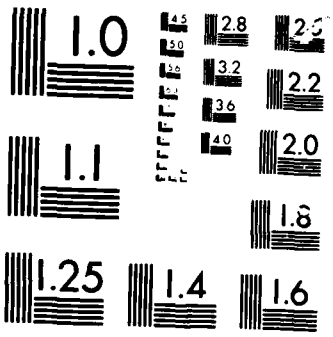
1.0
1.1
1.25
1.4
1.6
1.8
2.0
2.2
2.8
3.2
3.6
4.0
5.0

- Extension of the coupled flow deformation analysis to three dimensions and other block shapes is desirable.
- Implementation of the combined stochastic geometry and fracture models with field or laboratory verification is needed.
- The use of non-linear fracture mechanics needs to be considered to correctly model fractures approaching free surfaces or other joints.

6. Personnel and Acknowledgements

6.1 Personnel

Over the three year duration the following people have participated in the research reported here.

Faculty:

Professor H. H. Einstein, P.I.
Professor G. B. Baecher, Co-P.I.
Professor H. Herda [X]
Professor V. Li [X]
Professor D. Veneziano [X]

Visiting Scientist:

Dr. M. Gencer [XX]

Graduate Students:

H. C. Chan
W. S. Dershowitz
J. Kafritsas [XX]
O. Reyes [XX]

Undergraduate Students:

L. Fricke
B. M. Gordon
D. Sangster [XX]

[X] Served as thesis co-advisors, not funded by project.

[XX] Partially supported by project, remainder from fellowships.

6.2 Acknowledgement

Most of the research reported here has been supported by ARO under Grant No DAAG-29-83-K-0016 with Dr. G. S. Mock as Technical Monitor. The generous support and the knowledgable technical supervision provided by ARO, Dr. Mock and other experts in the Department of Defense were instrumental in making the many advances that have been reported here. For this the participants in the research project would like to express their gratitude. Initial phases of the

project and the fellowships were funded by the U.S. Bureau of Mines under the Mining and Minerals Resources Research Institute program. This support was essential and is gratefully acknowledged, as is the continuing help of Professor J. F. Elliott, Director MMRRI at M.I.T.

As was mentioned in 6.1 a number for faculty participated in the research as thesis advisors. They deserve the gratitude of the principal investigators and students for their advice and their devotion to the project.

7. Publications

Publication of research results is accomplished through this final report series and a number of papers in journals and symposia/conferences.

Published Papers:

"Coupled Deformation/Flow Analysis with the Distinct Element Method" by J. Kafritsas, M. Gencer. H. H. Einstein, Proc. Symp. 25th U.S. Symp. on Rock Mechanics, 1984.

"Methods of Artificial Intelligence in Rock Mechanics" by W. D. Dershowitz, H. H. Einstein, Proc. Symp. 25th U.S. Symp. on Rock Mechanics, 1984.

"A Three-Dimensional Model for Flow of Fractured Rock" by W. S. Dershowitz, B. M. Gordon, J. Kafritsas, H. Herda, Proc. 17th Int. Congress of the Int. Assoc. of Hydrology, 1985.

Papers submitted for Publication:

- "Conceptual Models for Characterization of Rock Joint Geometry" by W. S. Dershowitz, H. H. Einstein, submitted to Rock Mechanics and Rock Engineering.
- "Scale Effects in the Hydrology of Jointed Rock Masses" by W. S. Dershowitz, H. H. Einstein, submitted to Water Resources Resarch.

Planned Papers:

- Paper on parametric studies with 2-D and 3-D joint flow models.
- Paper on simplified measures for expressing joint geometry and flow on jointed media.
- Paper on parametric studies with flow/deformation analysis.
- Paper on wedge/block analysis with rotation and time dependent behavior.
- Two papers on fracturing of jointed media, one on fracture mechanics principles and numerical approaches, one on results.

THIS PAGE IS INTENTIONALLY LEFT BLANK

APPENDIX I
Literature References

Limited Listing only for complete listing see Volumes I to III

Baecher, G. B. and Lanney, N. A. (1978), "Trace Length Biases in Joint Surveys," Proceedings of the 19th U.S. Symposium on Rock Mechanics, American Institute of Mining Engineers, Vol. 1, pp. 56-65.

Childs, E. C. (1957), "The Anisotropic Hydraulic Conductivity of Soil," Journal of Soil Science, Vol. 8, No. 1, pp. 42-47.

Cundall, P. A. (1971), "A Computer Model for Simulating Progressive, Large-Scale Movements in Blocky Rock Systems", Proceedings, International Symposium on Rock Mechanics, Nancy.

Cundall, P. A. (1974), ""Rational Design of Tunnel Supports", Interim Report DACW 45-79-G-006, or University of Minnesota Report, MRD-2-74.

Einstein, H. H., Baecher, G. B., Veneziano, D. et al. (1980), "Risk Analysis for Rock Slopes in Open Pit Mines -- Final Technical Report," Publication No. R80-17, Order No. 669, Department of Civil Engineering, Massachusetts Institute of Technology, Cambridge, Massachusetts.

Einstein, H. H., Hirschfeld, R. C. (1973), "Model Studies on Mechanics of Jointed Rock," American Society of Civil Engineers Journal, Vol. 99, SM3.

Irmay, S. (1955), "Flow of Liquids through Cracked Media," Bulletin of the Resources Council, Israel, Vol. 5A, No. 1, p. 84.

Lajtai, E. Z. (1969), "Strength of Discontinuous Rocks in Direct Shear," Geotechnique, Vol. 19, No. 2, pp. 218-233.

Long, J.C.S. (1983), "Investigation of Equivalent Porous Medium Permeability in Networks of Discontinuous Fractures," Ph.D. Dissertation, Earth Sciences Division, Lawrence Berkeley Laboratory, University of California, Berkeley.

Schwartz, F. W., Smith, L. and Crowe, A. S. (1983), "A Stochastic Anaysis of Macroscopic Dispersion in Fractured Media," Submitted for Publication in Water Resources Research.

Snow, D. T. (1965), A Parallel Plate Model of Fractured Permeable Media, Ph.D. Dissertation, University of California, Berkeley, 331 pp.

Snow, D. (1968), "Rock Fracture Spacings, Openings, and Porosities," American Society of Civil Engineers, Journal, Vol. 94, SM1, pp. 73-91.

Veneziano, D. (1978), "Probabilistic Model of Joints in Rock", M.I.T. Manuscript (see also Einstein, Baecher, Veneziano, 1980).

END

DTIC

7-86